



Fluorescent Nano Materials and Their Sensing Ability Towards Organic Pollutants

A Dissertation

Presented in Partial Fulfillment of the Requirements for The Degree
of

Master of Philosophy

in

Department of Applied Chemistry and Chemical Engineering,
University of Dhaka.

SUBMITTED BY

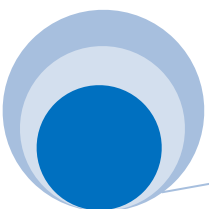
Reg No : 270

Session : 2009-2010

University of Dhaka



Dadicated to
Tabrize



ACKNOWLEDGEMENT

Thanks God for the wisdom and perseverance that He has been bestowing upon me during this research work.

I am highly pleased to express my best regards, profound gratitude, indebtedness thank and deep appreciation to my revered academic supervisors Professor, Dr. Md. Nurnabi, co-supervisor Associate Professor, Dr. A. F. M. Mustafizur Rhaman, Department of Applied Chemistry and Chemical Engineering, University of Dhaka, for their incessant supervision, enthusiastic encouragement, sagacious advice and rational criticism throughout the entire period of my research work. I really owe to them for giving me such an opportunity to work with them, because without their efforts and guidance it was impossible for me to make this thesis work a success.

Some part of my thesis work was carried out in the laboratory of Center for Advanced Research in Sciences (CARS). I am specially thankful to the Director of the Center for Advanced Research in Sciences (CARS).

I wish to express my heartiest thanks and gratefulness to the Chairman, course coordinators and all my honorable teachers of the Department of Applied Chemistry and Chemical Engineering, University of Dhaka.

Finally, I would like to say a big 'Thank-you' to my parents, siblings and my husband for their constant encouragement, cordial co-operation and all-out support to complete my thesis work.

September, 2013

The Author

ABSTRACT

Synthesis of 1,3-bis(1-butylbenzimidazol-2-yl)benzene (L-2), 2,5-bis(1-butylbenzimidazol-2-yl)thiophene(L-4), 2,5-bis(1-octylbenzimidazol-2-yl)thiophene (L-5), tetrarhenium metallacycles [$\{\text{Re}(\text{CO})_3\}_2(\mu\text{-dhaq})(\mu\text{-N-N})_2$] (L-6) and [$\{\text{Re}(\text{CO})_3\}_2(\mu\text{-thaq})(\mu\text{-N-N})_2$] (L-7), (N-N= 2,5-bis(1-octylbenzimidazol-2-yl)thiophene, H₂-dhaq= 1,4-dihydroxy-9,10-anthraquinone and H₂-thaq= 1,2,4-tri hydroxy-9,10-anthraquinone) were described in the present study. Metallacycles L-6 and L-7 underwent aggregation in THF-water mixtures and the morphology of the aggregate depends on the fraction of water. Compounds L-6 and L-7 formed granular or spongy spheres in THF solution, while they formed micron size rods in a THF-water mixture containing 40% and 30% water respectively. Besides, higher water content of 80% afforded amorphous materials. The micron size rods of L-6, L-7 showed better photoluminescence (PL) over granular or spherical aggregates, while PL is totally quenched in case of amorphous aggregates. Synthesized compounds showed sensing ability towards picric acid (PA) and 1-chloro-4-nitrobenzene. The absorbance spectra showed significance changes and photoluminescence was quenched on addition of nitroaromatics to the solutions of the sensing compounds. Binding properties were studied by Beneshi-Hildebrand and Stern-Volmer plots and found that the compounds had significant binding with nitroaromatics. This class of compounds may be applied for developing sensors for nitroaromatic pollutants in aqueous system.

List of Abbreviations

PL	Photoluminescence
PA	Picric acid
THF	Tetrahydrofuran
DCM	Dichloromethan
H	Host
G	Guest
FONs	Fluorescence Organic Nano Materials
HPS	Hexaphenylsilole
AIE	Aggregation-induced emission
AIEE	Aggregation-induced emission enhancement
SEM	Scanning electron microscopy
FESEM	Field emission scanning electron microscopy
TEM	Transmission electron microscopy
VD	Vapor deposition
VDSA	Vapor-driven self-assembly
NPs	Nanoparticles
CT	Charge transfer
NAC	Nitro-aromatic compound
TNT	Trinitrotoluene
DNT	Dinitrotoluene
GMCO	Graphene oxide–methyl cellulose hybrid
OMC	Ordered mesoporous carbon
NHCs	N-heterocyclic carbenes

List of Figures

Fig. 1.	Jablonski diagram	03
Fig. 2.	Beneshi-Hildebrand plot	05
Fig. 3.	Collisional quenching	07
Fig. 4.	Stern-volmer plot for dynamic quenching	07
Fig. 5.	Static quenching	08
Fig. 6.	Photoluminescence (PL) and UV/Vis absorption spectra of the Py-CN-MBE solution after nanoparticle formation	12
Fig. 7.	UV/Vis absorption and Photoluminescence (PL) spectra of the Py-CN-MBE/ PMMA film after nanoparticle formation	13
Fig. 8.	Fluorescence properties of compound (ABAN) in H ₂ O-THF solution	15
Fig. 9.	Schematic structures of TPP and DCM molecules	16
Fig. 10.	TEM and FESEM image of DCM-doped TPP NPs	16
Fig. 11.	UV-visible absorption spectra and fluorescence emission spectra of PDDP	18
Fig. 12.	FESEM photographs of PDDP nanoparticles	18
Fig. 13.	Structures of DPNP and Dye	20
Fig. 14.	SEM images of CN2Azo after exposure to UV light	21
Fig. 15.	Emission and UV-vis absorption spectra of CN2Azo in dichloromethane at ambient temperature	22

Fig. 16.	Fluorescence spectra of the TTP in solutions with different ratios of H ₂ O/ THF	23
Fig. 17.	Photopatterned array of Py-CN-MBE nanoparticles	26
Fig. 18.	Field emission SEM images of DAP nanoparticles	27
Fig. 19.	Reduction in the emission intensity of compound 9,10 bis(1,3 dicarboxylic- phenyl-5-ethynyl)anthracene upon gradual addition of PA	32
Fig. 20.	(a) The Benzimidazole skeleton is the fusion of benzene and imidazole, (b) 3D structure of Benzimidazole	35
Fig. 21.	'6+5' Heterocyclic structure with benzimidazoles, which includes Purine	35
Fig. 22.	Examples of antimicrobial, antiparasitic and antitumor agents containing the benzimidazole moiety	36
Fig. 23	UV-Visible spectra of L-2 with various amounts PA	57
Fig. 24.	UV-Visible spectra of L-4 with various amounts PA	57
Fig. 25.	UV-Visible spectra of L-5 with various amounts PA	58
Fig. 26.	UV-Visible spectra of L-6 with various amounts PA	58
Fig. 27.	UV-Visible spectra of L-7 with various amounts PA	59
Fig. 28.	UV-Visible spectra of L-5 with various amounts of 1-chloro-4-nitro benzene fraction	60
Fig. 29.	Beneshi-Hildebrand plot for the binding of L-2 with PA	61
Fig. 30.	Beneshi-Hildebrand plot for the binding of L-4 with PA	62
Fig. 31.	Beneshi-Hildebrand plot for the binding of L-5 with PA	62

Fig. 32.	Beneshi-Hildebrand plot for the binding of L-6 with PA	63
Fig. 33.	Beneshi-Hildebrand plot for the binding of L-7 with PA	63
Fig. 34.	PL quenching of L-2 by picric acid	65
Fig. 35.	PL quenching of L-4 by picric acid	65
Fig. 36.	PL quenching of L-5 by picric acid	66
Fig. 37.	PL quenching of L-6 by picric acid	66
Fig. 38.	PL quenching of L-7 by picric acid	67
Fig. 39.	Stern-Volmer plot for PL quenching of L-2 by PA	68
Fig. 40.	Stern-Volmer plot for PL quenching of L-4 by PA	68
Fig. 41.	Stern-Volmer plot for PL quenching of L-5 by PA	69
Fig. 42.	Stern-Volmer plot for PL quenching of L-6 by PA	69
Fig. 43.	Stern-Volmer plot for PL quenching of L-7 by PA	70
Fig. 44.	Modified Stern-Volmer plot for the PL quenching of L-4 by PA	71
Fig. 45.	Modified Stern-Volmer plot for the PL quenching of L-7 by PA	71
Fig. 46.	UV/visible spectra of L-6 and L-7 with various water fractions	73
Fig. 47.	PL spectra of L-6 and L-7 with various water fractions	73
Fig. 48.	SEM images of aggregated particles of L-6 (A) and L-7 (B) in water	75

Declaration

It is herewith certified that Reg. No.: 270, M. Phil, Session: 2009-2010, Department of Applied Chemistry and Chemical Engineering, University of Dhaka, Bangladesh, has carried out her M. Phil thesis entitled "**Fluorescent Nano Materials and Their Sensing Ability Towards Organic Pollutants**"

in the Department of Applied Chemistry and Chemical Engineering, University of Dhaka under our direct supervision. She has successfully carried out her research work and is ready to present her dissertation, which is required in partial fulfillment of her M. Phil degree. This is an original study of the author and no part of the thesis has been submitted to any other University or Institute for any degree.

We have gone through the final draft of the thesis and recommended its submission for her degree of M. Phil in Applied Chemistry and Chemical Engineering.

Supervisors:



Dr. Md. Nurnabi

Professor, Department of Applied Chemistry and Chemical Engineering,
University of Dhaka.



Dr. A. F. M. Mustafzur Rahman

Associate Professor, Department of Applied Chemistry and
Chemical Engineering, University of Dhaka.

Contents

Serial no.	Topics	Page no.
Chapter 1	Introduction	1-45
1.1 .	Luminescence	1
1.2 .	Fluorescence	1
1.3 .	Phosphorescence	4
1.4 .	Binding property and quenching	4-8
1.4.1.	Beneshi-Hildebrand method	
1.4.2.	Stern-Volmer relationship	
1.4.3	Quenching	
1.4.1.1	Collision (dynamic) quenching	
1.4.1.2	Static (complex formation)quenching	
1.5 .	Fluorescence Organic Nano Materials (FONs)	8-11
1.6 .	Methods of FONs preparation	11-23
1.7 .	Application of FONs	24-30
1.8 .	Nitoaromatic compounds and their detection	30-34
1.9 .	Benzimidazole	35-45
1.9.1	Synthesis of benzimidazole	
1.9.2	Characteristics shown by benzimidazole derivatives	
1.9.2.1.	Biological properties of benzimidazole derivatives	
1.9.2.2.	Photophysical properties of benzimidazole derivatives	
1.9.3.	Application of benzimidazole and its derivatives	
 Chapter 2	 Aim of the work	 46

Chapter 3	Experimental	47-51
3.1.	Materials and Methods	47
3.2.	Synthesis	47-50
3.2.1.	Synthesis of 1,3-bis(benzimidazolyl)benzene (compound L-1)	
3.2.2.	Synthesis of 1,3-bis(1-butylbenzimidazolyl)benzene (compound L-2)	
3.2.3.	Synthesis of 2,5-bis(1-butylbenzimidazol-2-yl)thiophene (compound L- 4)	
3.2.4.	Synthesis of 2,5-bis(1-octylbenzimidazol-2-yl)thiophene (compound L- 5)	
3.2.5.	Synthesis of [$\{\text{Re}(\text{CO})_3\}_2(\mu\text{-dhaq})(\mu\text{-1})_2$] (compound L-6)	
3.2.6.	Synthesis of [$\{\text{Re}(\text{CO})_3\}_2(\mu\text{-thaq})(\mu\text{-1})_2$] (compound L-7)	
3.3.	Fabrication of nano particles	50-51
3.3.1.	Fabrication of nano particles of L-6	
3.3.2.	Fabrication of nano particles of L-7	
Chapter 4	Result and Discussion	52-75
4.1.	Synthesis	52-55
4.2.	Binding property study	56-63
4.3.	Photoluminescence (PL) quenching study	64-72
4.4.	Absorption and Fluorescence spectroscopy of nanomaterials of L-6 and L-7	72-73
4.5.	Spectral properties of aggregates	73-74
4.6.	Morphology of the aggregates	74-75
Chapter 5	Conclusion	76
References		77-107
Appendix		108-116

1.1. Luminescence

Luminescence is emission of light by a substance not resulting from heat; it is thus a form of cold body radiation. It can be caused by chemical reactions, electrical energy, subatomic motions, or stress on a crystal. Historically, radioactivity was thought of as a form of "radio-luminescence", although it is today considered to be separate since it involves more than electromagnetic radiation. The term 'luminescence' was introduced in 1888 by Eilhard Wiedemann[1,2]. Several investigators reported luminescence phenomena during the seventeenth and eighteenth centuries. The luminescence properties of benzimidazole have been extensively studied[3-6], but little work has been reported on substituted species, for example thiabendazol and its major metabolite, 5-hydroxythiabendazole were shown to have luminescence properties[7].

Photoluminescence is a form of luminescence process, in which a substance absorbs photons (electromagnetic radiation) and then re-radiates photons. Quantum mechanically, this can be described as an excitation to a higher energy state and then a return to a lower energy state accompanied by the emission of a photon. The period between absorption and emission is typically extremely short, in the order of 10 nanoseconds. Under special circumstances, however, this period can be extended into minutes or hours.

Photoluminescence is formally divided into two categories, fluorescence and phosphorescence.

1.2. Fluorescence

Fluorescence is a member of the ubiquitous photoluminescence family, in which susceptible molecules emit light from electronically excited states created by either a physical (for example, absorption of light), mechanical (friction), or chemical reason. It is the property of some atoms and molecules to absorb light at a particular wavelength and to subsequently emit light of longer wavelength after a brief interval. It was British scientist Sir George G. Stokes who first described fluorescence in 1852 and was

responsible for coining the term in honor of the blue-white fluorescent mineral fluorite (fluorspar).

In the excited state, the electron has higher potential energy and will relax back to a lower state by emitting photon energy. This is fluorescence can be detected in the spectrum. In most cases, the emitted light has a longer wavelength, and therefore lower energy, than the absorbed radiation. The most striking examples of fluorescence occur when the absorbed radiation is in the ultraviolet region of the spectrum, and thus invisible to the human eye, and the emitted light is in the visible region.

Fluorescence is generally studied with highly conjugated polycyclic aromatic molecules. The category of molecules capable of undergoing electronic transitions that ultimately result in fluorescence are known as fluorescent probes, fluorochrom, or simply dyes. Fluorochrom that are conjugated to a larger macromolecule (such as a nucleic acid, lipid, enzyme, or protein) through adsorption or covalent bonds are termed fluorophores. In general, fluorophores are divided into two broad classes, termed- intrinsic and extrinsic. Intrinsic fluorophores, such as aromatic amino acids, neurotransmitters, porphyrins, and green fluorescent protein are those that occur naturally. Extrinsic fluorophores are synthetic dyes or modified biochemicals that are added to a specimen to produce fluorescence with specific spectral properties.

The study of chemical reactions of molecules in electronically excited states produced by the absorption of infrared (700–1000 nanometers), visible (400–700 nm), ultraviolet (200–400 nm), or vacuum ultraviolet (100–200 nm) light known as photochemistry. Bond making and bond breaking as well as electron transfer and ionization are often observed in both organic and inorganic compounds as a consequence of such excitation. The excited state produced by absorption of a photon is not generally a stable species. After a characteristic lifetime that can vary from femtoseconds (10^{-15} s) to hours, the excited molecule will either relax to its ground-state precursor or undergo a chemical

transformation. The term photo physics is used to describe nonreactive relaxation processes, which include radiative (taking place with the emission of light) and nonradiative (taking place without the emission of light) pathways.

The energies of the lowest singlet and triplet excited states (relative to the ground state) can be obtained from the longest wavelength band of the fluorescence and phosphorescence spectra, respectively. This band is called a 0, 0 band to indicate a transition between the lowest vibrational levels of the lowest-lying states. Singlet and triplet energies can also be determined indirectly by measuring quenching efficiencies. The shift between the 0, 0 bands for absorption and emission in a single molecule is called its Stokes shift. A small Stokes shift is usually observed when the excited state has geometry similar to the ground state. A Jablonski diagram (see illustration) is often used to graphically depict the relationship between competing photo physical processes.

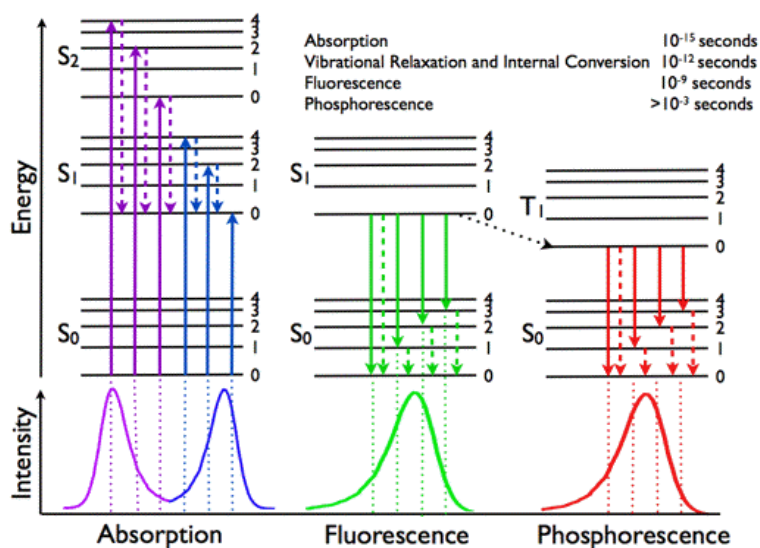


Figure-1 : Jablonski diagram. S terms = singlet states; T terms = triplet states.

1.3. Phosphorescence

Phosphorescence is a form of photoluminescence which is a result of triplet–singlet electronic relaxation (typical lifetime: milliseconds to hours). In which the energy from absorbed photons undergoes intersystem crossing into a state of higher spin multiplicity, usually a triplet state. Once the energy is trapped in the triplet state, transition back to the lower singlet energy states is quantum mechanically forbidden, meaning that it happens much more slowly than other transitions. The result is a slow process of radiative transition back to the singlet state, sometimes lasting minutes or hours. The process of phosphorescence occurs in a manner similar to fluorescence, but with a much longer excited state lifetime.

1.4. Binding property and Quenching

To observe one-to-one binding between host (H) and guest (G) molecule using UV-Visible absorption, Beneshi-Hildebrand method can be used. On the other hand, Stern-Volmer method is used to observe the intermolecular deactivation i.e. quenching of luminescent material.

1.4.1. Beneshi-Hildebrand Method

The Beneshi-Hildebrand method is a mathematical approach used in physical chemistry for the determination of the equilibrium constant K and stoichiometry of non-bonding interactions. This method has been typically applied to reaction equilibria that form one-to-one complexes, such as charge-transfer complexes and host-guest molecular complexation.



The theoretical foundation of this method is the assumption that when either one of the reactants (host) is present in excess amounts over the other reactant, the characteristic electronic absorption spectra of the other reactant(trace amount/guest) will be transparent

in the collective absorption/emission range of the reaction system[8]. Therefore, by measuring the absorption spectra of the reaction before and after the formation of the product and its equilibrium, the association constant of the reaction can be determined.

The kinetics of Beneshi-Hildebrand method is –

$$1/\Delta A = 1/(\Delta \epsilon K[H][G]) + 1/(\Delta \epsilon [H])$$

Where, $\Delta A = A_0 - A$ = the change of absorbance before (A_0) and after (A) of HG complex.

$\Delta \epsilon$ = represents the change in value between ϵ^{HG} and ϵ^G .

K = the equilibrium constant.

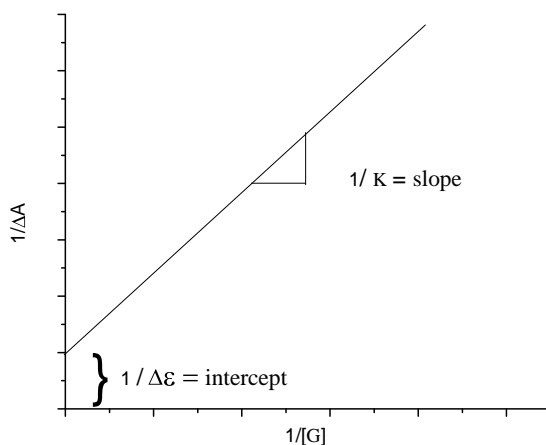


Figure-2 : Beneshi-Hildebrand plot.

Limitations of Beneshi-Hildebrand plot:

1. $[H] \gg [G]$ is must ($[H]$ must be almost 10 fold excess than $[G]$); if not then linearity breaks down to scatter plot.
2. Strongly bound complex formation should be 1:1 product complex; if it is 2:1 weakly bound complex then accuracy would be lost.
3. Only one parameter, K or ϵ , can be evaluated independently of the other.

1.4.2. Stern–Volmer relationship

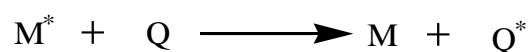
The Stern–Volmer relationship, named after Otto Stern and Max Volmer[9] allows us to explore the kinetics of a photophysical intermolecular deactivation process. Processes such as fluorescence and phosphorescence are examples of intramolecular deactivation (quenching) processes. An intermolecular deactivation is where the presence of another chemical species can accelerate the decay rate of a chemical in its excited state. In general, this process can be represented by a simple equation:



Where, A is one chemical species, Q is another (known as a quencher) and * designates an excited state.

1.4.3. Quenching

The process by which an excited state molecule, M*, in an excited singlet or triplet state transfers all or part of its excitation energy to a reaction partner or quencher, Q, is called energy transfer or quenching when the molecule of interest is M.



A number of processes can lead to a reduction in fluorescence intensity, which is referred to as quenching. These processes can occur during the excited state lifetime, for example collisional quenching, energy transfer, charge transfer reactions or photochemistry or they may occur due to formation of complexes in the ground state. There are two quenching processes usually encountered-

1. Collisional (dynamic) quenching
2. Static (complex formation) quenching

1.4.3.1. Collisional (dynamic) Quenching

Collisional quenching occurs when the excited fluorophore experiences contact with an atom or molecule that can facilitate non-radiative transitions to the ground state. Common quenchers include O_2 and acrylamide.

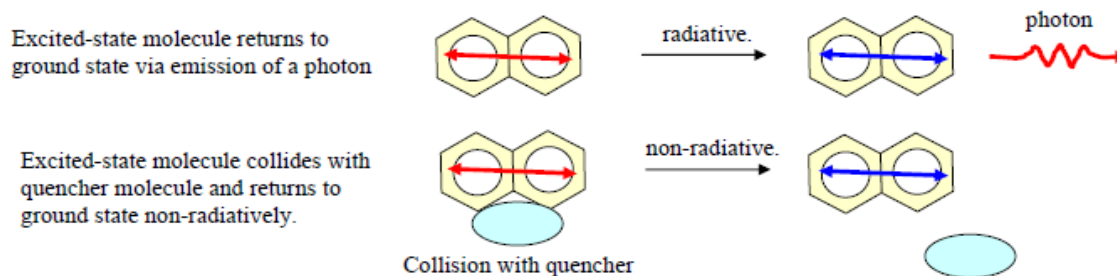


Figure-3 : Collisional quenching.

In the simplest case of collisional quenching, the following relation, called the Stern-Volmer equation, holds:

$$I_0/I = K_{sv} [Q] + 1$$

Where, I_0 is the intensity, or rate of fluorescence, without a quencher, I , is the intensity, or rate of fluorescence, with a quencher, K_{sv} , is the quencher rate coefficient and Q , is the concentration of the quencher[10].

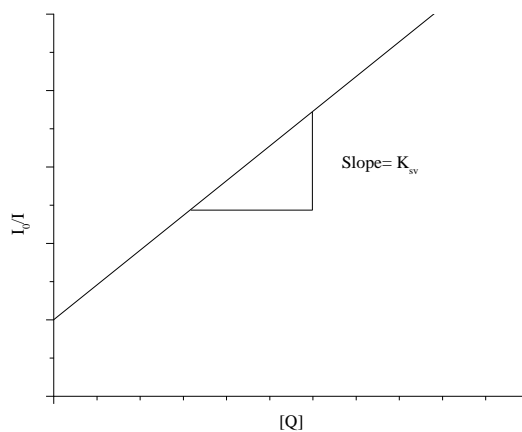


Figure-4 : Stern-Volmer plot for dynamic quenching.

1.4.3.2. Static (complex formation) Quenching

Static quenching only affects the complexed fluorophores. The properties of the uncomplexed fluorophores are not changed.

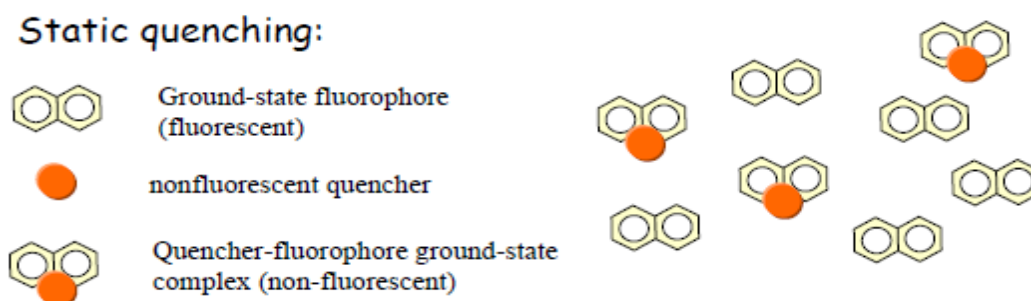


Figure-5 : Static quenching.

In some cases, the fluorophore can form a stable complex with another molecule. If this ground-state is non-fluorescent then we say that the fluorophore has been statically quenched. In such a case, the dependence of the fluorescence as a function of the quencher concentration follows the relation:

$$I_0/I = 1 + K_a [Q]$$

Where, K_a is the association constant of the complex. Such cases of quenching via complex formation were first described by Gregorio Weber.

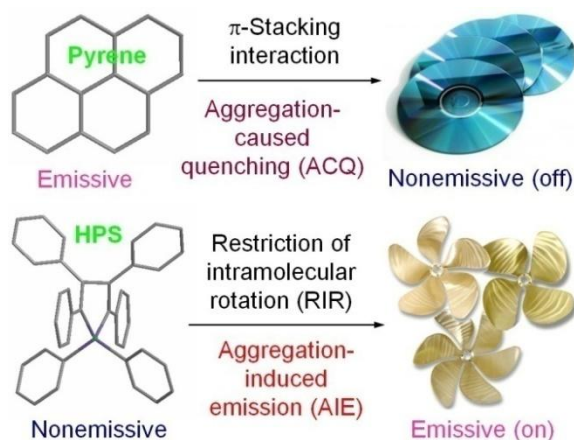
1.5. Fluorescence Organic Nano Materials (FONs)

During the past two decades, more and more research attention has been paid to nanomaterials- those functional materials composed of objects in the range 1–100 nm. If hybrids are neglected, nanomaterials can be divided into two categories-inorganic nanomaterials and organic nanomaterials. Besides inorganic counterparts, nanomaterials based on traditional functional small organic molecules have been the subject of research interest in recent years, because many routes are introduced for fabricating small organic

compounds into nanostructures. Besides the exploration of the synthetic strategies, much effort has also been made to investigate the unique optical and/or electronic properties of the organic nanomaterials obtained by molecular aggregation in the nanostructures.

One of the example of quenching is aggregation of fluprophor in solvent. Fluorophor aggregation generally quence the light emission. Most of the organic luminogens are highly emissive. But when they undergo aggregation, the luminescence is totally quenched by aggregation or the emission is induced by aggregation. Pentacenequinone derivatives form fluorescent nano aggregates in aqueous media and show aggregation-induced enhancement[11].

Planar luminogens such as pyrene tend to aggregate due to strong π - π stacking interaction, which commonly turns “off” light emission, whereas nonplanar propeller-shaped luminogens such as hexaphenylsilole (HPS) behave oppositely, with their light emissions turned “on” by aggregate formation, due to the restricted intramolecular rotation in the aggregates. The additional thing is hexylphenylsilole (HPS) dissolved in its good solvent is nonemissive. But addition of large amounts of water into the solution causes the silole molecules to aggregate and induces them to emit efficiently. This is “aggregation-induced emission enhancement” (AIEE), because the nonluminescent silole molecules are induced to emit by aggregation.



Scheme-1 : Planar luminogens such as pyrene tend to aggregate just as discs pile, which commonly turns “off” light emission, whereas nonplanar propeller-shaped luminogens such as hexaphenylsilole (HPS) behave oppositely, with their light emissions turned “on” by aggregate formation.

Only a limited number of organic compounds display AIE (aggregation-induced emission) characteristics such as siloles, aminobenzoic acids, arylethene and arylbenzene derivatives. There are two types of aggregate: J-aggregate and H-aggregate.

It was found that the optical and electronic properties of organic nanomaterials are fundamentally different from those of their inorganic counterparts, because the intermolecular interactions in organic materials are basically of weak types, such as hydrogen bonds, π - π stacking, van der Waals contacts, and CT (charge transfer) interactions. For organic nanomaterials, a series of unique PL behaviors have been achieved, which resulted from the special aggregation modes of the organic molecules, the crystallinity of the materials, and the deliberate introduction of at least one kind of guest compound into the host material matrices. In the following sections, we introduce the various methods for fabrication of nanoparticle and the particular PL (photoluminescence) properties of them, including emission enhancement in amorphous nanostructures, fluorescence narrowing and defect emission from organic crystalline

nanomaterials, size dependent optical properties and tunable and switchable emissions from doped organic nanosystems.

1.6. Methods of FONs preparation

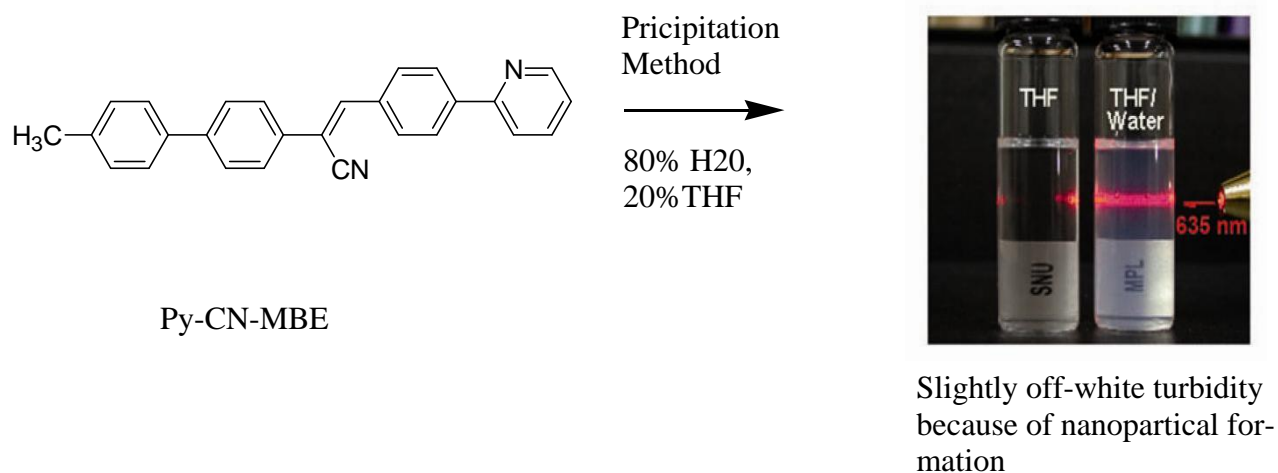
Most of the current works focus on organic nanoparticles with a single chemical composition dispersed in an aqueous system. Of all the preparation methods, reprecipitation is the most facile and commonly used one. Reprecipitation, which is a solvent displacement method, was first reported by Nakanishi and coworkers[12-14]. With this method, a series of organic nanoparticles were successfully fabricated by several groups.

For example, after their pioneer work on this method, Nakanishi and coworkers prepared pyrene nanoparticles and observed the emissions from both free excitons and self-trapped excitons[15,16].

Horn and coworkers prepared nanoparticles from β -carotene and observed the influence of both supramolecular structure and particle size on the absorption spectra[17].

Majima's group[18] and Barbara's group[19] prepared nanocrystals from perylene and a perylene derivative, respectively, and studied the spectroscopy of single nanoparticles.

Byeong's group[20] prepared colloidal nanoparticles of 1-cyano-trans-1-(4'-methylbiphenyl)-2-[4'-(2'-pyridyl)phenyl]ethylen (Py-CN-MBE) by reprecipitation method where water was added as a nonsolvent to its solution ($2 \times 10^{-5} \text{ molL}^{-1}$) in THF and observed that after the addition of an 80% volume fraction of water to the THF solution, the suspension was macroscopically homogeneous with no precipitates but had a slightly off-white turbidity as a result of light scattering from the nanoparticles[21] and confirmed the fine spherical structure of nanoparticles by scanning electron microscopy (SEM) image.



Scheme -2: Nanoparticle formation of (Py-CN-MBE) by reprecipitation method.

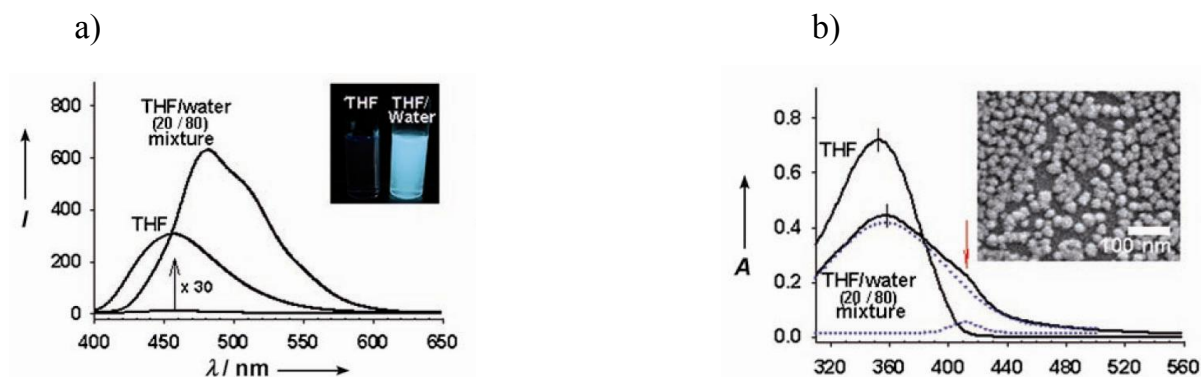


Figure-6 : a) Photoluminescence (PL) spectra of the Py-CN-MBE solution after nanoparticle formation. Insets: the fluorescence emission changes of the Py-CN-MBE solution after nanoparticle formation under illumination by UV light at 365 nm. b) UV/Vis absorption spectra of the Py-CN-MBE solution after nanoparticle formation. Blue dotted lines show the peak separation of Py-CN-MBE nanoparticles in the case of 80% water addition and exposure to dichloromethane vapor for 20 s. Insets: SEM images of the Py-CN-MBE colloidal nanoparticles obtained with the reprecipitation method.

Vapor deposition (VD) is also a facile and feasible method for preparing nanomaterials and has achieved great success in fabricating organic nanostructures. Byeong-Kwan and

coworkers[20] also fabricated a photopatterned FONs arrays of 1-cyano-trans-1-(4'-methylbiphenyl)-2-[4'-(2'-pyridyl)ethylene (Py-CN-MBE), which is based on the principles of vapor-driven self-assembly (VDSA) and they found that this molecule has strong nanoparticle formation capability through self-assembly with concomitant fluorescence turn-on (so-called aggregation-induced emission enhanced (AIEE)[22-24].

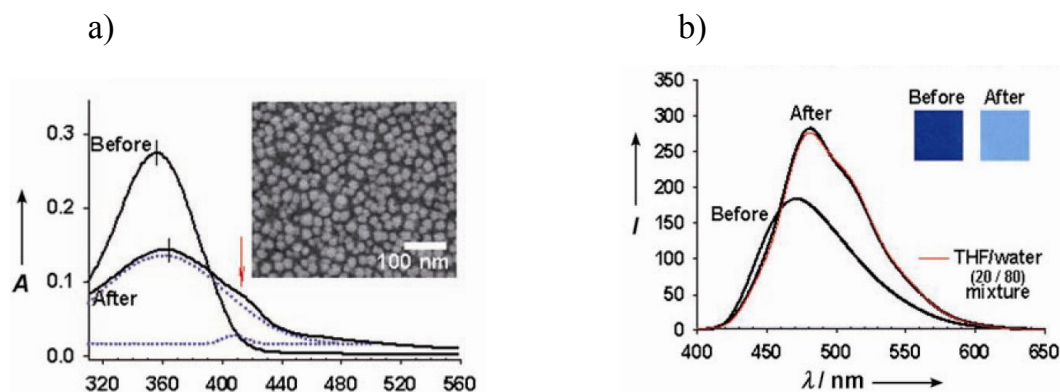
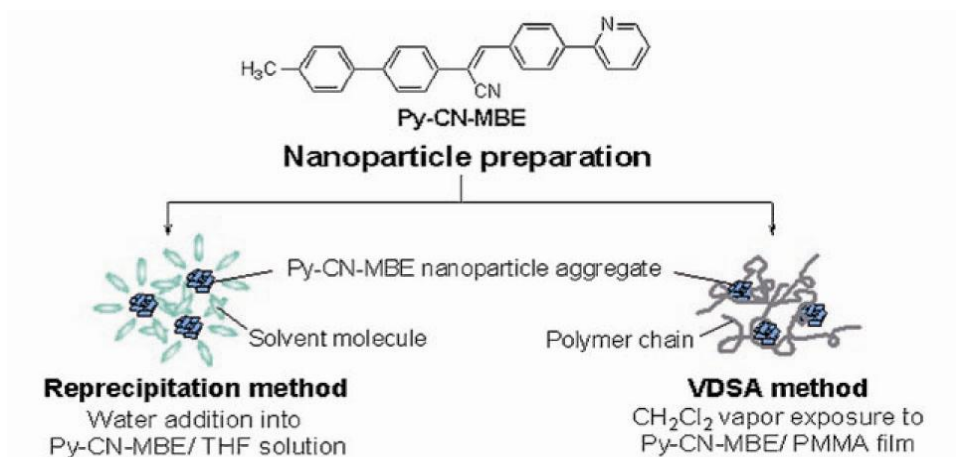
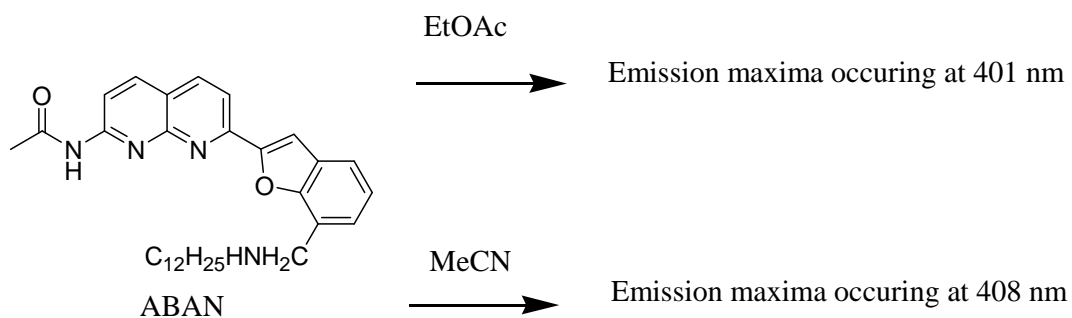


Figure-7 : a) UV/Vis absorption spectra of the Py-CN-MBE/PMMA film after nanoparticle formation. Blue dotted lines show the peak separation of Py-CN-MBE nanoparticles in the case of 80% water addition and exposure to dichloromethane vapor for 20 s. Insets: SEM images of the Py-CN-MBE colloidal nanoparticles obtained with the VDSA process. b) Photoluminescence (PL) spectra of the Py-CN-MBE/PMMA film after nanoparticle formation. Insets: the fluorescence emission changes of the Py-CN-MBE/PMMA film after nanoparticle formation under illumination by UV light at 365 nm.



Scheme-3 : Preparation of nanoparticles of 1-cyano-trans-1-(4'-methylbiphenyl)-2-[4'-(2'-pyridyl)phenyl]ethylen(Py-CN-MBE).

Yeh-Yang Sun and coworkers[25] fabricated nanoparticles of ethynyl-linked benzofuran-naphthyridine compounds (ABAN) by reprecipitation method [13,24,26] and observed that the emission spectra of the benzofuran-naphthyridine linked molecules were solvent sensitive. The fluorescence of ABAN displayed red shifts as the polarity of aprotic solvents increased, e.g., the emission maxima occurring at 401 and 408 nm in EtOAc and MeCN, respectively. That means as the polarity of the solvent increased, the fluorescence peak underwent a bathochromic shift.



Scheme-4 : The emission maxima of ABAN in various solvent.

They also investigated the photophysical properties of the benzofuran-naphyridine linked molecules in H₂O-THF solutions and showed that the fluorescence intensity increased remarkably in H₂O-THF solutions with appropriate fractions of water and determined the morphology of nanoparticles by scanning electron microscopy (SEM).

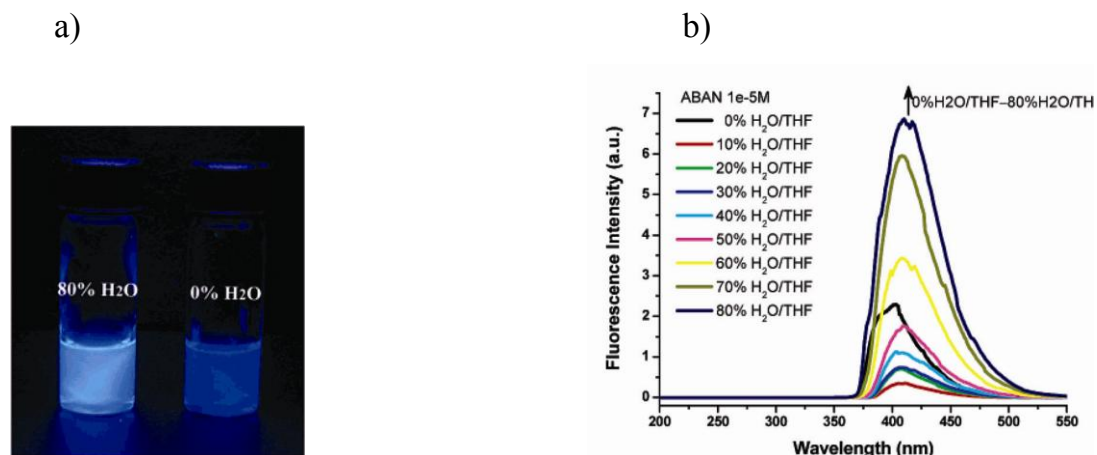


Figure-8 : Fluorescence properties of compound (ABAN) in H₂O-THF solution. (a) Enhanced fluorescence of compound (ABAN) in H₂O-THF solution (v/v, 4:1) with excitation at 378 nm. (b) Emission spectra of ABAN in H₂O-THF solution (1×10^{-5} M).

Ai-Dong's group[27] fabricated nanoparticles of 1,3,5-triphenyl-2-pyrazoline (TPP) doped with 4-(dicyanomethylene)-2-methyl-6-(p-dimethyl-aminostyryl)-4H-pyran (DCM) by simple reprecipitation method[12] and investigated that the fluorescence emission from the nanoparticles can be tuned by changing the content of DCM and confirm the size of those nanoparticles are spherical with a mean size of about 30-40 nm by field emission scanning electron microscopy (FESEM) and transmission electron microscopy (TEM).

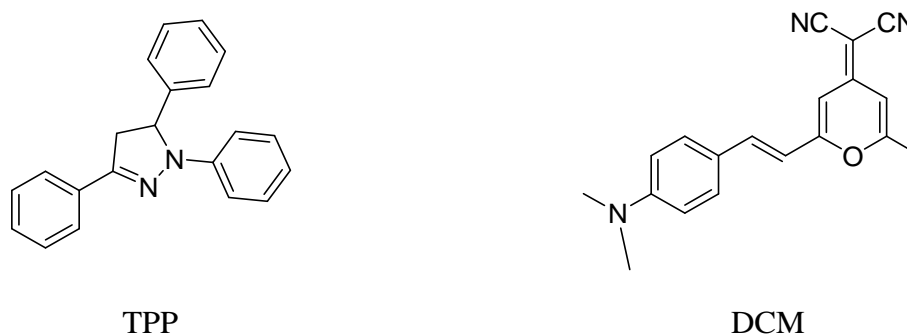


Figure-9 : Schematic structures of TPP (left) and DCM (right) molecules.

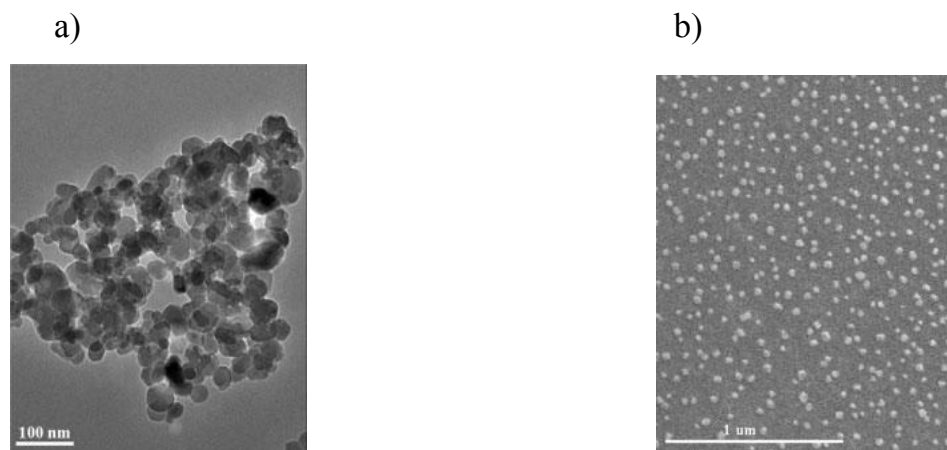
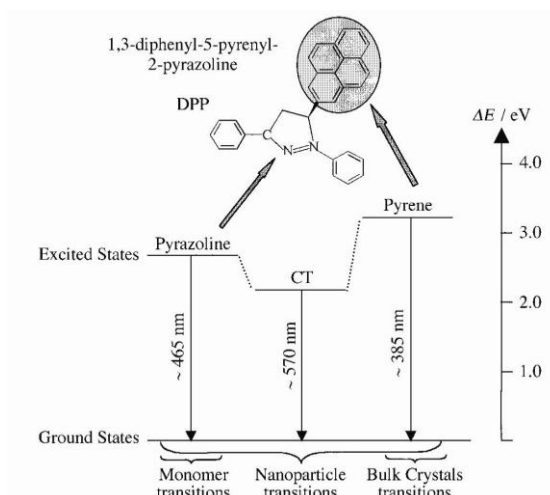


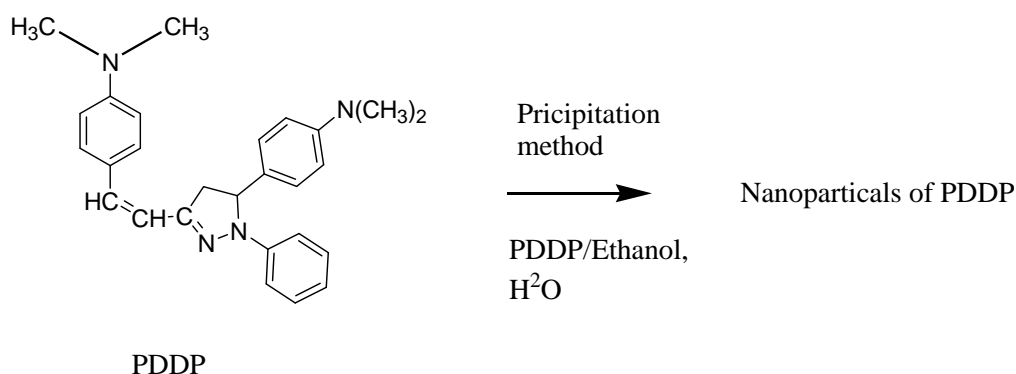
Figure -10 : a)TEM & b)FESEM images of DCM-doped TPP NPs.

Hongbing Fu, B. H. Loo and coworkers[28] synthesized 1,3-diphenyl-5-pyrenyl-2-pyrazoline (DPP) nanoparticles by reprecipitation method and they found that DPP nanoparticles exhibit multiple emissions from both pyrene and pyrazoline groups and from a CT (charge transfer) complex between pyrene and pyrazoline. Where they molecularly disperse the solution of DPP in a water miscible solvent, acetonitrile and mixed vigorously with an aqueous phase. Mixing the solvent and water phases change the character of the solvent and induced the nucleation and growth of DPP nanoparticles.



Scheme-5 : The emission transitions for DPP in monomers, nanoparticles, and bulk crystals.

Nanoparticles of 1-phenyl-3-((dimethylamino)styryl)-5-((dimethylamino)phenyl)-2-pyrazoline (PDDP) ranging from tens to hundreds of nanometers were fabricated by using the reprecipitation method by Hong-Bing Fu and Jian-Nian Yao[26b]. They were injected quantities of PDDP/ethanol solution($1 \times 10^{-3} \text{ molL}^{-1}$) into $10 \mu\text{L}$ of water.



Scheme-6 : Nanoparticles formation of PDDP.

They observed that their absorption and emission depended on particle size. As the nanoparticle size increases from 20 to 310 nm the absorption and fluorescence observed to shift to longer wavelength.

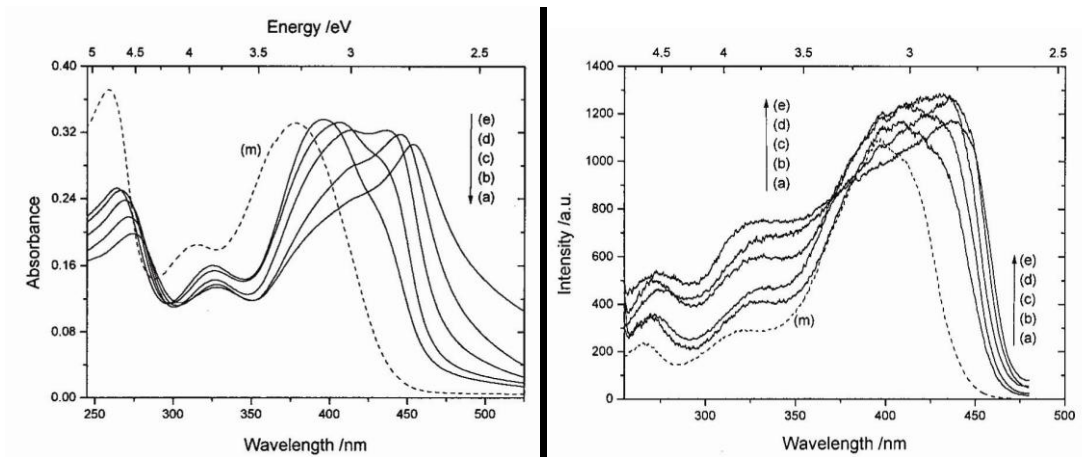


Figure-11 : UV-visible absorption spectra and fluorescence emission spectra of PDDP nanoparticles dispersions in water with different sizes: (a) 20 nm, (b) 50 nm, (c) 105 nm (d)190 nm and (e) 310 nm. (m) The spectrum of the PDDP/ ethanol solution ($1.0 \times 10^{-5} \text{ molL}^{-1}$).

They also confirm the size of nanoparticles by FESEM.

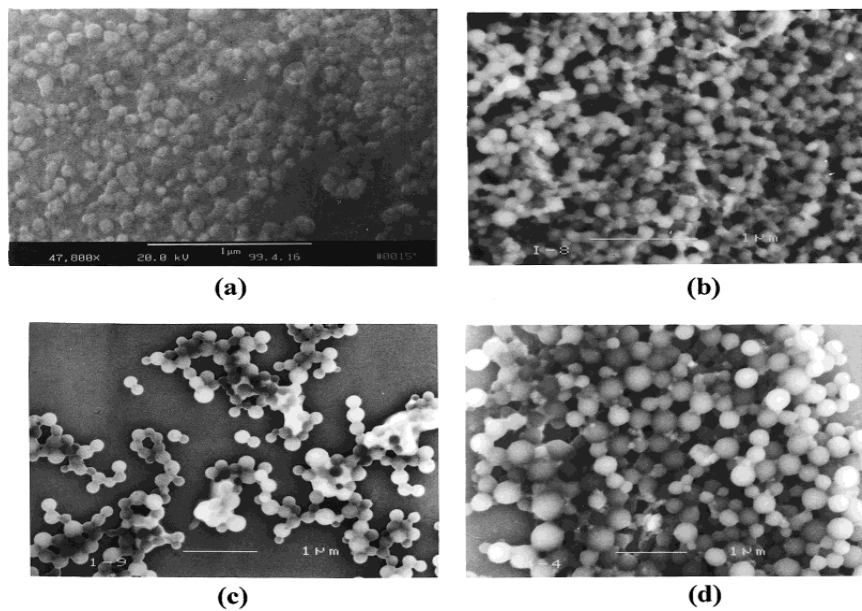
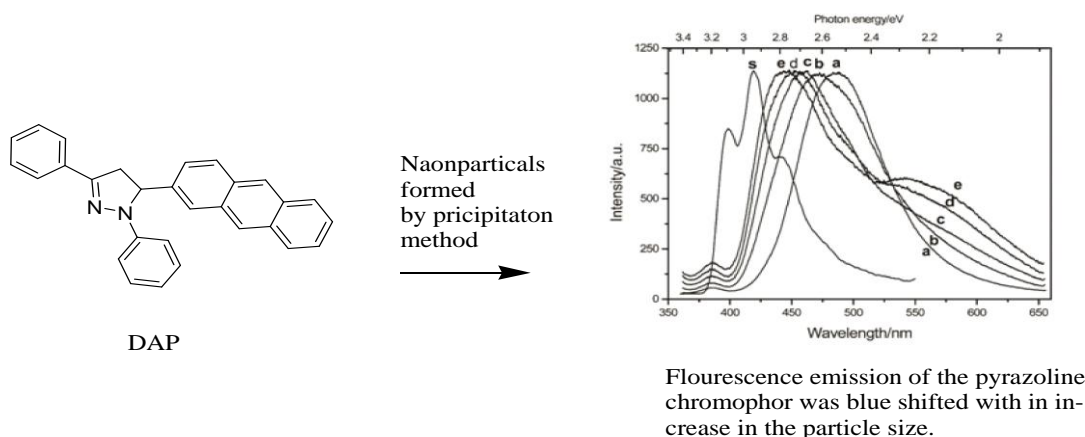


Figure-12 : FESEM photographs of PDDP nanoparticles: (a) 50 nm, (b) 105 nm, (c) 190 nm, and (d) 310 nm.

Debao Xiao, Lu Xi and their group[29] prepared organic nanoparticles of 1,3-diphenyl-5-(2-anthryl)-2-pyrazoline (DAP) ranging in average diameters from 40 to 160 nm through the reprecipitation method. The average diameters of the particles were controlled by variation of the aging time. They found that DAP nanoparticles exhibit the size-dependent optical properties, which demonstrated that the nanoparticle emission in the blue light region from pyrazoline chromophore shifts to shorter wavelengths with increasing particle size.



Scheme-7 : Fluorescence emission spectra of DAP nanoparticle dispersions with different sizes and DAP solution in acetonitrile. Line s, the spectrum of DAP solution; a, 40 nm; b, 60 nm; c, 90 nm; d, 120 nm; e, 160 nm. The excitation wavelength is at 350 nm.

Nanoparticle dispersion of 1-(4-chlorobenzoyl)-3-(5-(pyrid-4-yl)-1,3,4-thiadiazol-2-yl)thiourea was prepared by a simple reprecipitation method by Al-Kaysi group[30].

Longtian Kang and coworkers[31] fabricated organic core/diffuse-shell nanorods of 1,5-diphenyl-3-(naphthalene-4-yl)-1H-pyrazoline (DPNP) and 2,5-bis(2-(N-hexadecylpyridinium-4-yl)-vinyl)pyrrole iodide by two steps: (i) the preparation of uniform DPNP nanorods by a simple reprecipitation method; (ii) the adsorption of dye on the surface of DPNP nanorods through hydrophobic interactions, which presents fluorescence resonance energy transfer from the core to shell components and they observed that the nanorods of DPNP have an average width of 200 nm by SEM.

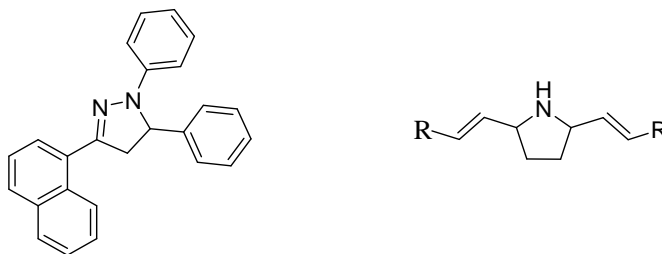


Figure-13 : Structures of DPNP (left) and Dye (right).

Similarly, Yao and co-workers[31] have successfully fabricated organic core/diffuse shell 1,5-diphenyl-3-(naphthalene-4-yl)-1H-pyrazoline (DPNP) nanorods by reprecipitation.

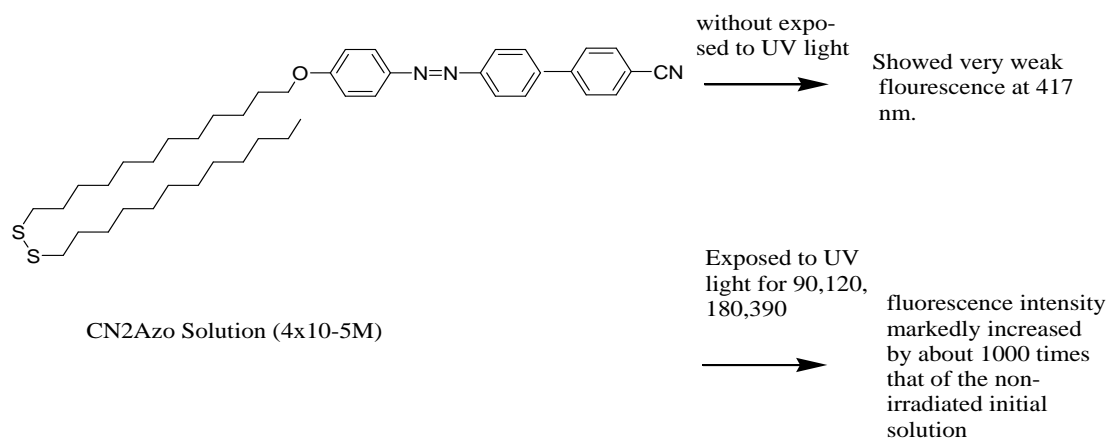
Among them molecular self-assembly is another strategy for nanofabrication that involves designing molecules and supramolecular entities[32]. The assembly of organic molecules to nanostructures needs the driving forces from the molecules themselves and sometimes initiation from the surroundings.

For example, Shelnutt and coworkers prepared porphyrin nanotubes by ionic self-assembly of two oppositely charged porphyrins in aqueous solution and investigated the photocatalytic behavior of the nanotubes[33].

With a similar method of self-assembly, Zhang and coworkers also prepared tubular structures of an intramolecular charge-transfer compound;[34] Wang and coworkers obtained luminescent nanowires from several quinacridone derivatives; [35] while Zang and coworkers prepared nanofibers and nanobelts from several kinds of small conjugated molecules[36-38].

Mina Han and Masahiko Hara[39] prepared highly fluorescent self-assembled spherical aggregates of an azobenzene derivatives [12-{4-(4c-cyanobiphenylazo)phenoxy}dodecyl] dodecyl disulfide (CN2Azo), consisting of a photoisomerizable azobenzene core coupled directly to biphenyl fluorophore as a head segment and a long alkyl chain as a tail seg-

ment and describe the highly fluorescent self-assembled spherical aggregates of azobenzene molecules without a specific ionic component under UV light illumination, even though azobenzene itself is negligibly fluorescent in nonirradiated initial solution.



Scheme-8 : Upon irradiation with UV light, change in emission intensities of CN2Azo.

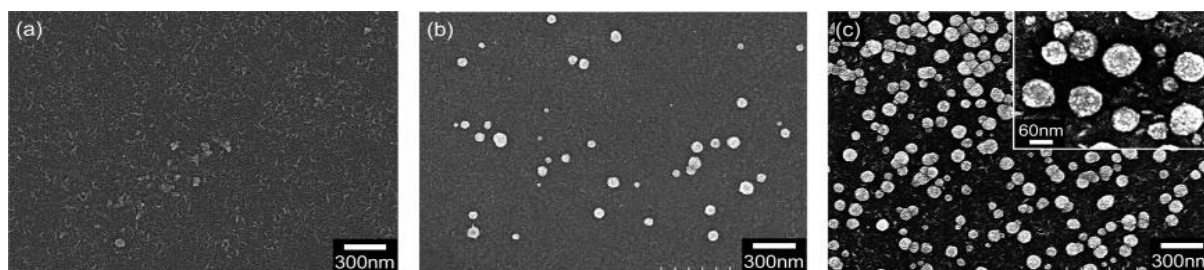


Figure-14 : SEM images of CN2Azo ($4 \times 10^{-5} \text{M}$) after exposure to UV light (a) for 120 min, (b) 180 min, and (c) for 390 min. (Inset) magnified SEM images.

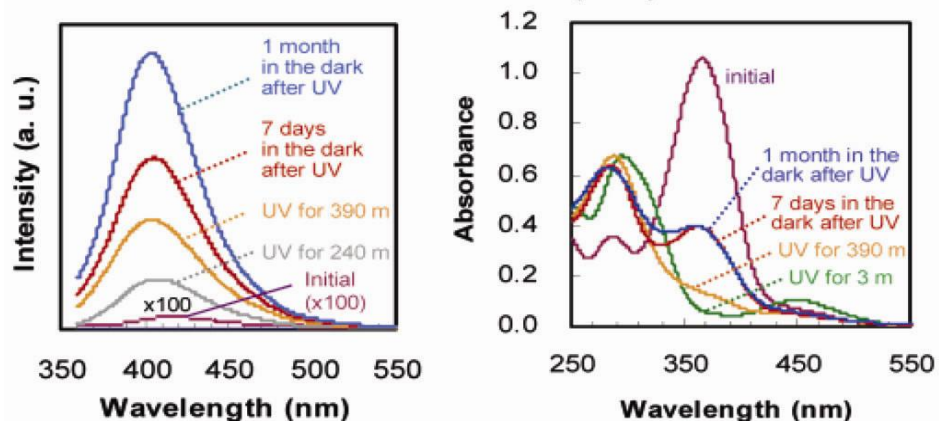
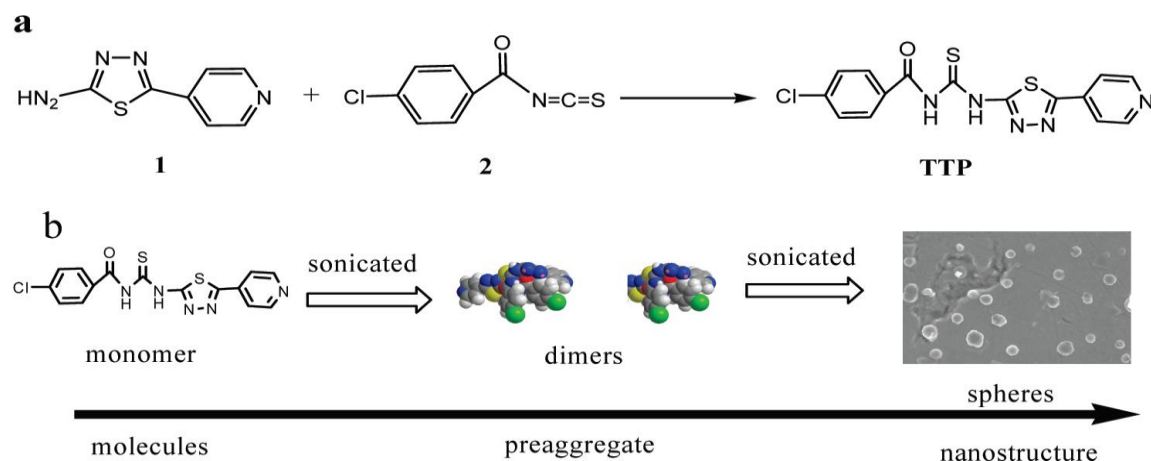


Figure-15 : (a) Emission spectra of CN2Azo (4×10^{-5} M) in dichloromethane at ambient temperature (325 nm excitation). (b) Changes in UV-vis absorption spectra of CN2Azo (4×10^{-5} M) in dichloromethane.

Takazawa and coworkers induced the selfassembly of 3-ethyl-2-[(3-ethyl-2(3H)-benzothiazolydene)-methyl]benzothiazolium iodide to form wire structures by cooling the hot solutions, and then studied the optical waveguiding behavior of the wires[40,41]. Shimizu and coworkers fabricated nanotubes by the self-assembly of amphiphilic molecules in solutions[42].

Haibing Li and Huijuan Yan[43] found that 1-(4-chlorobenzoyl)-3-(5-(pyrid-4-yl)-1,3,4-thiadiazol-2-yl)thiourea (TTP) molecules readily self-assembled into colloidal nanoparticles as a result of reprecipitation when water was added as a nonsolvent to its solution in THF. They observed that the fluorescence intensity of TTP increased remarkably in H₂O/THF solutions with appropriate fractions of water and they determined the size and morphology of TTP nanomaterials by SEM.



Scheme-9 : (a) Synthesis of TTP and (b) Representation for the formation processes of nanoscale materials of TTP.

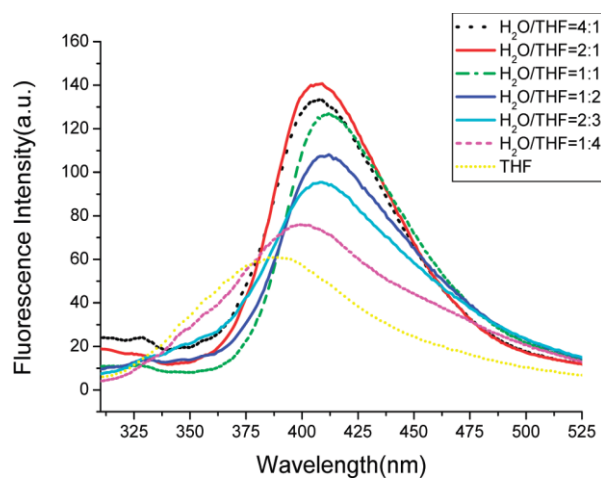


Figure -16 : Fluorescence spectra of the TTP in solutions with different ratios of H₂O/THF.

Debuigne and co-workers have reported the preparation of cholesterol, rhovanil, and rhodirome nanoparticles by microemulsions[44].

1.7. Application of FONs

Nanoparticles determine our life in the form of protein complexes and other cell components, as viruses, colloidal particles in drinking water, surface water and sea water, and as aerosols. They have been found to use as dispersion colors and as adhesives; in industry they play an important role in the formulation of pigments and in the production of catalysts. Numerous attempts are being made to deliver nanoparticulate forms of pharmaceutically active compounds specifically to the desired site of the action in the body. Finally nanoparticles find use as quantum dots with special properties for electronic components. Beyond these practical aspects there is scientific interest in nanoparticles owing to their special properties which lie between the properties of molecules and those of bulk material.

During the past few years organic nanomaterials have been increasingly studied because of their unique optical and optoelectronic properties as well as their potential applications in nanoscale devices[22,26b,45a,45b,46,47]. Hongbing Fu and coworkers synthesized 1,3-diphenyl-5-pyrenyl-2-pyrazoline (DPP) is used as a model compound, in the light emitting layer of an electroluminescent device, because of its strong, blue pyrazoline fluorescence[48].

Monodisperse polystyrene nanomaterials and microspheres[49,50] have been widely documented for the construction of photonic crystals.

Micro/nanostructured conductive polymers, such as polyaniline[51] and polypyrrole[52], attracted growing attention because of their good electrical conductivity, redox properties, environmental stability, and potential applications in sensors[53], biomedicine[54], actuators[55], etc.

Nanostructures based on semiconductor conjugated polymers, such as polyfluorene (PF), polythiophene (PT), polyphenylenevinylene (PPV) are attracting significant research interest, owing to their many novel optoelectronic properties and applications such as field effect transistors[56], optically pumped lasers[57], photodetectors [58], and electroluminescent diodes[59].

Fluorescent organic nanoparticles (FONs) have become the subject of ever-increasing attention in recent years, because of their large diversity in molecular structure and optical properties that are of potential use in optoelectronics and biologics[22,25,26b,26d,27,39,60,61,62,63]. Byeong-Kwan and co-workers[20] develop a new approach to the fabrication of photopatterned assemblies of FONs on the surfaces of solid substrates, which is based on the principles of vapor-driven self-assembly (VDSA) and patternwise photoacid generation to explore the collective properties of FONs as well as to realize practical device applications. This technology has the potential advantage to eliminate the difficulties of transferring preformed colloidal FONs onto fixed locations on substrates, thereby opening up a new approach to the realization of practical optoelectronic nanodevice applications of FONs.

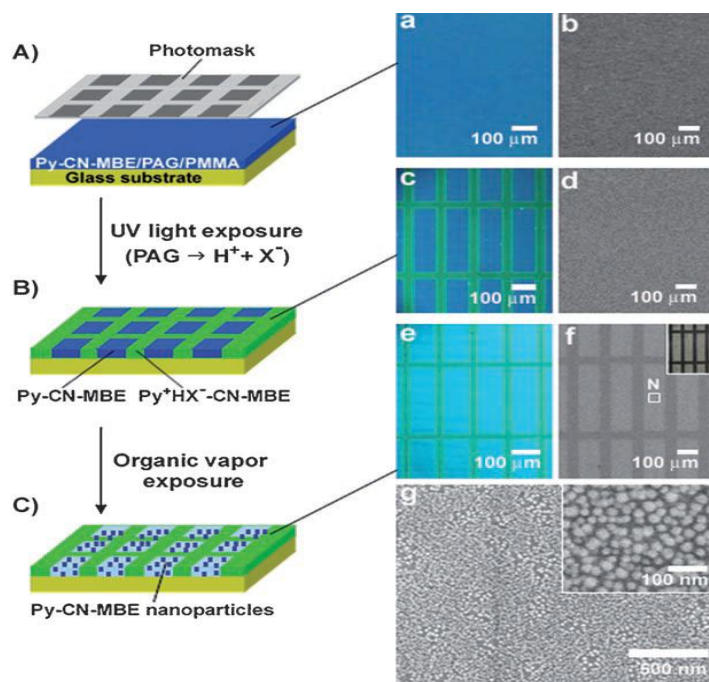


Figure-17 : Photopatterned array of Py-CN-MBE nanoparticles. A–C) Schematic diagram of the procedure for photopatterning Py-CN-MBE nanoparticles. a–g) Fluorescence emission and SEM images at each step. The inset photo in (f) shows a microscope image of the patterned array of Py-CN-MBE nanoparticles, obtained with a platinum- sputtering treatment.

Organic low-dimensional nanostructures used as nanoscale building blocks have attracted considerable research interest in the development of novel nanodevices[68].

Organic nanomaterials used as light-emitting candidates have attracted in the development of novel optoelectronic devices and full color flat panel displays due to their advantages such as high luminescence efficiencies[65]. Recently, a study has been reported on the changes in the emission spectra of organic nanoparticles[15,28,66]. For example, perylene nanoparticles were found to exhibit size-dependent emission[15] because of the reduction of the barrier from S-exciton to F-exciton states in the nanoparticles. In light of the fact that pyrazoline derivatives have been widely used as optical brightening agents for textiles and paper because of their strong

fluorescence[67,68] and as the hole-conducting medium in photoconductive materials[69,70] and electroluminescence (EL) devices, Debao Xiao and group has investigated the size-dependent optical properties of the nanoparticles from a series of pyrazoline compounds. The following scheme displays some field emission scanning electron microscope images of the as-prepared DAP nanoparticles, in which the average sizes were 60 nm (A) and 160 nm (B), respectively. These results confirm that the particles are unambiguously amorphous. Such an amorphous character of DAP nanoparticles should be profitable to the light-emitting efficiency because of the reduction in quenching from the internal conversion process which is dominant in the crystalline systems[65]

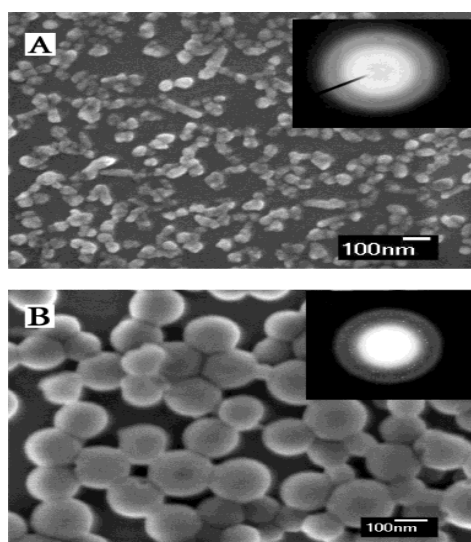


Figure-18 : Field emission SEM images of DAP nanoparticles with average diameters of (A) 60 nm and (B) 160 nm. The insets are electron diffraction patterns of the corresponding particles.

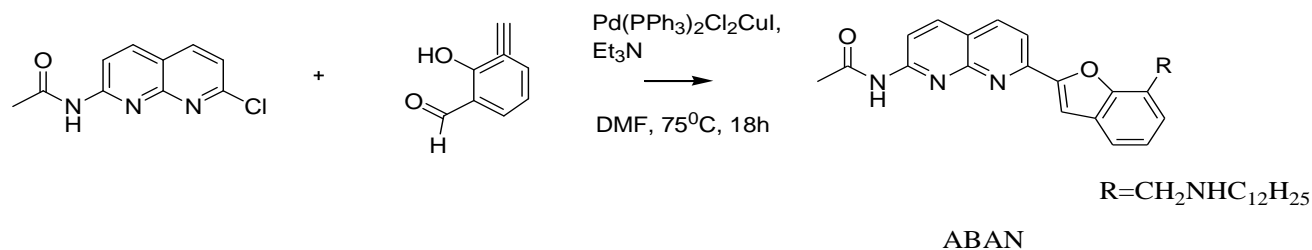
The development of fluorescent sensors with high selectivity and sensitivity for heavy and transition metal ions has always been of particular interest[71]. As mercury and its derivatives are widely used in industry and they have inherent high toxicity, the detection of Hg^{2+} is attracting particular attention[72,73]. Some fluorescent Hg^{2+} sensors have been explored[74], including polymers[75], foldamers[76], biomolecules[77-79], and small

molecules[80-82]. Nanoparticles of organic materials could have interesting applications in the pharmaceutical field because the microemulsions can be potential systems for drug delivery[83]. Nanospheres and nanocapsules are already used to entrap a drug or adsorb it[84-86]. Organic π -conjugated molecules play special and key roles in conductance, superconductance, magnetic, optical, and photo-electronic conversion, and luminescence[87].

Carotenoids nanoparticles is used as active compounds in pharmaceuticals and cosmetics or as coloring agents in the foodstuffs and animal feeds[88-91]. Monitoring pH in biological tissue or cells *via* fluorescence spectroscopy has become a widespread research area, including fluorescent nanoparticles with physically[92,93] or covalently entrapped dyes[94-97] and fiber-optics[98,99]. The nanosensors are based on materials such as polyacrylamide[92,94,97,99], silica[93], phospholipid-coated or amino-modified polystyrene[95,96] and methacrylate hydrogels[98].

Among the nanostructures formed by the self-assembly of specifically designed molecules, has proved to be particularly interesting for applications such as nanowires, gels, and biomimetic systems[100,51].

It has been shown that 2-acetamido-1,8-naphthyridine (AN) derivatives bind via triple hydrogen bondings with guanine (G)[101] preferably over other nitrogenous bases of adenine, cytosine, thymine, and uracil. This property of AN-G complexation has been demonstrated in supramolecular chemistry[113], HPLC separation[102], molecular sensing[103], and mapping of the guanine sequence in DNA[104]. For the development of molecular sensors having the core structure of naphthyridine[105], Yeh-Yang sun and their group intended to prepare 2-acetamido-7-(3-formyl-2-hydroxyphenyl) ethynyl-1,8-naphthyridine (compound **X**) via the Sonogashira coupling reaction⁵ of 2-acetamido-8-chloro-1,8-naphthyridine **1b** with 3-ethynyl-2-hydroxybenzaldehyde.



Scheme-10 : Synthesis of the Benzofuran-Naphthyridine Linked Compound ABAN.

Among a variety of nanostructured materials, nanoparticles have attracted much attention because of their wide-spread applications in biology[106], for example Au- or conjugated Au- nanoparticles are fabricated and applied for monitoring bioreactions[107] and recognition of biomolecules[108]. Other applications include detection of hazardous organic and radioactive materials[109], toxic cations and anions[110], and pH[111]. Due to their intrinsic localized surface plasmon (LSP) resonance, photophysical and electrochemical properties, metal nanoparticles are widely explored for the development of colorimetric[107, 109a, 109b, 109c, 110c, 111], fluorometric[108d, 108c, 110a, 110b, 110d] and electrochemical [108a, 113a] sensors. Up to now, nanoparticles that consist of metals e.g. Au and Au-conjugates[107-110], Ag[112], Pd[113], inorganic semiconductors[114], (e.g. PbS, ZnS, CdS, CuS, CdSe), metal oxides or metal oxide composites[115], and silica[116] have been widely reported. A few reports are available on nanoparticles of transition metal complexes[117], and coordination polymers[118], where the morphology of the nano- and microparticles of coordination polymers are generally controlled by employing different ligating solvents which block the growth of the particle in some direction[118a,118d,117c].

Rhenium-complexes are extensively studied because of their outstanding photophysical and electrochemical properties[119] and found a wide range of applications as functional materials such as in OLED[120], in opto-electronic polymers[121], and in biology for binding proteins[122], and DNA[123], for biological labeling[124], and as biological probe[125]. Rhenium complexes also demonstrated the ability to sense cations and anions[126], pH[127], oxygen[128] and selective molecular recognition[129].

Surprisingly, studies on the formation of micro- or nanoparticles based on rhenium complexes are lacking so far. Only our group has previously revealed that Re(I) metallacycles undergo aggregation induced emission enhancement[130], thus, an efficient methodology for the fabrication of micro- or nanoparticles and demonstration of their application for sensing purposes will add new tools for the materials scientists.

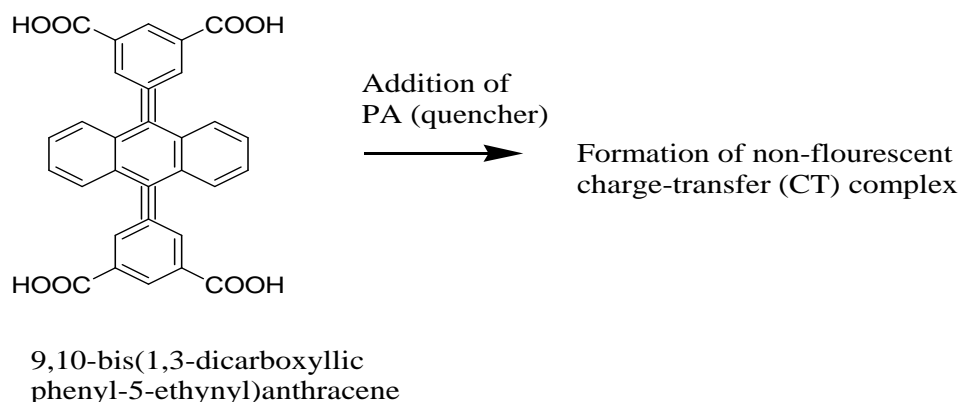
1.8. Nitroaromatic compounds and their detection

Nitroaromatic compounds (NAC) such as trinitrotoluene (TNT), dinitrotoluene (DNT), and picric acid (PA) are considered as environmental contaminants and toxic to living organisms[131-133]. They are well-known primary constituents of many unexploded land mines worldwide and used as dyes, pesticides and explosives and the factory sites that produce such chemicals are highly contaminated with these substances. Further, soil and groundwater of war zone and military facilities can contain toxic levels of these compounds and their degradation products. Polymers[134], siloles[135], metalloporphyrins[136] and aromatic compounds containing fused ring systems[137] are already reported to show efficient NACs sensing ability. Beside these various fluorescent chemosensors, fluorescent polymers, and nanoparticles have been developed for detection of nitroaromatics[8,138-151]. The concern over the adverse effects of nitroaromatics on environment and health provide the sufficient impetus to develop cost efficient, selective, portable, fast, and sensitive method for detection of nitroaromatics[152-154] Currently, a wide range of instrumental techniques are being employed to detect explosives such as TNT (2,4,6-trinitrotoluene), DNT (2,4-dinitrotoluene) and PA (picric acid), which are the primary constituents of many unexploded land mines worldwide[155]. Among these competing methods, fluorescence quenching based detection of explosives has grown enormously owing to its high sensitivity, easy visualization and real-time monitoring with fast response time[156]

A few reports on fluorescence quenching of Re(I) metallacycles by aromatic nitro compounds are reported[157,158]. Herein we report a simple one-step method to

synthesize tetrahemium metallacycles employing bis-benzimidazolylthiophene as a ditopic N-heterocyclic clip and 1,4-dihydroxy- and 1,2,4-trihydroxy-9,10-anthraquinones as bis-chelating bridging ligands. We also document a simple precipitation methods for the fabrication of micron-sized particles of the synthesized matallacycles and their ability to sense nitroaromatic compounds.

Bappaditya Gole and coworkers[159] synthesized a p-electron rich supramolecular polymer 9,10-bis(1,3-dicarboxylicphenyl-5-ethynyl)anthracene and their analogues which are used as chemosensor for detection of nitroaromatic explosives such as TNT and PA both insolutions aswell as in thin-film. They report that the incorporation of ethynyl groups enriches π -conjugation in 9,10-bis(1,3-dicarboxylicphenyl-5-ethynyl)anthracene and thereby they exhibit strong fluorescence emission and also observed that the emission intensity is reduced because of theformation of a non-fluorescent charge-transfer (CT) complex between the electron donor (fluorophore) and the electronacceptor (quencher).



Scheme-11 : Quenching of 9,10-bis(1,3-dicarboxylicphenyl-5-ethynyl)anthracene by Picric acid.

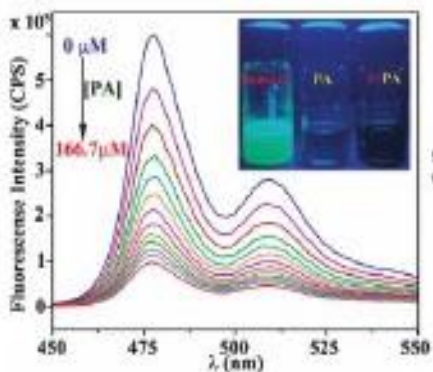


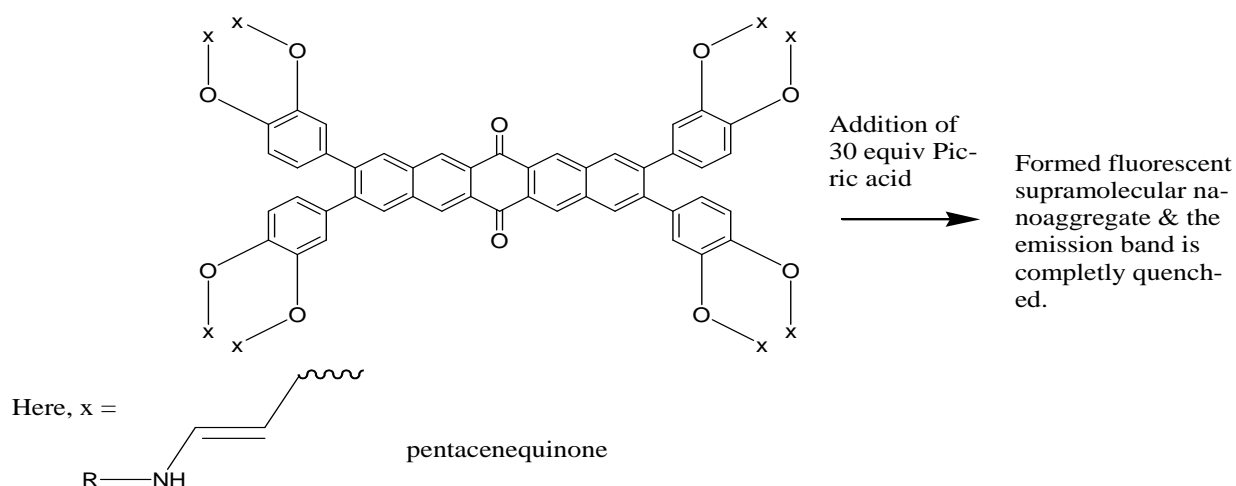
Figure-19 : Reduction in the emission intensity of compound 9,10-bis(1,3-dicarboxylicphenyl)-5-ethynylanthracene upon gradual addition of PA.

New triphenylene derivatives was synthesized by Vandana and coworkers[160] by using a Suzuki–Miyaura coupling protocol and by a click reaction respectively, serve as potent chemosensors for various electron deficient nitroaromatic explosives, such as picric acid, trinitrotoluene, dinitrotoluene and dinitrobenzene.

Pyrene-functionalized Ru nanoparticles were synthesized by Chen W and coworkers[161] by olefin metathesis reactions of carbene-stabilized Ru nanoparticles with 1-vinylpyrene and 1-allylpyrene (the resulting particles were denoted as Ru=VPy and Ru=APy, respectively) and they examined this sensitive chemosensors for the detection of nitroaromatic compounds, such as 2,4,6-trinitrotoluene (TNT), 2,4-dinitrotoluene (2,4-DNT), 2,6-dinitrotoluene (2,6-DNT), 1-chloro-nitrobenzene (CNB), and nitrobenzene (NB), by their effective quenching of the nanoparticle fluorescence. They was found that the detection sensitivity increased with increasing nitration of the molecules.

Recently, several fluorescent conjugated polymers[162] and fluorescent nanofibers obtained by molecular self-assembly have been reported as sensing materials for detection of nitroaromatic explosives[163-165] Vandana Bhalla and coworkers reported that pentacenequinone derivative forms fluorescent supramolecular nanoaggregates[11]

in aqueous media that selectively sense picric acid in solution phase[166]. They have chosen pentacenequinone moiety as the motif for preparation of luminescent supramolecular aggregates because of the tendency of 6,13-pentacenequinones to form ordered thin films which make them good candidates for preparation of organic electronic devices[167-169]. They carried out fluorescence studies of compound pentacenequinone with picric acid. The following scheme shows that Upon addition of 30 equiv of picric acid, the emission band of pentacenequinone (1.0×10^{-5} M) at 515 nm in toluene/DCM (8:2) is completely quenched.



Scheme-12 : fluorescence studies of compound pentacenequinone with picric acid.

Aniruddha Kundu and coworkers[170] reported on their paper that there is a drastic decrease in PL intensity on addition of nitroaromatics to the GMCO (graphene oxide–methyl cellulose hybrid) system and it is very large (91%) for the addition of picric acid. Thus, the hybrid system acts as a good sensor for the detection of nitro aromatics by instantaneous photoluminescence quenching with a detectable limit of 2 ppm.

Fang Q and coworkers[171] report that an inverted opal fluorescence chemosensor for the ultrasensitive detection of explosive nitroaromatic vapors through resonance-energy-transfer-amplified fluorescence quenching. They fabricated the inverted opal silica film

with amino ligands by the acid-base interaction between 3-aminopropyltriethoxysilane and surface sulfonic groups on polystyrene microsphere templates. Then they chemically anchored the fluorescent dye onto the interconnected porous surface to form a hybrid monolayer of amino ligands and dye molecules and observed that amino ligands can efficiently capture vapor molecules of nitroaromatics such as 2,4,6-trinitrotoluene (TNT) through the charge-transfer complexing interaction between electron-rich amino ligands and electron-deficient aromatic rings.

A sensitive electrochemical sensor has been fabricated by Zang J. and coworkers[172] to detect ultratrace nitroaromatic explosives using ordered mesoporous carbon (OMC) and they reported that as low as 0.2 ppb TNT, 1 ppb 2,4-dinitrotoluene and 1 ppb 1,3-dinitrobenzene can be detected on OMC based electrodes.

Content S and coworkers[173] detect nitroaromatic molecules in air by the quenching of the photoluminescence of porous silicon (porous Si) films. They achieved the detection by monitoring the photoluminescence (PL) of a nanocrystalline porous Si film on exposure to the analyte of interest in a flowing air stream. They quenched the photoluminescence on exposure to the nitroaromatic, presumably by an electron-transfer mechanism and observed detection limits of 500 parts-per-billion (ppb), 2 ppb, and 1 ppb for nitrobenzene, 2,4-dinitrotoluene (DNT), and 2,4,6-trinitrotoluene (TNT), respectively (exposure times of 5 min for each, in air).

1.9. Benzimidazole

Benzimidazole is a bicyclic aromatic compound involves the fusion of a fundamental structural characteristic of six-member benzene fused to five member imidazole.

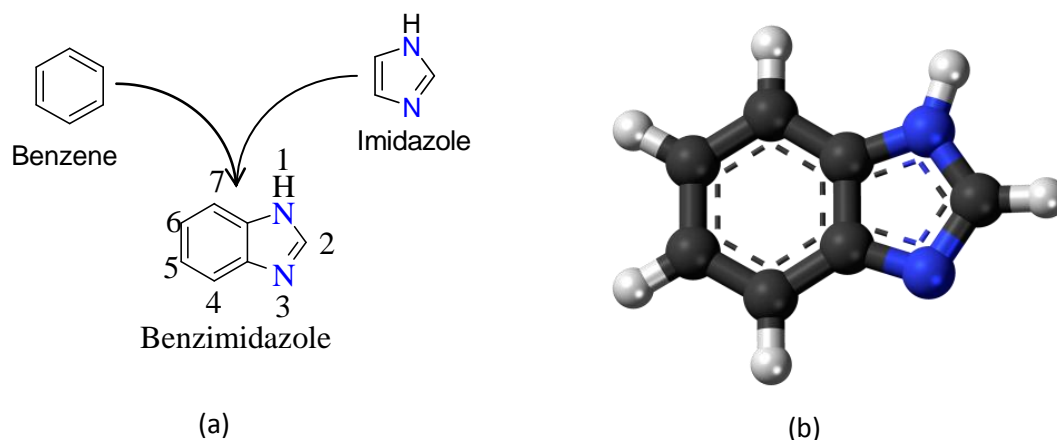


Figure-20 : The Benzimidazole skeleton is the fusion of benzene and imidazole (a), 3D structure of Benzimidazole (b).

This basic ‘6+5’ heterocyclic structure is shared by another class of chemical compounds, the purines. Among the members of this group are several very well-known and important biomolecules, such as adenine and guanine, two of the four nucleic acid bases, uric acid, and caffeine[9].

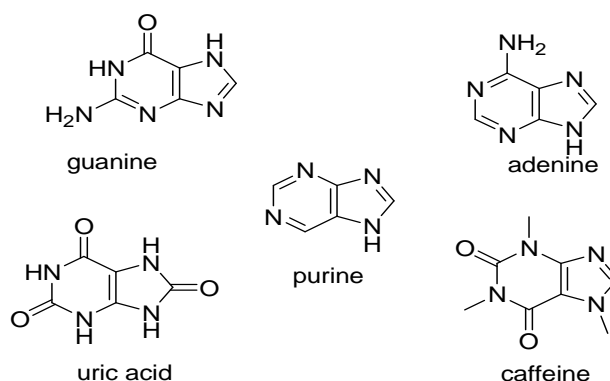


Figure-21 : Purines, which include some of the most well-known biomolecules, share the ‘6+5’ heterocyclic structure with benzimidazoles.

From this fundamental structural similarity, it is not too surprising that benzimidazole containing molecules and benzimidazole derivatives have been found to be biologically active small molecules, such as vitamin B₁₂ and a variety of antimicrobial, antiparasitic, and even antitumor agents[9,10].

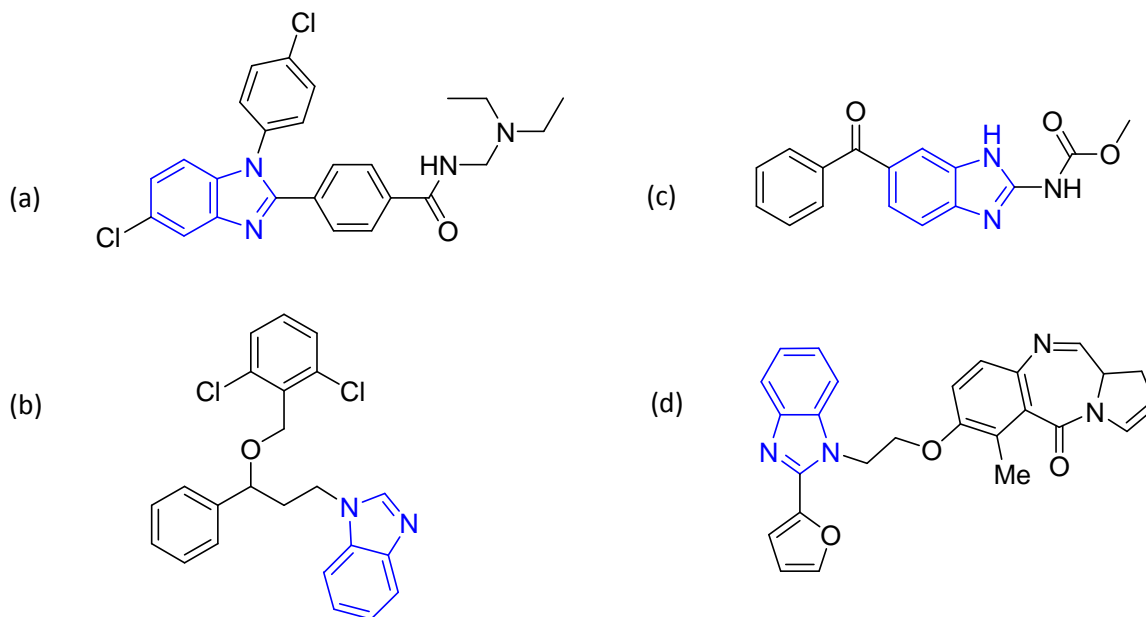
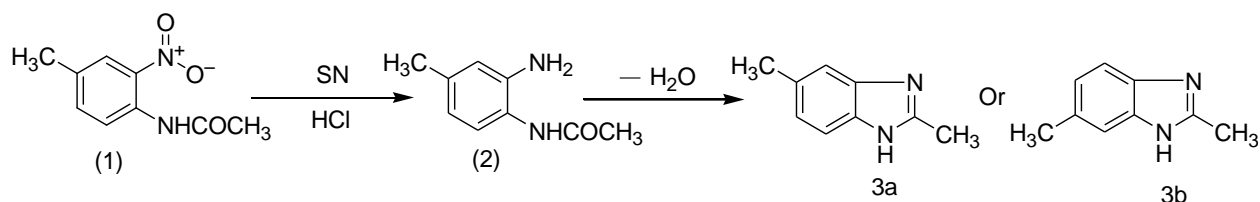


Figure-22 : Examples of antimicrobial (a, b), antiparasitic (c), and antitumor agents (d) containing the Benzimidazole moiety (colored blue).

Aside from their place in biomedical research, benzimidazoles also have a prominent place in organocatalysis, organometallic[174], and materials chemistry[175] for two reasons stemming from their molecular architecture: the imidazole is a precursor to N-heterocyclic carbenes; and the benzene ring provides a convenient scaffold to which additional functionality may be easily added to modify the spatial and electronic characteristics of a benzimidazole derivative.

1.9.1. Synthesis of benzimidazole

The benzimidazole nucleus does not appear to occur very widespread in nature. Historically, the first benzimidazole was prepared in 1872 by Hoebrecker, who obtained 2,5 (or 2,6) di-methyl-benzimidazole (3) by the reduction of 2-nitro-4-methyl-acetanilide (1). Several years later Ladenburg obtained the same compound by refluxing 3, 4-diaminotoluene with acetic acid[176].

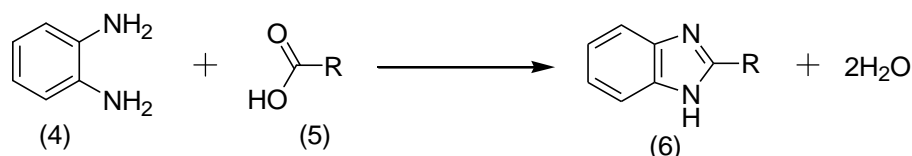


Scheme-13 : Synthesis reaction of first synthesized benzimidazole.

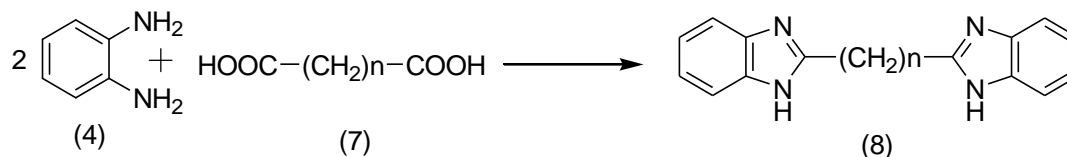
A number of methods developed for the synthesis of benzimidazole derivatives, which include conversion of esters using an aluminum reagent, the reaction between N-ethoxycarbonylthioamides with 1,2-diamines, the reaction of an appropriate 1,2-phenylenediamine with carboxylic acid and its derivative, nitriles, or orthoesters in the presence of a strong acid at elevated temperature. Recently, several methods had introduced, where aldehydes, acid chloride, o-dinitrobenzene, Gold's reagent, and 2-nitroanilines are used as starting materials for this synthesis. Brain and coworker developed a new procedure for the preparation of these compounds by palladium-catalyzed aryl-amination chemistry. Although these methods are suitable for certain synthetic conditions, sometimes, there exist some drawbacks such as long reaction time, high temperature, low yields of products in some cases, use of an additional microwave oven, corrosive reagents and large amounts of solid supports which would eventually result in the generation of a large amount of toxic waste. Moreover more than one step is involved in the synthesis of these compounds in some procedures.

Some common synthetic procedures for benzimidazoles [176].**A. From by Reaction o-phenylenediamine with Carboxylic Acids****a. Monobasic Acids**

O-phenylenediamines reacts readily with most carboxylic acids to give 2-substituted benzimidazoles, usually in very good yield. The reaction is carried out usually by heating the reactants together on a steam bath, by heating together under reflux or at an elevated temperature or by heating in a sealed tube.

**Scheme-14:** Synthesis reaction of benzimidazole from monobasic acids.**b. Dibasic Acids**

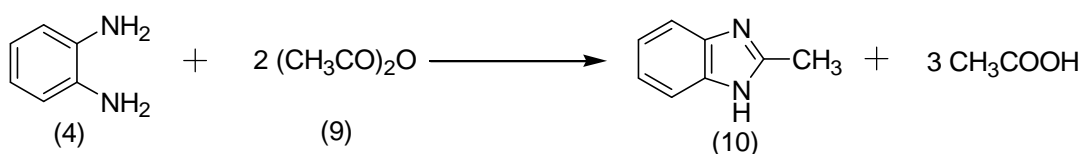
When dibasic acids react with o-phenylenediamine the products formed depend on the mole ratio of the reactants and the experimental conditions. Two or more moles of the o-phenylenediamines are heated with one mole of the dibasic acid to give bisbenzimidazole as the product.

**Scheme-15:** Synthesis reaction of Benzimidazole from dibasic acid.

B. By Reaction with acid Anhydrides

a. Anhydrides of Monobasic Acids

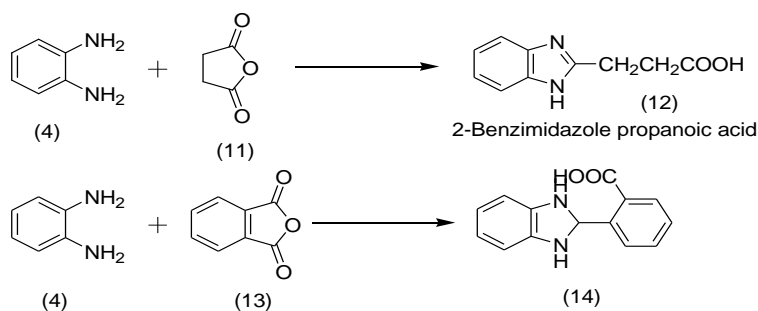
The reaction of acid anhydrides and o-phenylenediamine will lead to benzimidazoles or to N, N'-diacylphenylenediamines depending on the conditions employed. It was formerly thought that o-phenylenediamine yield benzimidazoles with acids and diacyl derivatives with acid anhydrides; however, this was shown to be incorrect. Time appears to be a decisive factor and if the refluxing is continued long enough benzimidazoles may be obtained, usually in good yield. O-phenylenediamines when heated under reflux for several hours with acetic anhydride is completely converted to 2-methylbenzimidazole.



Scheme-16 : Synthesis reaction of benzimidazole from anhydrides of monobasic acid.

b. Anhydrides of Dibasic Acids

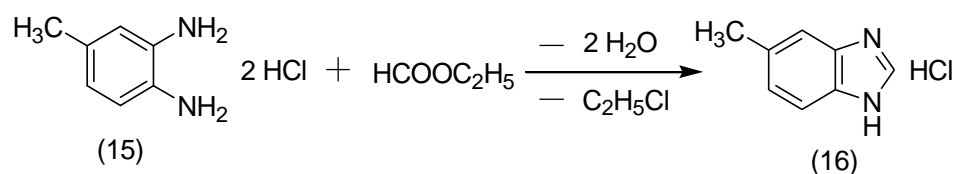
The anhydrides of dibasic acids react as monobasic acids; for example, succinic anhydride with o-phenylenediamines gives β -(2-benzimidazole) propionic acid (12) & phthalic anhydride gives o-(2-benzimidazole) benzoic acid (14). In several cases amides or phthalanils have been obtained as byproducts[10].



Scheme-17 : Synthesis reaction of benzimidazole derivatives from the anhydrides of dibasic acids.

C. By Reaction with Esters

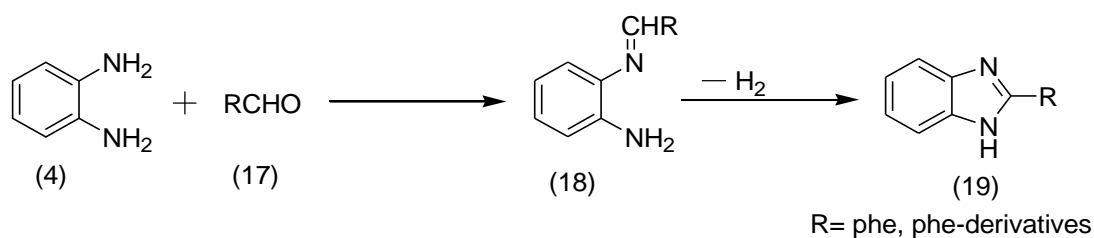
Reaction of o-phenylenediamine with esters also yields benzimidazoles. Von Niementowski first investigated the reaction of esters and o-phenylenediamine to give benzimidazoles. Equimolecular amounts of 3, 4-diaminotoluene dihydrochloride and ethyl formate when heated in a sealed tube for 3 hr. at 225°C give 84 per cent of 5(or 6)-methylbenzimidazole hydrochloride.



Scheme-18 : Synthesis reaction of benzimidazole derivatives by the esters.

D. By Reaction with Aldehydes

Under the correct conditions aldehydes may react with o-phenylenediamines to yield 2-substituted benzimidazoles.



Scheme-19 : Synthesis of Benzimidazole derivatives by aldehydes.

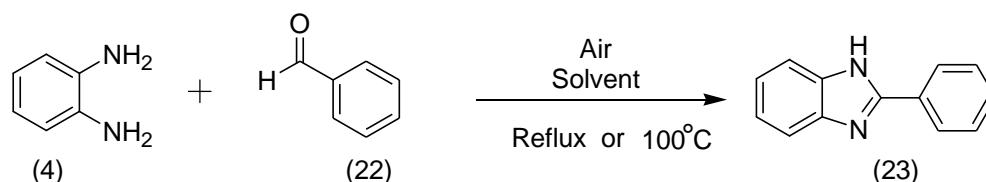
Since an oxidation is involved, the reaction is best carried out under oxidative conditions. This oxidation may be brought about by the air or, more conveniently, by the use of other oxidizing agents such as cupric acetate. This latter reagent was first introduced by Weidenhagen.

E. Synthesis of 2-Substituted Benzimidazoles

The widespread interest in benzimidazole-containing structures has prompted extensive studies for their synthesis of 2-substituted benzimidazoles. One is the coupling of phenylenediamines and carboxylic acids or their derivatives (nitriles, imidates, or ortho-esters), which often requires strong acidic conditions, and sometimes combines with very high temperatures (i.e., PPA, 180°C) or the use of microwave irradiation[177]. The other way involves a two step procedure that includes the oxidative cyclo-dehydrogenation of aniline Schiff's bases, which are often generated in situ from the condensation of phenylenediamines and aldehydes.

(1) Direct One-Step Air Oxidation Procedure[178]

In this method, various benzimidazoles are synthesized from phenylenediamines and aldehyde using air as the oxidant. The reaction scheme involves:

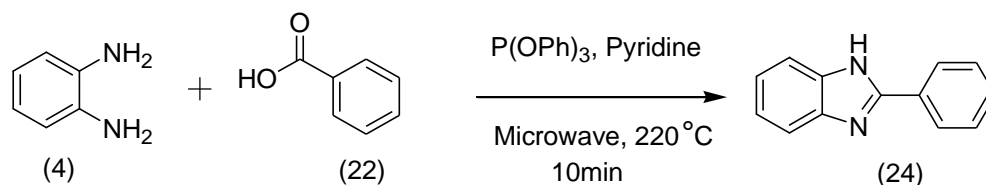


Scheme-20 : Synthesis reaction of 2-substituted benzimidazole derivatives.

The salient features of this method include a simple procedure, mild conditions, no coupling agents or commercial oxidants/additives used, no waste produced (only by-product being water), easy purification, and high generality.

(2) Microwave Assisted One Step High Throughput Synthesis Process[179]

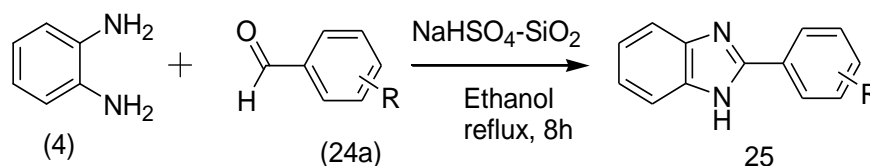
In this process, various benzimidazoles are synthesized from diamines and carboxylic acids under microwave irradiation condition. The reaction scheme involves:



Scheme-21 : Synthesis reaction of benzimidazole derivatives through microwave-assisted process.

(3) $NaHSO_4$ - SiO_2 Promoted Synthesis Process[180]

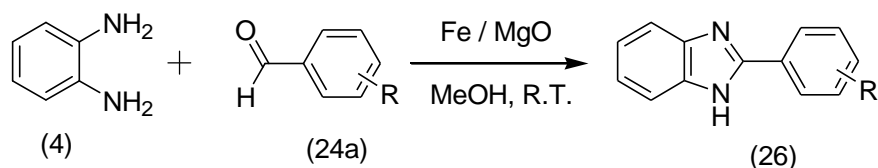
A library of benzimidazole derivatives have been prepared through the reaction of o-phenylenediamine and aldehydes in the presence of catalytic amount of silica supported sodium hydrogen sulphate ($NaHSO_4$ - SiO_2) under refluxing in ethanol solvent to obtained excellent yields. This method is simple, convenient, environmental friendly, reusable, efficient and practical.



Scheme-22: Synthesis reaction of $NaHSO_4$ - SiO_2 Promoted Synthesis of benzimidazole derivatives.

(4) Cyclization–Oxidation processes[181]

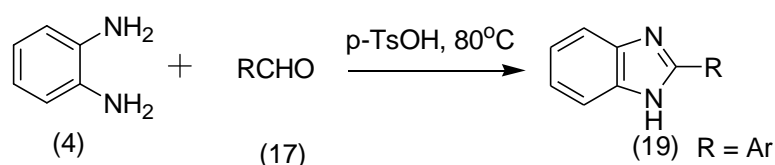
A convenient and straight forward method has been developed for the synthesis of benzimidazole using aryl aldehydes and o-phenylene diamine in the presence of Fe containing Magnesium oxide (Fe/MgO), at room temperature. The salient feature of this method includes mild condition, short reaction time, high yield, easy purification, recyclable catalyst, large scale synthesis and simple procedure. The catalyst can be reused for several cycles without decrease in activity.



Scheme-23 : Synthesis reaction of benzimidazole derivatives through cyclization-oxidation.

(5) p-TsOH Catalyzed Synthesis Process[182]

p-TsOH (20 mol%) was used to be a catalyst for the synthesis of 2-arylsubstituted benzimidazoles efficiently. Simple and convenient procedure, easy purification and shorter reaction time are the advantageous features of this method.



Scheme-24 : Synthesis reaction of benzimidazole derivatives through p-TsOH Catalyzed process.

1.9.2. Characteristics Shown by benzimidazole Derivatives

1.9.2.1. Biological Properties of benzimidazole

Benzimidazoles are remarkably effective compounds both with respect to their inhibitory activity and their favorable selectivity ratio. Extensive biochemical and pharmacological studies have confirmed that benzimidazole molecules are effective against various strains of microorganisms. Benzimidazoles are regarded as a promising class of bioactive heterocyclic compounds that exhibit a range of biological activities. Specifically, this nucleus is a constituent of vitamin-B₁₂. This ring system is present in numerous antiprotozoal[183], antihelmintics[184], anti-HIV[185], anticonvulsant[186], anti-inflammatory[187], antihepatic[188], antineoplastic[189] and antiulcer[190] activities. Now-a-days Infectious microbial diseases are causing problems world-wide, because of

resistance to number of antimicrobial agents (β -lactam antibiotics, macrolides, quinolones, and vancomycin). A variety of clinically significant species of microorganisms has become health problem globally [191]. In particular, increasing drug resistance among Gram-positive bacteria such as *staphylococci*, *enterococci* and *streptococci* is a significant for health. One way to fight with this challenge is the appropriate usage of the available marketed antibiotics the other is the development of novel antimicrobial agents[192]. Hence, there will always be a vital need to discover new chemotherapeutic agents to overcome the emergence of resistance and ideally shorten the duration of therapy. Due to the structural similarity to purine, antibacterial ability of benzimidazoles are explained by their competition with purines resulting in inhibition of the synthesis of bacterial nucleic acids and proteins[193,194].

1.9.2.2. Photophysical Properties of benzimidazole Derivatives

Benzimidazole has been used as carbon skeletons for N-heterocyclic carbenes (NHCs), which is an extension of the well elaborated imidazole system. The NHCs are usually used as ligands for transition metal complexes. They are often prepared by deprotonating an N, N'-disubstituted benzimidazolium salt at the 2-position with a base[195,196]. The luminescence properties of benzimidazole have been extensively studied[197-200], but little work have been reported on substituted species. Thiabendazole and its major metabolite, 5-hydroxythiabendazole shows luminescence properties[201].

1.9.3. Application of benzimidazole & Its Derivatives

Benzimidazoles are the important among the heterocyclic compounds found in several natural and non-natural products such as Vitamin B₁₂[202], marine alkaloid kealiquinone[203], benzimidazole nucleosides[204] etc. Some of their derivatives are marketed as anti-fungal agents such as Carbendazim[205], anti-helminthic agents such as Mebendazole and thiabendazole[206] and anti-psychotic drug such as Pimozide[207] and other derivatives have been found to possess some interesting bioactivities such as anti-tubercular[208], anti-cancer[209] etc. Besides these applications benzimidazole

derivatives also used in the treatment of HBV infection, in suppressing the proton pump function, and in the textile industry[210]. A large number of patents describe benzimidazole derivatives of use in the textile industry as wetting, emulsifying, foaming, or softening agents or as dispersants for use in dyeing. In the main, these compounds are sulfonated benzimidazoles. Another use is in the treatment of fibers to improve whiteness of the undyed material or as optical bleach. A number of aminobenzimidazoles have been used for the preparation of sulfur and azo dyes of use in the textile industry. Another use has been in the preparation of fluorescent dyes for use in such preparations as inks for marking clothes to be dry-cleaned. Benzimidazole derivatives have wide range of biological actions & industrial applications.

Research on suitable chemical sensors with high sensitivity for the detection of explosives has attracted much attention in recent time for wide applications in security screening and environment monitoring [211]. Currently, a wide range of instrumental techniques are being employed to detect explosives such as TNT (2,4,6-trinitrotoluene), DNT (2,4-dinitrotoluene) and PA (picric acid), 1-chloro-4-nitrobenzene, which are the primary constituents of many unexploded land mines worldwide [212]. Among these competing methods, fluorescence quenching based detection of explosives has grown enormously owing to its high sensitivity, easy visualization and real-time monitoring with fast response time [213]. The benzimidazole ring is an important pharmacophore in modern drug discovery. In recent years, attention has increasingly been given to the synthesis of benzimidazole derivatives. The synthesis of novel benzimidazole derivatives remains a main focus of medicinal research. Recent observations suggest that benzimidazole derivatives show easy interactions with nitroaromatic compound and act as sensor for them. Since now, researchers have been attracted toward designing more potent benzimidazole derivatives having wide diverse of biological activity.

So the objectives of my research can be summarized as following:

1. To synthesis a series of novel benzimidazole derivatives having biological as well as photo physical properties.
2. Synthesis of tetrahenium complexes applying the benzimidazole derivatives obtained.
3. Nanomaterials fabrication of the benzimidazole derivatives and tetrahenium complexes.
4. To Study of their photophysical properties (binding and quenching with nitroaromatic compound).
5. Evaluation of the potency/efficiency of these compounds as sensor for nitroaromatic compounds.
6. To apply these compounds as chemical sensor.

3.1. Materials and Methods

Caution : Picric acid is explosive in nature and should be handled in small quantities. It also forms shock-sensitive compounds with heavy metals. All reagents were purchased commercially and were used as received without further purification. Tetrahydrofuran (THF) and dichloromethan (DCM) used in this study was of spectroscopic grade and deionized water was used throughout the experiment. Prior to use, the solvents were checked for spurious emissions in the region of interest and found to be satisfactory. ^1H NMR spectra were measured on Bruker AC 300 and AMX-500 FT-NMR spectrometers. Infrared spectra were recorded on a Perkin-Elmer Paragon 882 FT-IR spectrometer. Elemental analyses were performed using a Perkin-Elmer 2400 CHN elemental analyzer. Mass data were obtained using a JEOL JMS-700 for FAB or Waters LCT-Premier XE for ESI. Scanning electron microscopy (SEM) experiments were carried out in a JSM-5400 scanning microscope to examine the morphology and microstructure of the aggregated samples. Electronic absorption spectra were recorded on a UV-1700 spectrophotometer. Emission spectra were obtained in THF and DCM solution at ambient temperature with a Hitachi F7000 fluorescence spectrophotometer.

3.2. Synthesis

3.2.1. Synthesis of 1,3-bis(benzimidazolyl)benzene (compound L-1)

1,3-bis(benzimidazolyl)benzene was synthesized following a literature procedure[214] and the product was obtained as brown powder. The melting point of the compound was 250-255° c.

3.2.2. Synthesis of 1,3-bis(1-butylbenzimidazol-2-yl)benzene (compound L-2)

1,3-Bis(2'-benzimidazolyl)benzene (4.00 g, 12.9 mmol) in DMSO (80.0 mL) was cooled to 8 °C on an ice-water bath, KOH (7.20 g, 128.8 mmol) was added, during which, the bath temperature was maintained at 8 °C. The mixture was stirred for 15 min, 1-bromobutane (8.82 g, 64.4 mmol) was added and the solution then allowed to reach room

temperature and left for 24 h. The mixture was diluted with water (200 mL) and the solution extracted with dichloromethane (2×200 mL). The combined organic layer was washed with water (2×200 mL), dried (MgSO_4), filtered and evaporated under reduced pressure and purified by flash column chromatography on silica gel with hexane-ethylacetate as the eluent, to give a colorless solid (4.86 g, 11.5 mmol, 89%). ^1H NMR (300 MHz, CDCl_3 , ppm): δ 0.67 (t, 6H, $J = 6.9$ Hz, CH_3), 1.05 (sextet, 4H, $J = 7.5$ Hz, $-\text{CH}_2-\text{CH}_3$), 1.59 (quintet, 4H, $J = 7.5$ Hz, $-\text{CH}_2-\text{CH}_2-\text{CH}_3$) 4.08 (t, 4H, $J = 7.5$ Hz, $-\text{CH}_2-(\text{CH}_2)_2-\text{CH}_3$), 7.08 (m, 4H, ArH), 7.23 (m, 2H, ArH), 7.50 (m, 1H, ArH), 7.67 (m, 4H, ArH), 7.92 (s, 1H, ArH). MS (ESI^+): m/z 423.5 ($\text{M} + \text{H}^+$). Anal. calcd for $\text{C}_{28}\text{H}_{30}\text{N}_4 \cdot 0.5 \text{H}_2\text{O}$: C, 78.02; H, 7.25; N, 12.99. Found: C, 78.21; H, 7.33; N, 13.01.

3.2.3. Synthesis of 2,5-bis(1-butylbenzimidazol-2-yl)thiophene (compound L-4)

2,5-Bis(2'-benzimidazolyl)thiophene (4.00 g, 12.6 mmol) in DMSO (80.0 mL) was cooled to 8°C on an ice-water bath, KOH (7.10 g, 126.4 mmol) was added, during which, the bath temperature was maintained at 8°C . The mixture was stirred for 15 min, 1-bromobutane (12.21 g, 63.2 mmol) was added and the solution then allowed to reach room temperature and left for 24 h. The mixture was diluted with water (200 mL) and the solution extracted with dichloromethane (2×200 mL). The combined organic layer was washed with water (2×200 mL), dried (MgSO_4), filtered and evaporated under reduced pressure and purified by flash column chromatography on silica gel with hexane-ethylacetate as the eluent to give an yellowish solid (4.86 g, 11.5 mmol, 89%, m.p. $105-107^\circ\text{C}$). For $\text{C}_{26}\text{H}_{30}\text{N}_4\text{S}$: C, 75.51; H, 8.20; N, 10.36; S, 5.93%. Found: C, 70.1456; H, 6.5934; N, 12.4661; S, 8.0406%.

3.2.4. Synthesis of 2,5-bis(1-octylbenzimidazol-2-yl)thiophene compound L-5)

2,5-Bis(2'-benzimidazolyl)thiophene (4.00 g, 12.6 mmol) in DMSO (80.0 mL) was cooled to 8 °C on an ice-water bath, KOH (7.10 g, 126.4 mmol) was added, during which, the bath temperature was maintained at 8 °C. The mixture was stirred for 15 min, 1-bromooctane (12.21 g, 63.2 mmol) was added and the solution then allowed to reach room temperature and left for 24 h. The mixture was diluted with water (200 mL) and the solution extracted with dichloromethane (2 × 200 mL). The combined organic layer was washed with water (2 × 200 mL), dried (MgSO₄), filtered and evaporated under reduced pressure and purified by flash column chromatography on silica gel with hexane-ethylacetate as the eluent to give a yellowish solid (4.86 g, 11.5 mmol, 89%). ¹H NMR: (300 MHz, CDCl₃): 0.83 (t, 6H, J = 7.0), 1.23-1.40 (m, 20H), 1.93 (quintet, 4H, J = 7.5 Hz), 4.42 (t, 4H, J = 7.5 Hz), 7.28-7.33 (m, 4H), 7.37-7.40 (m, 2H), 7.67 (s, 2H), 7.79-7.82 (m, 2H). Calcd. For C₃₄H₄₄N₄S: C, 75.51; H, 8.20; N, 10.36; S, 5.93%. Found: C, 75.23; H, 8.35; N, 9.95; S, 5.8%. m/e (ES): 541.3 (M⁺ + H).

3.2.5. Synthesis of [Re(CO)₃]₂(μ-dhaq)(μ-1)]₂ (compound L-6)

A suspension consisting of a mixture of Re₂(CO)₁₀ (0.130 g, 0.20 mmol), 1,4-dihydroxy-9,10-anthraquinone (H₂-dhaq, 0.053 g, 0.22 mmol), and L-5 (0.088 g, 0.21 mmol) in *p*-xylene (6 mL) was sealed in a Teflon-lined stainless steel autoclave. The autoclave was placed in an oven maintained at 160 °C for 48 h and then cooled to room temperature to afford black colored crystalline products (0.19 g, 0.079 mmol, 79%). ¹H NMR (500 MHz, THF-d⁸): 0.75 (12H, t, J = 7.0 Hz, Me), 1.1-1.29 (32H, m), 1.35-1.47 (8H, m), 1.69-1.79 (4H, m, underneath THF), 1.80-1.90 (4H, m), 2.26 (s, Me, *p*-xylene guest) 4.17-4.27 (8H, m), 6.86 (4H, s, H^{5,6}-bBImth), 7.01 (s, *p*-xylene guest), 7.27-7.29 (8H, dd, 5.9, 3.2, H^{2,3}-bBImth), 7.54-7.56 (4H, dd, 5.9, 3.2, H⁴-bBImth), 7.75 (4H, s, H^{1,2}-dhaq), 7.92-

7.94 (4H, dd, 5.8, 5.3, H^{4,5}-dhaq), 8.54-8.56 (4H, dd, 5.9, 3.2, H¹-bBI_mth), 8.63-8.65 (4H, dd, 5.8, 5.3, H^{3,6}-dhaq) IR (KBr, pellet, cm⁻¹): ν_{CO} 2012.1 (s), 1906.7 (s), 1875.5 (s). MS (FAB, ¹⁸⁷Re): m/z 2637.2 (M⁺ - H). Anal. Calcd for C₁₀₈H₁₀₀N₈O₂₀S₂Re₄ · 0.5 C₈H₁₀: C, 49.97; H, 3.93; N, 4.16; S, 2.38%. Found: C, 49.76; H, 4.02; N, 4.20; S, 2.36%. UV-vis (10⁻⁵ M, THF, nm): λ_{max} 231, 281, 403 (MLCT), 609, 661. Emission (THF, nm): λ_{max} 470.

3.2.6. Synthesis of [$\{\text{Re}(\text{CO})_3\}_2(\mu\text{-thaq})(\mu\text{-1})\}_2$ (compound L-7)

Complex L-7 was synthesized followed a procedure similar to that for 23a using H₂-thaq(1,2,4-trihydroxy-9,10-anthraquinone) instead of H₂-dhaq(1,4-dihydroxy-9,10-anthraquinone). Yield: 80% (0.21 g, 0.080 mmol). ¹H NMR (500 MHz, THF-d₈): 0.77 (12H, t, J = 7.2 Hz, Me), 1.18-1.32 (32H, m), 1.35-1.55 (8H, m), 1.69-1.79 (4H, m, underneath THF), 1.85-2.0 (4H, m), 2.28 (s, Me, *p*-xylene guest) 4.20-4.30 (8H, m), 6.77 (4H, s, H^{5,6}-bBI_mth), 7.01 (s, *p*-xylene guest), 7.26-7.35 (8H, m H^{2,3}-bBI_mth), 7.52-7.63 (4H, m, H⁴-bBI_mth), 7.76-7.80 (4H, m, H^{1,2}-dhaq), 7.89-7.97 (4H, m, H^{4,5}-dhaq), 8.60 (2H, s, dhaq), 8.62-8.67 (4H, m, H¹-bBI_mth). IR (KBr, pellet, cm⁻¹): ν_{CO} 2012.7 (s), 1907.0 (s), 1877.0 (s). MS (FAB, ¹⁸⁷Re): m/z 2669.5 (M⁺ - H). Anal. calcd for C₁₀₈H₁₀₀N₈O₂₂S₂Re₄ · C₈H₁₀: C, 50.17; H, 3.99; N, 4.03; S, 2.31%. Found: C, 49.78; H, 4.13; N, 4.12; S, 1.99%. UV-vis (10⁻⁵ M, THF, nm): λ_{max} 221, 266, 408 (MLCT), 590, 638. Emission (THF, nm): λ_{max} 470.

3.3. Fabrication of nano particles

3.3.1. Fabrication of nano particles of compound L-6

Aggregates were fabricated by adding 0.5 mL of a stock solution of compound L-6 (2 × 10⁻⁴ M, THF) in round bottom flasks containing THF-water mixture of the required ratio (9.5 mL) with vigorous stirring for 30 min. at room temperature to give a final concentration of 1 × 10⁻⁵ M. For example, for a 40% water fraction 0.5 mL of the stock

solution of 7a (2×10^{-4} M, THF) was added to 9.5 mL of solvent mixture containing 5.7 mL THF and 3.8 mL H₂O.

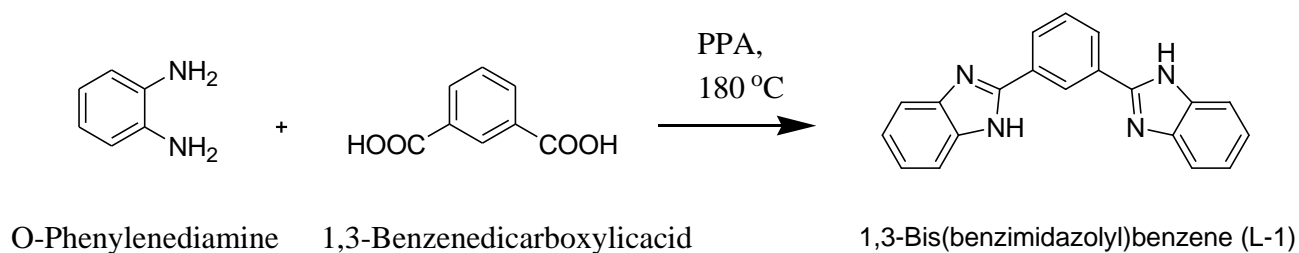
3.3.2 Fabrication of nano particles of compound L-7

Aggregates were fabricated by adding 0.5 mL of a stock solution of compound L-7 (1×10^{-4} M, THF) in round bottom flasks containing THF-water mixture of the required ratio (9.5 mL) with vigorous stirring for 30 min. at room temperature to give a final concentration of 0.5×10^{-5} M. For example, for a 40% water fraction 0.5 mL of the stock solution of 7a (2×10^{-4} M, THF) was added to 9.5 mL of solvent mixture containing 5.7 mL THF and 3.8 mL H₂O.

4.1. Synthesis

Synthesis of compound L-1 and L-3

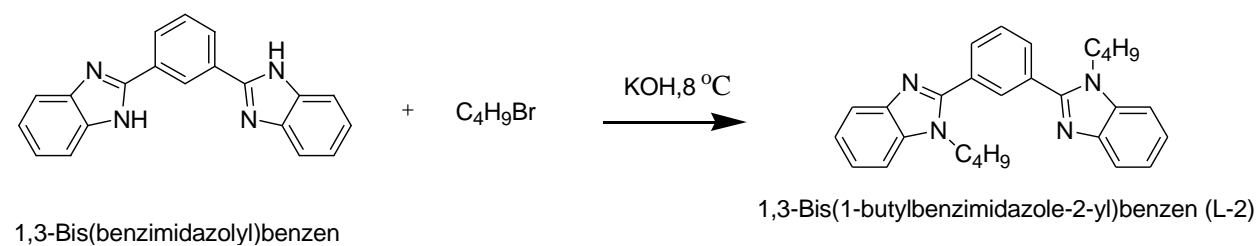
1,3-Bis(benzimidazolyl)benzene (L-1) was synthesized by reacting O-phenylenediamine (2 mole) with 1,3-benzenedicarboxylic acid (1 mole) in strong acidic condition and at very high temperature (i.e., PPA, 180 °C). Melting point of the compound was 250-255 °C (decompose).



Scheme-25 : Synthesis of L-1[1,3-bis(benzimidazolyl)benzene].

Synthesis of compound L-2

1,3-Bis(1-butylbenzimidazol-2-yl)benzene (L-2) was synthesized by reacting 1,3-bis(benzimidazolyl)benzene with 1-bromobutane in DMSO and KOH at 8 °C for 24 h. In this process N-alkylation of both the secondary amino groups took place. The compound was extracted from DMSO-H₂O mixture with DCM. The combined DCM layers were dried over MgSO₄ and DCM was evaporated to afford light yellow to brown powder. The product was sufficiently pure for analysis and tests.

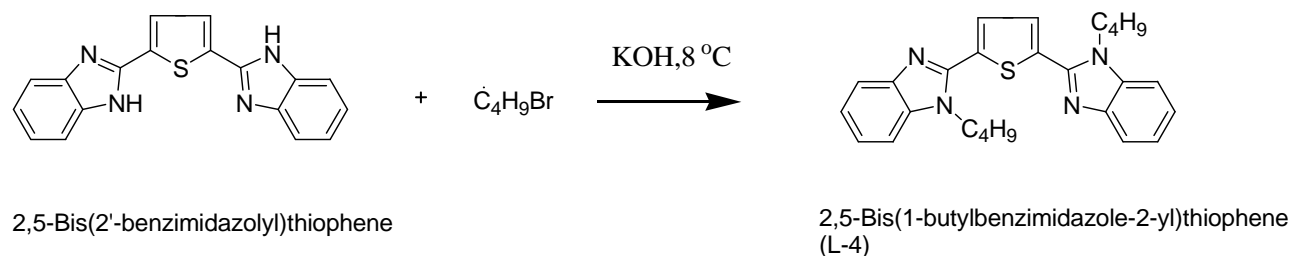


Scheme-26 : N-Alkylation of of L-2 [1,3-bis(1-butylbenzimidazol-2-yl)benzene].

Compound L-2 were characterized by ^1H NMR, elemental analysis, FAB-MS data. The ^1H NMR spectra and mass data indicated the formation of compound L-5 in the reaction. The proton ^1H NMR of this compound showed two triplet at 0.67 and 4.08 which were assigned for methyl protons and N-CH₂ protons, a sextet at 1.05 and a quintet at 1.59 for methylene protons and two multiplets at 7.08 and 7.23 for aromatic protons.

Synthesis of compound L-4

2,5-Bis(1-butylbenzimidazol-2-yl)thiophene (L-4) were synthesized in high yields (89%) by reacting 2,5-bis(2'-benzimidazolyl)thiophene in DMSO with 1-bromobutan and KOH at 8°C for 24 h applying same method as for compound L-2.

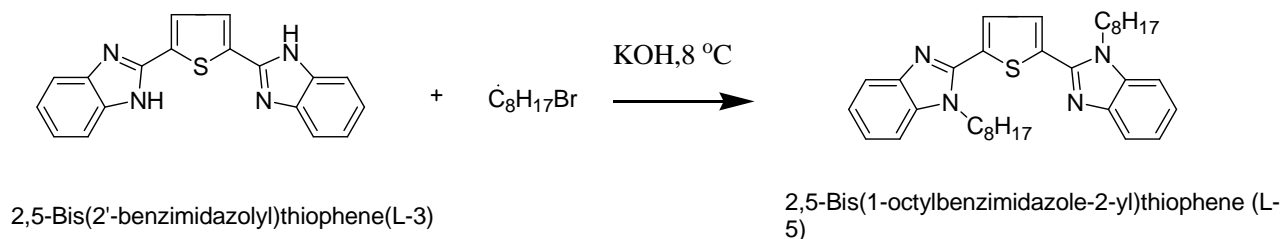


Scheme-27 : N-Alkylation of L-4(2,5-bis(1-butylbenzimidazol-2-yl)thiophene).

Compound L-4 was purified by same method as compound L-2 and melting point measured was 105-107° c (literature m. p. 104-105 °C)[215].

Synthesis of compound L-5

2,5-Bis(1-octylbenzimidazol-2-yl)thiophene (L-5) was obtained in high yield (89%) by reacting 2,5-bis(2'-benzimidazolyl)thiophene with 1-bromooctane in DMSO and KOH at 8°C for 24 h following the same method as for compound L-2.

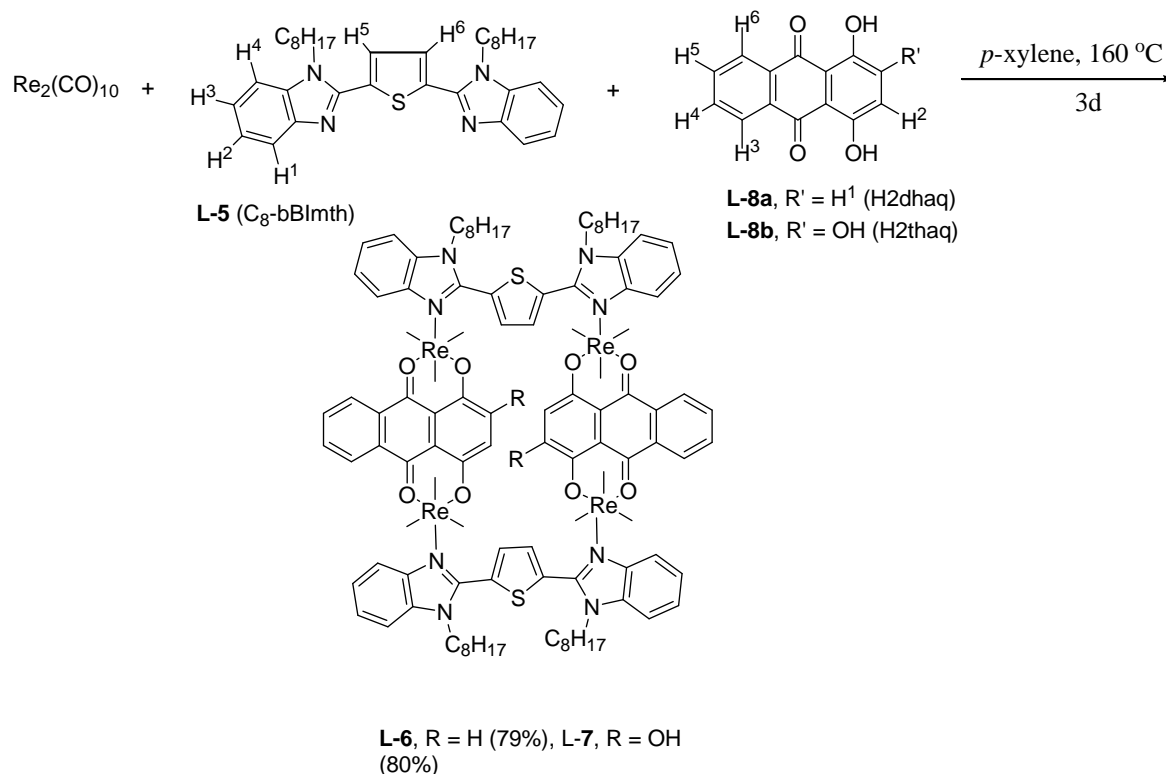


Scheme-28 : N-alkylation of L- 5 (2,5-bis(1-octylbenzimidazol-2-yl)thiophene).

Compound L-5 was characterized by 1H NMR, elemental analysis, FAB-MS data. The 1H NMR spectra and mass data indicate the formation of compound L-5 in the reaction. The 1H NMR of this compound showed a singlet at 7.67 attributed for two thiophenyl protons, two triplets at 0.83 and 4.42 and a quintet at 1.93 for methylene protons and a multiplet at 1.23-1.40 and three multiplets at 7.28-7.33, 7.37-7.40 and 7.79-7.82 which were assigned for aromatic protons.

Synthesis of compound L-6 and L-7

Complexes [$\{Re(CO)_3\}_2(\mu-dhaq)(\mu-N-N)$] $_2$ (L-6) and [$\{Re(CO)_3\}_2(\mu-thaq)(\mu-N-N)$] $_2$ (L-7) (H_2-dhaq = 1,4-dihydroxy-9,10-anthraquinone; H_2-thaq = 1,2,4-trihydroxy-9,10-anthraquinone; N-N = 2,5-bis(1-octylbenzimidazol-2-yl)thiophene) were prepared in high yields (79%) by reacting $Re_2(CO)_{10}$, H_2dhaq or H_2-thaq , an *N*-heterocyclic ditopic bridging ligand L-5 in *p*-xylene at 160 °C for 48 h under solvothermal conditions.



Scheme-29 : Solvothermal synthesis of metallacycles L-6 and L-7

Complexes L-6, L-7 were characterized by ^1H NMR, IR spectra, FAB-MS data, and microanalyses. The ^1H NMR spectra and mass data indicate the possible formation of tetrarhenium metallacycles in the reactions. The proton ^1H NMR of this compound showed triplet at 0.75 which is assigned for methyl proton, singlet at 6.86 for bBlmth proton and at 7.75 for $\text{H}^{1,2}$ -dhaq proton, singlet at 7.01 for P-xylene guest proton and at 7.75 which assign for $\text{H}^{1,2}$ -dhaq proton, five multiplets at 1.1-1.29, 1.35-1.47, 1.80-1.90, which account for alkyl protons and three double doublets at 7.93, 8.55, 8.64. The IR spectra of all the compounds exhibited strong and characteristic CO stretching vibrations in the range of $2013\text{-}1873\text{ cm}^{-1}$ region and were consistent with literature values[216]. X-ray diffraction analyses further confirmed the structures of compounds L-6 and L-7.

4.2. Studies on Binding property

Binding properties of PA with L-2, L-4, L-5, L-6, L-7 were studied using UV-Visible spectroscopy. Different amounts of PA, such as 50, 75, 100, 125, 150, 200, 275 μL of 10^{-3} (M) DCM stock solution was added with 2 mL of the solution of L-2 in DCM (0.25×10^{-4} M), where the final conc. of picric acid were $[\text{PA}] \times 10^{-4}$ M = 0, 0.24, 0.36, 0.47, 0.58, 0.69, 0.9, 1.1 and the absorption spectra were recorded immediately. Similarly the binding was monitored by adding different amounts of PA, such as 50, 75, 100, 125, 150, 175, 200, 225, 275, 325 μL 10^{-3} (M) DCM stock solution with 2 mL of the solution of L-4 in DCM (0.25×10^{-4} M), where the final conc. of picric acid were $[\text{PA}] \times 10^{-4}$ M = 0, 0.24, 0.36, 0.47, 0.58, 0.69, 0.8, 0.9, 1, 1.1, 1.39 and the absorption spectra were recorded immediately. For L-5 the amounts of PA, such as 25, 50, 60, 70, 80, 90, 100, 120 μL of 10^{-3} (M) DCM stock solution were added with 2 mL of the solution of L-5 in DCM (0.25×10^{-4} M), where the final conc. of picric acid were $[\text{PA}] \times 10^{-4}$ M = 0, 0.12, 0.24, 0.29, 0.33, 0.38, 0.43, 0.47, 0.57 and the absorption spectra were recorded immediately. For L-6 the amounts of PA, such as 50, 75, 100, 150, 175, 225, 375, 450 μL 10^{-4} (M) THF stock solution were added with 2 mL of the solution of L-6 in THF (1×10^{-5} M), where the final conc. of picric acid were $[\text{PA}] \times 10^{-5}$ M = 0, 0.24, 0.36, 0.69, 0.8, 1, 1.5, 1.8 and the absorption spectra were recorded immediately. For L-7 the amounts of PA, such as 75, 150, 200, 250, 300, 350 μL 10^{-4} (M) THF stock solution were added with 2 mL of the solution of L-7 in THF (0.5×10^{-5} M), where the final conc. of picric acid were $[\text{PA}] \times 10^{-5}$ M = 0, 0.36, 0.47, 0.69, 0.9, 1.1, 1.3, 1.48 and the absorption spectra were recorded immediately.

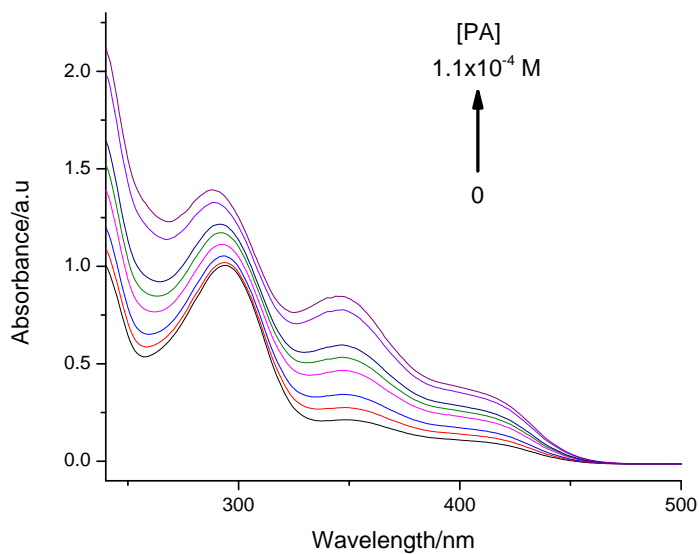


Figure-23 : UV-Visible spectra of L-2 with various amounts PA from bottom, $[\text{PA}] \times 10^{-4} \text{ M} = 0, 0.24, 0.36, 0.47, 0.58, 0.69, 0.9, 1.1$.

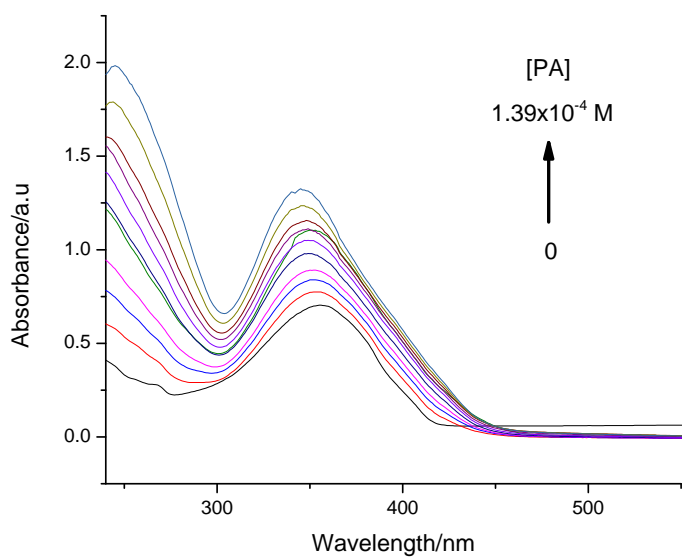


Figure-24 : UV-Visible spectra of L-4 with various amounts PA from bottom, $[\text{PA}] \times 10^{-4} \text{ M} = 0, 0.24, 0.36, 0.47, 0.58, 0.69, 0.8, 0.9, 1, 1.1, 1.39$.

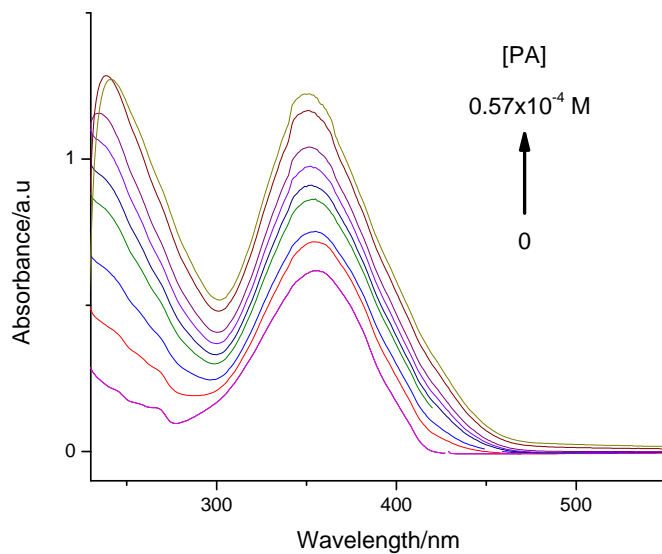


Figure-25 : UV-Visible spectra of L-5 with various amounts PA from bottom, $[\text{PA}] \times 10^{-4} \text{ M} = 0, 0.12, 0.24, 0.29, 0.33, 0.38, 0.43, 0.47, 0.57$.

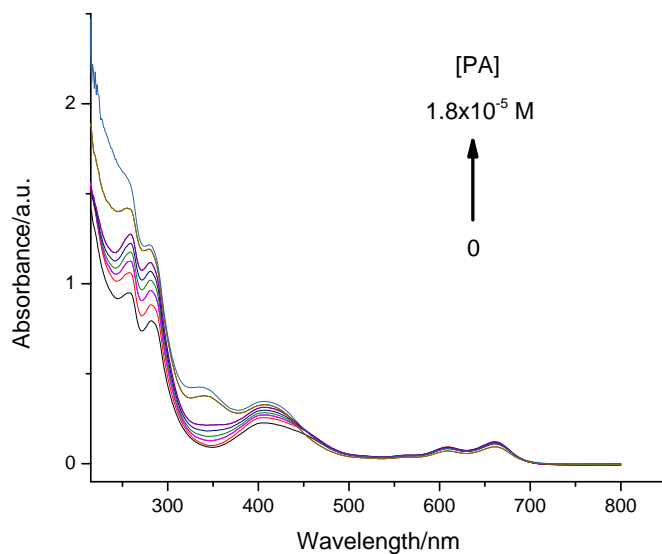


Figure-26 : UV-Visible spectra of L-6 with various amounts PA from bottom, $[\text{PA}] \times 10^{-4} \text{ M} = 0, 0.24, 0.36, 0.69, 0.8, 1, 1.5, 1.8$.

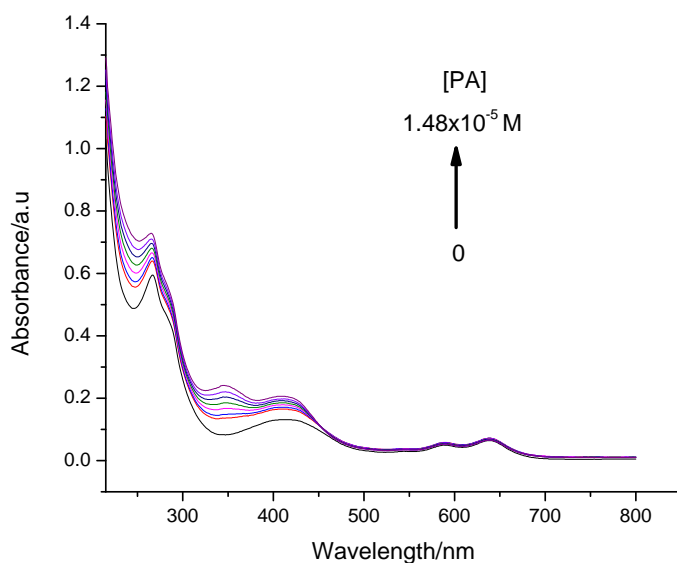


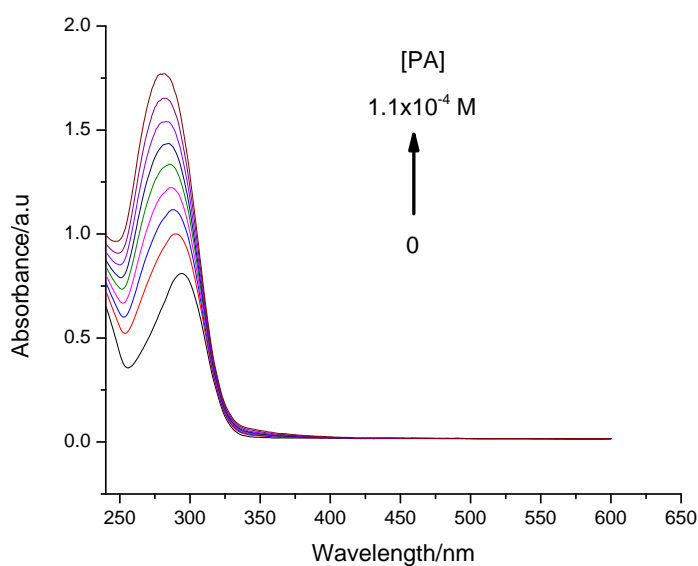
Figure-27 : UV-Visible spectra of L-7 with various amounts PA from bottom, $[PA] \times 10^{-4} M = 0, 0.36, 0.47, 0.69, 0.9, 1.1, 1.3, 1.48$.

The absorption spectrum of L-2, L-4, L-5 in DCM ($0.25 \times 10^{-4} M$) showed an intense band at 300 nm (L-2) and at 350 (L-2, L-4, L-5) corresponding to the $\pi-\pi^*$ transitions on addition of picric acid ($1 \times 10^{-3} M$). The absorption spectrum of L-6 in THF ($1 \times 10^{-5} M$) showed an intense band at 250 nm with shoulders at 280 nm, corresponding to the $\pi-\pi^*$ transitions of the dhaq and L-5 ligands and a broad and weak band at 400 nm, assigned to the MLCT transition. In addition, two weak bands appeared at 610 and 660 nm, which are assigned to intraligand transitions of the dhaq moiety. For compound L-7 the bands are situated at 250, 300 ($\pi-\pi^*$ transitions), 410 (MLCT), and at 590, 630 nm.

Table-6 : Absorption maxima of compound L-2, L-4, L-5, L-6, L-7

Compound	λ_{\max} (nm)
L-2	300, 350
L-4	350
L-5	350
L-6	250, 280, 400, 610, 660
L-7	250, 350, 410, 590, 630

1-Chloro-4-nitrobenzene were also used to study the binding properties of L-2. Different amounts such as 50, 75, 100, 125, 150, 175, 225, 275 $\mu\text{L } 10^{-3}$ (M) DCM stock solution of 1-Chloro-4-nitrobenzene were added with 2 mL of the solution of L-2 (0.25×10^{-4} M), where the final conc. of picric acid were $[\text{PA}] \times 10^{-4}$ M = 0, 0.24, 0.36, 0.47, 0.58, 0.69, 0.9, 1, 1.1 and the absorption spectra were recorded immediately. The absorption spectrum of L-2 in DCM (0.25×10^{-4} M) showed an intense band at 285 nm(L-2) corresponding to the $\pi-\pi^*$ transitions.

**Figure-28 : UV-Visible spectra of L-5 with various amounts of 1-chloro-4-nitrobenzene**

fraction from the top, $[PA] \times 10^{-4} M = 0, 0.24, 0.36, 0.47, 0.58, 0.69, 0.9, 1, 1.$

The current observations support that PA forms non-emissive ground state complex with (L-2, L-4, L-5, L-6, L-7). To observe one-to-one binding between host (H) and Guest (G) molecule using UV-Visible absorption, Beneshi-Hildebrand method can be used.

Beneshi-Hildebrand plot is,

$$1/\Delta A = 1/(\Delta\epsilon K[H][G]) + 1/(\Delta\epsilon[H])$$

Where ΔA is the difference of absorbance in absence and in the present of host, $\Delta\epsilon$ is the difference of the molar extinction coefficient in absence and in the present of host, K is the binding constant, and $[H]$, $[G]$ represent host and guest molar concentration respectively.

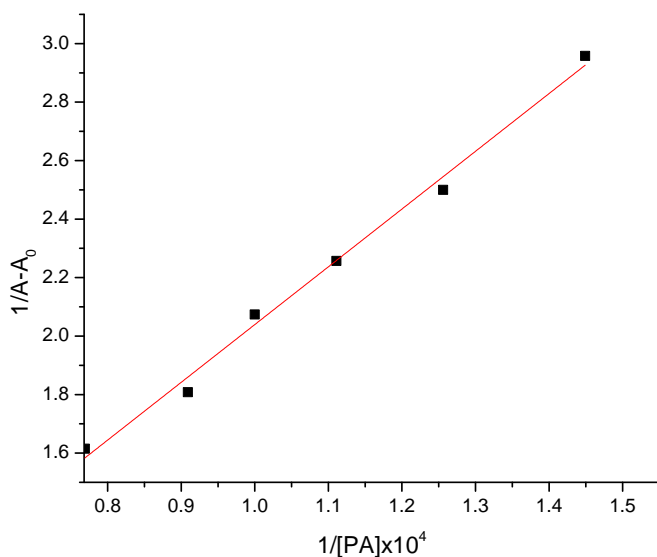


Figure-29 : Beneshi-Hildebrand plot for the binding of L-2 with PA.

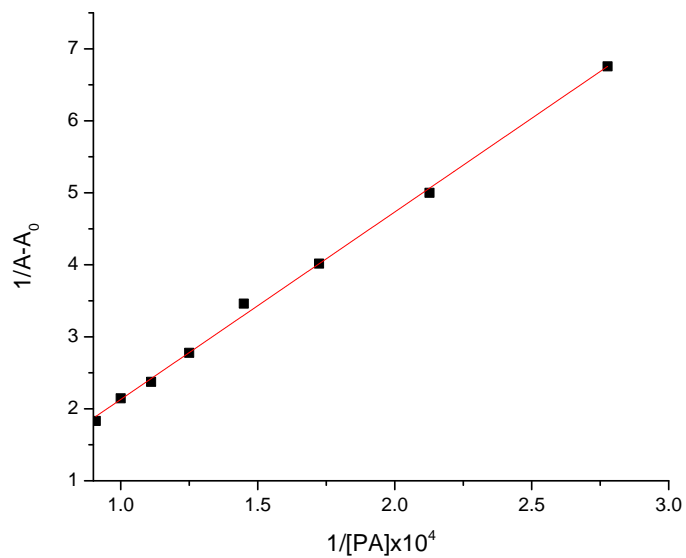


Figure-30 : Beneshi-Hildebrand plot for the binding of L-4 with PA.

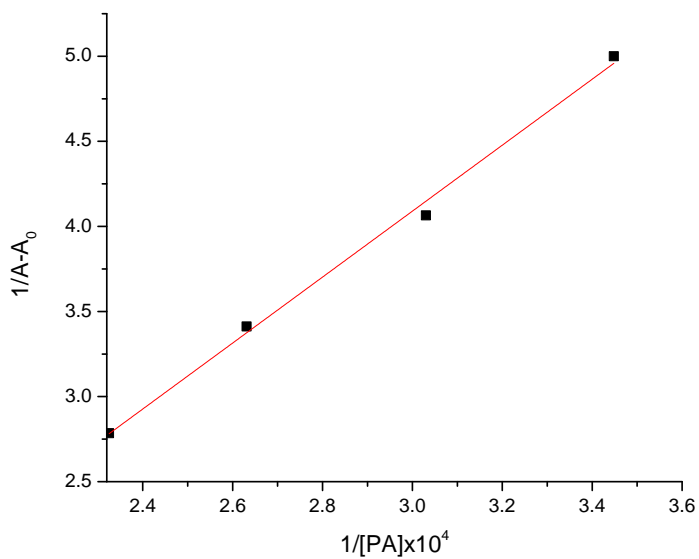


Figure-31 : Beneshi-Hildebrand plot for the binding of L-5 with PA.

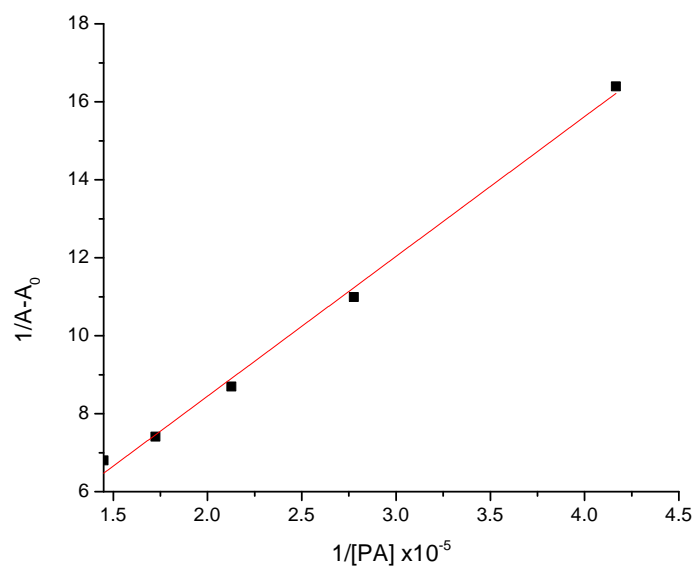


Figure-32 : Beneshi-Hildebrand plot for the binding of L-6 with PA.

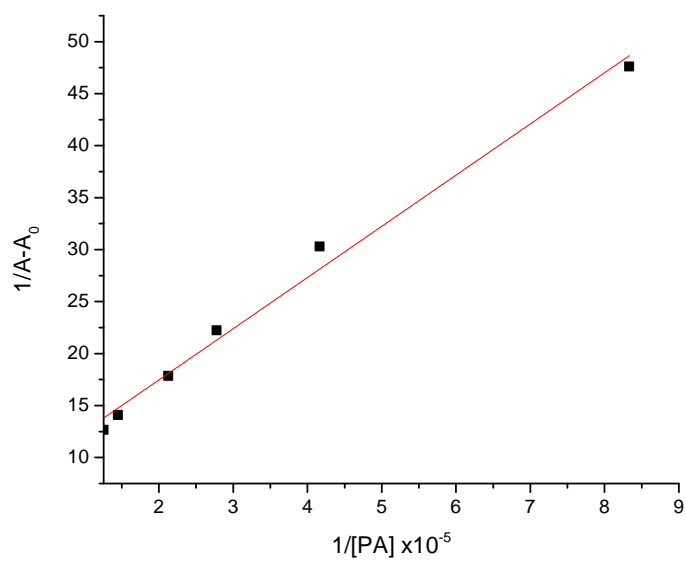


Figure-33 : Beneshi-Hildebrand plot for the binding of L-7 with PA.

4.3. PL Quenching Study:

Picric acid (PA) were used to study the quenching properties of L-2, L-4, L-5, L-6, L-7 by using fluorescence spectroscopy. The quenching was monitored by adding different amounts, such as 50, 75, 100, 125, 150, 175, 200, 225 μL 10^{-3} M DCM stock solution of quencher(PA) with 2 mL of the solution of L-2 (0.25×10^{-4} M), where the final conc. of picric acid were $[\text{PA}] \times 10^{-4}$ M = 0, 0.24, 0.36, 0.47, 0.58, 0.69, 0.9, 1 and the PL spectra were recorded immediately. Similarly different amounts of quencher(PA), such as 25, 50, 75, 100, 125, 150, 175, 200, 275 μL 10^{-3} M DCM stock solution were added with 2 mL of the solution of L-4 (0.25×10^{-4} M), where the final conc. of picric acid were $[\text{PA}] \times 10^{-4}$ M = 0, 0.24, 0.36, 0.47, 0.58, 0.69, 0.9, 1.1 and the PL spectra were recorded immediately. For L-5 different amounts of quencher(PA), such as 25, 50, 60, 70, 80, 90, 100, 110, 120, 130 μL 10^{-3} M DCM stock solution were added with 2 mL of the solution of L-5 (0.25×10^{-4} M), where the final conc. of picric acid were $[\text{PA}] \times 10^{-4}$ M = 0, 0.12, 0.24, 0.29, 0.33, 0.38, 0.43, 0.52, 0.62 and the PL spectra were recorded immediately . For L-6 the amounts of quencher(PA), such as 0, 125, 175, 225, 275, 300, 325, 375 μL 10^{-4} M THF stock solution of were added with 2 mL of the solution of L-6 in THF (1×10^{-5} M), where the final conc. of picric acid were $[\text{PA}] \times 10^{-5}$ M = 0, 0.24, 0.58, 0.8, 1, 1.2, 1.3, 1.39, 1.5 and the PL spectra were recorded immediately. And for L-7 different amounts of quencher(PA), such as 50, 100, 150, 250, 350, 450 μL 10^{-4} M THF stock solution were added with 2 mL of the solution of L-7 in THF (0.5×10^{-5} M), where the final conc. of picric acid were $[\text{PA}] \times 10^{-5}$ M = 0, 0.24, 0.47, 0.69 1.1, 1.48, 1.8 and the PL spectra were recorded immediately.

Upon excitation at 355 nm L-2, L-4, L-5 emitted a structureless PL band at 420 nm, 455 nm and L-6, L-7 at 415 nm, 440 nm, which originates from the singlet MLCT excited states as the Stock shift is small (100 nm for L-2, L-4, L-5 and 85 nm for L-6, L-7).

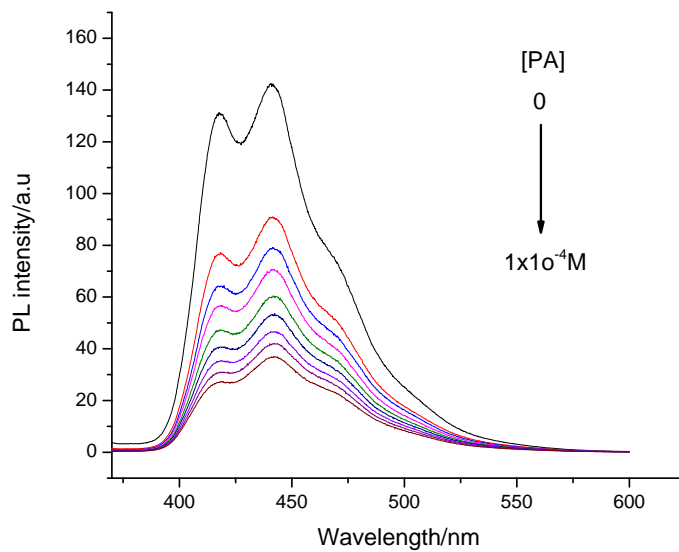


Figure-34 : PL quenching of L-2 by picric acid from top, $[PA] \times 10^{-4} \text{ M} = 0, 0.24, 0.36, 0.47, 0.58, 0.69, 0.9, 1$.

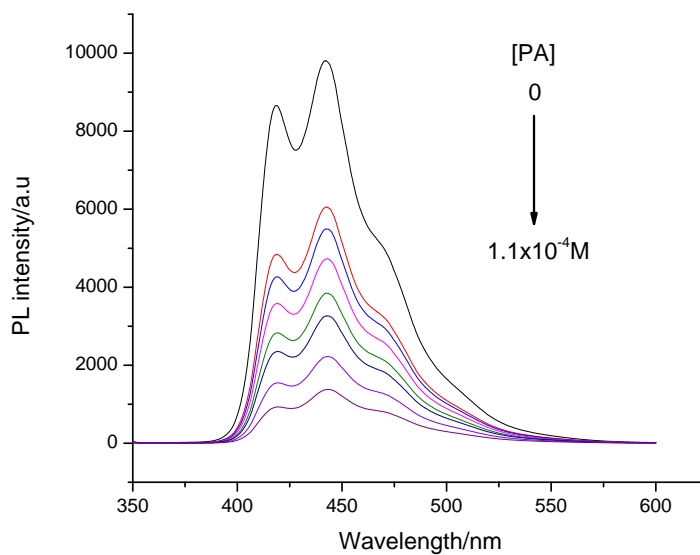


Figure-35 : PL quenching of L-4 by picric acid from top, $[PA] \times 10^{-4} \text{ M} = 0, 0.24, 0.36, 0.47, 0.58, 0.69, 0.9, 1.1$.

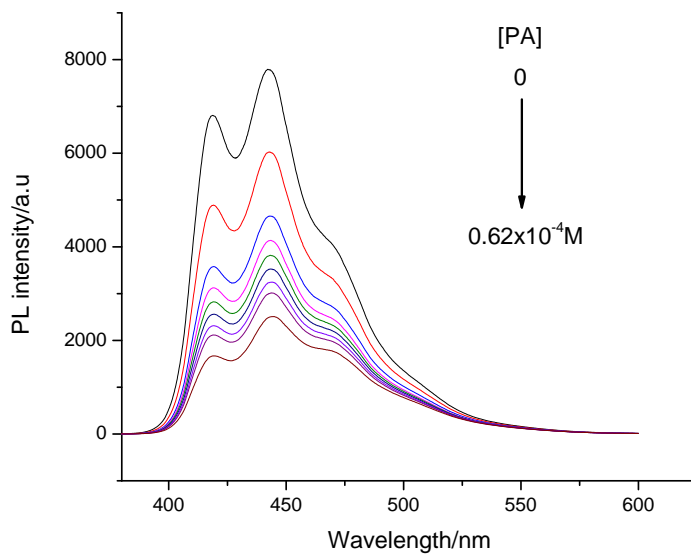


Figure-36 : PL quenching of L-5 by picric acid from top, $[PA] \times 10^{-4} \text{ M} = 0, 0.12, 0.24, 0.29, 0.33, 0.38, 0.43, 0.52, 0.62$.

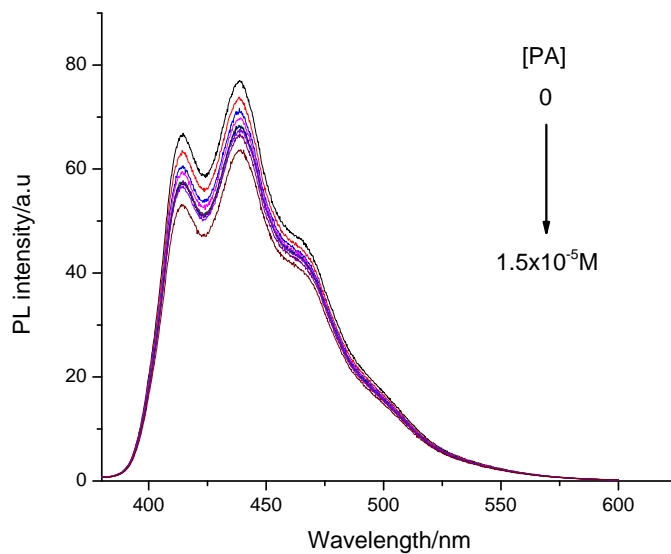


Figure-37 : PL quenching of L-6 by picric acid from top, $[PA] \times 10^{-5} \text{ M} = 0, 0.24, 0.58, 0.8, 1, 1.2, 1.3, 1.39, 1.5$.

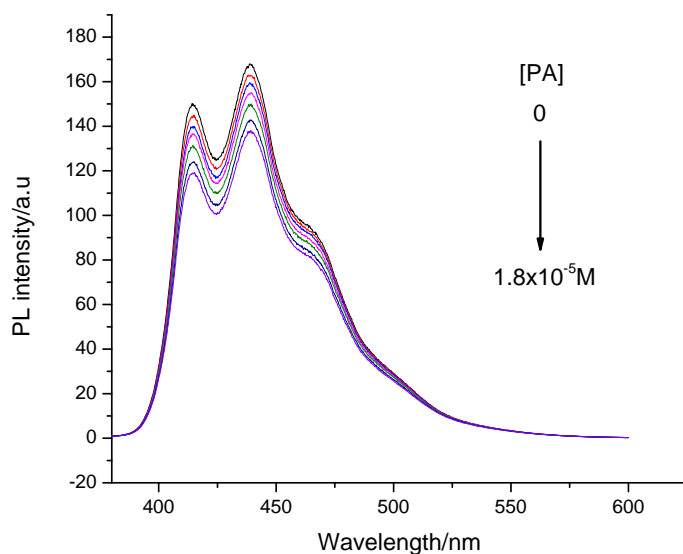


Figure-38 : PL quenching of L-7 by picric acid from top, $[PA] \times 10^{-5} \text{ M} = 0, 0.24, 0.47, 0.69, 1.1, 1.48, 1.8$.

PL intensity were quenched on addition of PA. Among the compounds studied L-2, L-4, L-5 showed significant quenching, where change is not significant for L-6 and L-7.

The quenching of luminescent material is normally analyzed using the Stern-Volmer equation[8] as long as a linear plot is obtained.

$$I_0/I = K_{sv}[Q] + 1$$

According to the equation the Stern-Volmer plot for PL quenching of L-2 and L-5 by picric acid showed linear curvature and L-4, L-6, L-7 showed positive curvature. So modified stern-Volmer were plotted for L-4 and L-7.

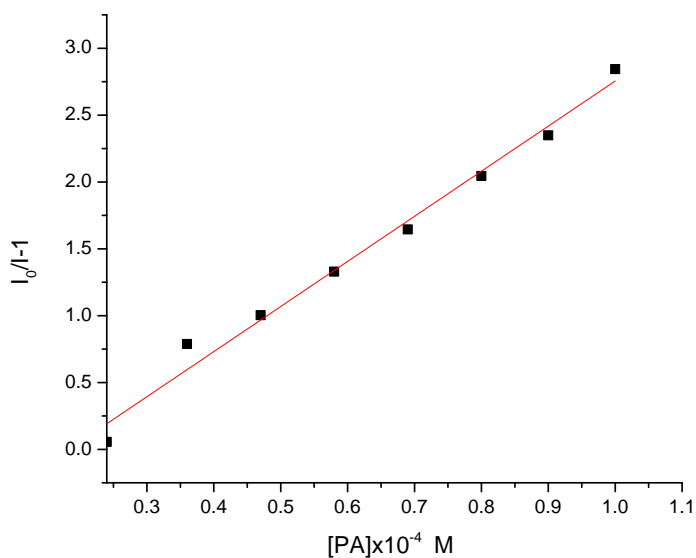


Figure-39 : Stern-Volmer plot for PL quenching of L-2 by PA.

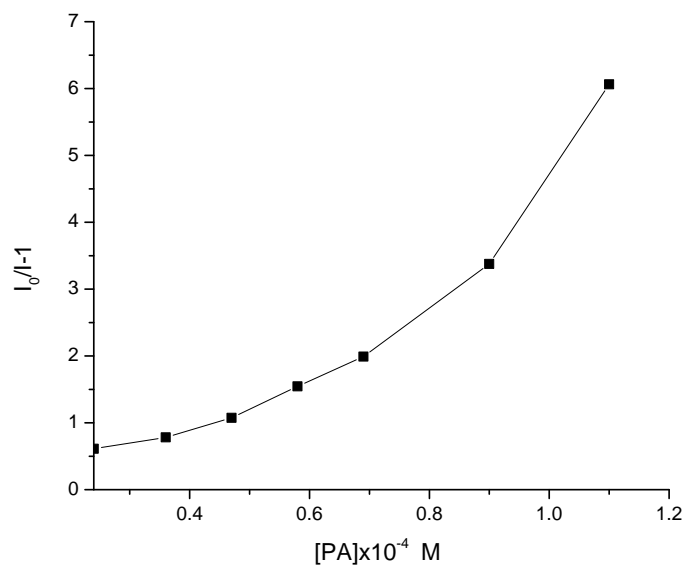


Figure-40 : Stern-Volmer plot for PL quenching of L-4 by PA.

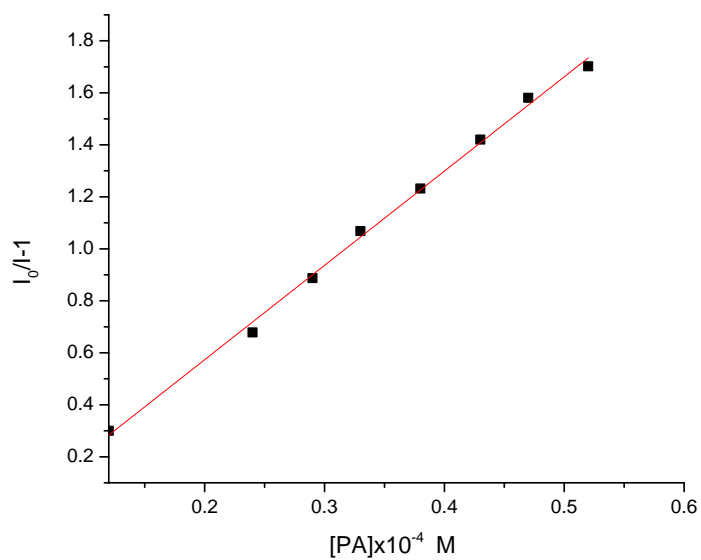


Figure-41 : Stern-Volmer plot for PL quenching of L-5 by PA.

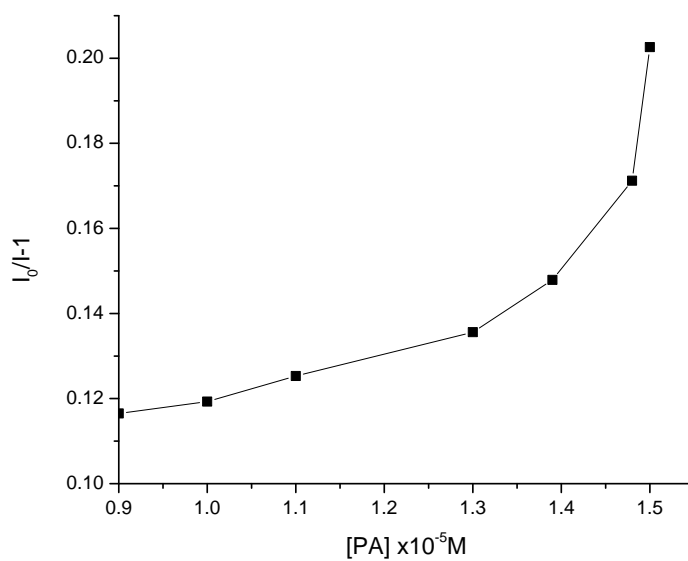


Figure-42 : Stern-Volmer plot for PL quenching of L-6 by PA.

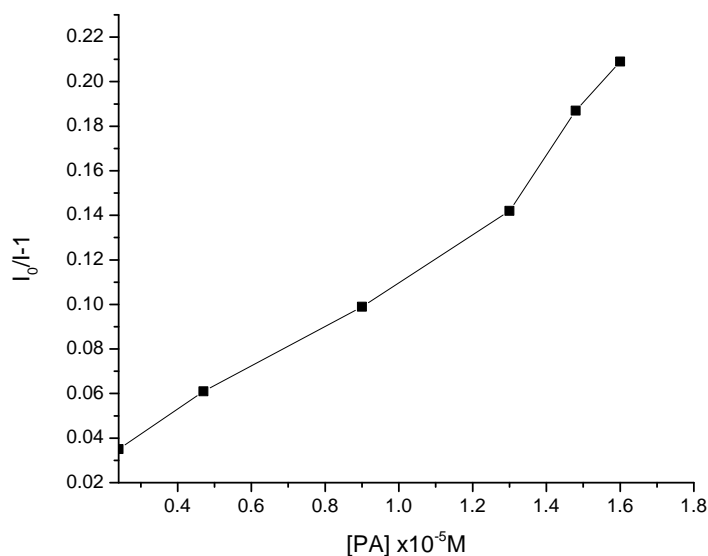


Figure-43 : Stern-Volmer plot for PL quenching of L-7 by PA.

A positive curvature at higher quencher concentration is attributed to the static quenching mechanism at higher quencher concentrations and need modified Stern-Volmer equation[217].

$$(I_0/I-1)/[Q] = (K_s + K_{sv}) + K_s K_{sv} [Q]$$

Where K_s is the formation constant of the ground state 1:1 complex. For L-4, L-7 the plot of $(I_0/I-1)/[PA]$ vs. $[PA]$ produced linear plots and from the intercept the sum of the formation constant K_s and Stern-Volmer constant K_{sv} were obtained.

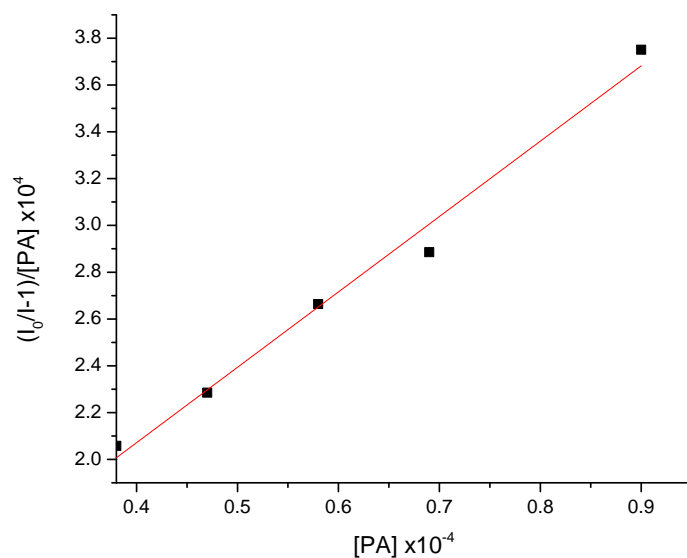


Figure-44 : Modified Stern-Volmer plot for the PL quenching of L-4 by PA.

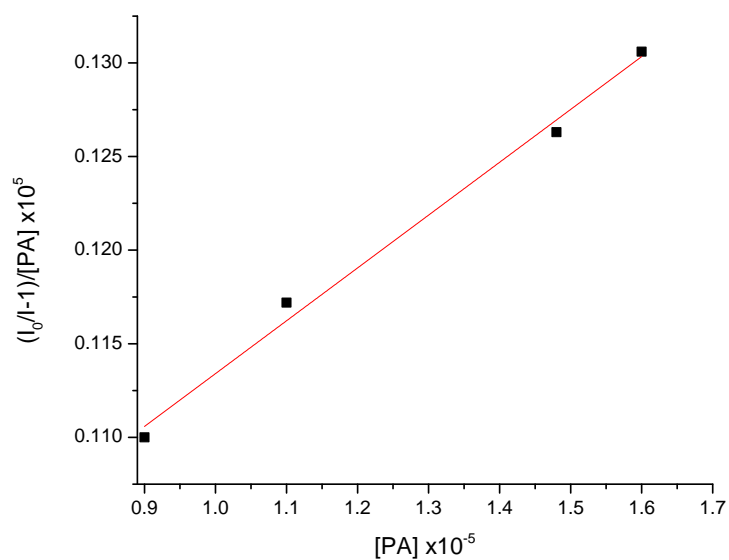


Figure-45 : Modified Stern-Volmer plot for the PL quenching of L-7 by PA.

In this case K_s is also considered as the static quenching constant[218], which was obtained from Beneshi-Hildebrand plot using equation.

Table-25 : Dynamic and Static Stern-Volmer constants for L-2, L-4, L-5, L-6, L-7.

Compound	K_{sv}, M^{-1}	K_s, M^{-1}
L-2	3.37312	0.0327
L-4	18.397 ^a	0.1751
L-5	3.62719	0.8900
L-6		0.3563
L-7	0.01824 ^a	1.5470

Here, a = K_{sv} for modified Stern-Volmer plot.

4.4. Absorption and Fluorescence spectroscopy of nanomaterials of L-6 and L-7

Aggregates of L-6 were fabricated by adding 0.5 mL of a stock solution of compound (2×10^{-4} M, THF) in round bottom flasks containing THF-water mixture of the required ratio (9.5 mL) with vigorous stirring for 30 min. at room temperature to give a final concentration of 1×10^{-5} M. Similarly aggregates of L-7 were also fabricated by adding 0.5 mL of a stock solution of compound (1×10^{-4} M, THF) in round bottom flasks containing THF-water mixture of the required ratio (9.5 mL) with vigorous stirring for 30 min. at room temperature to give a final concentration of 0.5×10^{-5} M.

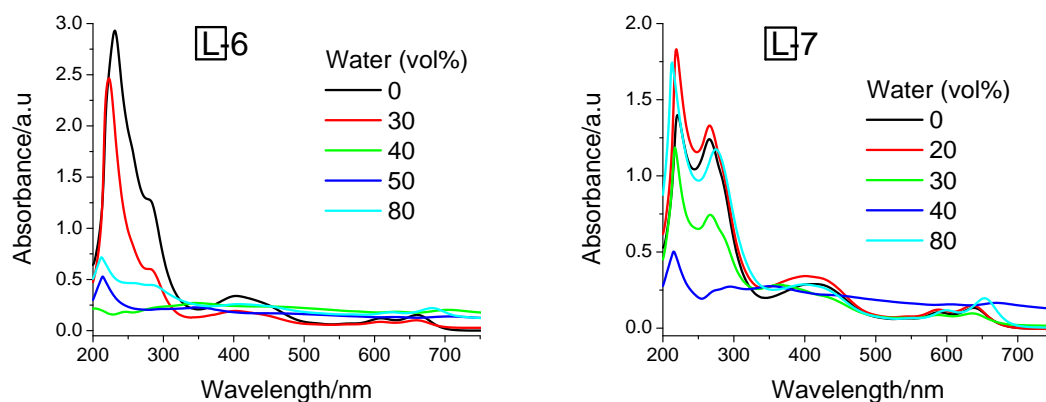


Figure-46 : UV/visible spectra of L-6 and L-7 with various water fractions.

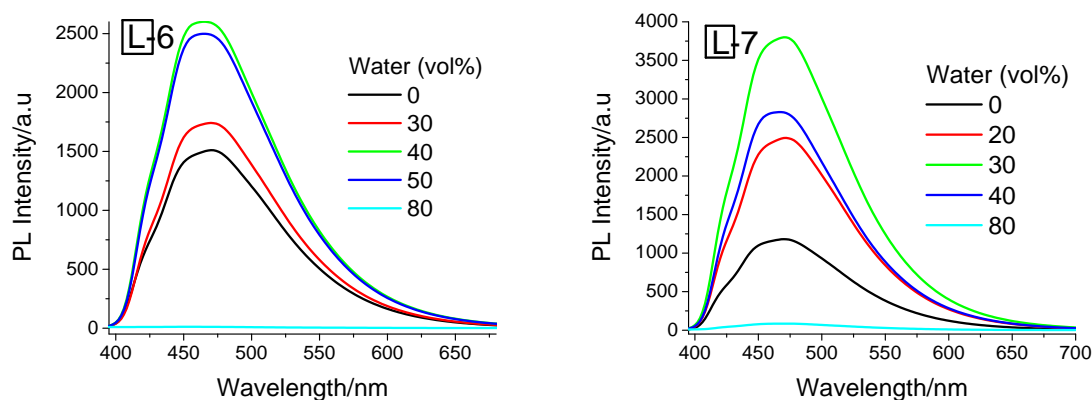


Figure-47 : PL spectra of L-6 and L-7 with various water fractions.

4.5. Spectral properties of aggregates

Aggregates of different morphologies were fabricated by simple precipitation method. A dilute solution of the compound in THF was added drop-wise to THF-water mixture of a required composition with vigorous stirring for 30 min. Solutions of compounds L-6 and L-7 in 40% and 30% water content precipitated on standing, while solutions with lesser or higher water contents were macroscopically homogenous and visually clear without precipitation. For compound L-6 the UV-vis bands at 231 and 281 nm are blue shifted by 10-20 nm upon addition of increased amount of water [Figure 46]. The MLCT band and

the bands at 609, 661 nm was blue shifted slightly (up to 40% water) and then red shifted. Similar shifts of UV-vis bands were observed for compounds L-7 [Figure-46]. The red shift in the UV-vis spectra can be attributed to aggregation analogous to J-aggregation[219]. Moreover, tailing of the UV-vis absorption spectra into the visible region was observed, which is a common feature of aggregated particles[220], due to the Mie effect. The PL spectra of aggregated particles of L-6 showed slight blue shift with increasing water fraction, while the change is not significant for L-7.

4.6. Morphology of the aggregates

The formation of aggregates of compound L-6, L-7 was confirmed by SEM analysis (Figure-48). SEM samples were prepared by casting a drop of a sample solution onto an individual copper holder and coated with gold. In THF solution L-6 formed granular type aggregates admixture with some nanorods, while L-7 in THF formed spongy spheres composed of nanorods. In a solution containing 40% water, L-6 produced open-ended micron size rods of wide lengths (3.8–8.8 μm), while L-7 in solution with a water content of 30% afforded smaller micron size rods (1.1–3.1 μm). In 80% water content both L-6 and L-7 afforded amorphous aggregates. The intermolecular interactions in aggregates are not clear to us. Presumably, the presence of four alkyl chains in the periphery of the metallacycle imparts sufficient hydrophobicity to drive the aggregation process[221]. The morphology change as a function of water content can be due to two reasons: (a) Re–CO \cdots H–O type hydrogen bonding between the carbonyl ligand and water could play a crucial role in nanoparticle formation, since a coordinated carbonyl ligand has been reported to be a hydrogen bond acceptor[222], (b) rapid nucleation of the aggregation process in the solvent with a higher water (a non solvent) content offers the aggregates little opportunity to grow and thus smaller particles are formed[223].

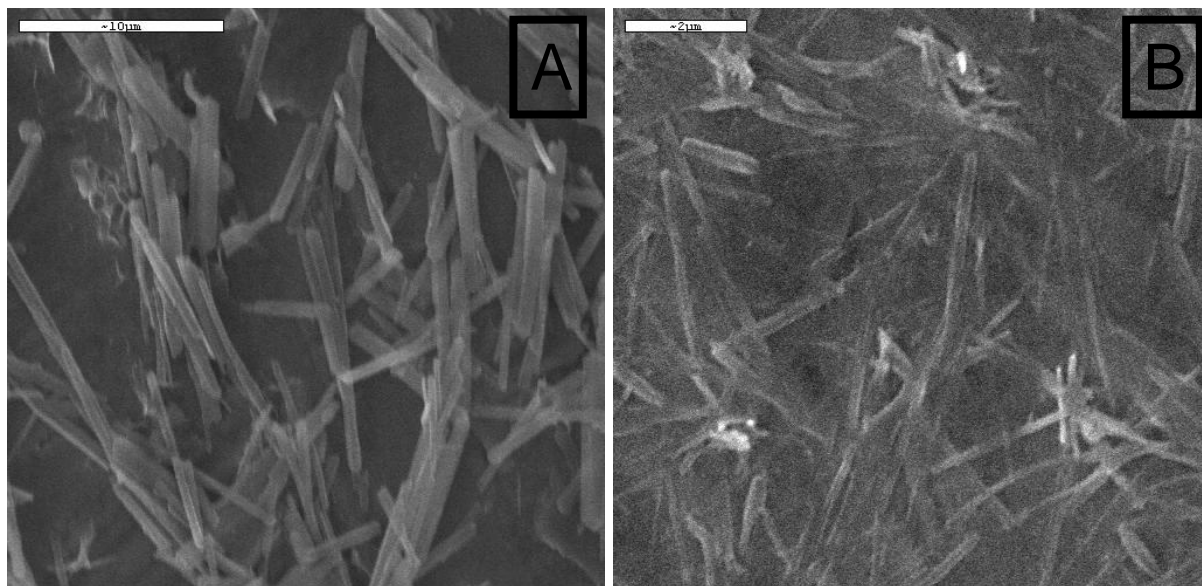


Figure-48 : SEM images of aggregated particles of L-6 (A) and L-7 (B) in water fraction 40% and 30% respectively.

Increased environmental awareness and societal needs serve as a catalyst for developing new method to detect organic pollutants. From this panorama, this investigation involved synthesis of various benzimidazole derivatives such as 1,3-bis(benzimidazolyl)benzene (L-1) by reacting O-phenylenediamine with dicarboxylic acid in strong acidic condition and at very high temperature (i.e., PPA, 180°C). N-alkylated derivatives such as 1,3-bis(1-butylbenzimidazol-2-yl)benzene(L-2), 2,5-bis(1-butylbenzimidazol-2-yl) thiophene (L- 4) and 2,5-bis(1-octylbenzimidazol-2-yl)thiophene compound L-5) were obtained by N-alkylation of amino groups. Rhenium(I) metallacycles [$\{\text{Re}(\text{CO})_3\}_2(\mu\text{-dhaq})(\mu\text{-1})\}_2$ (L-6) [$\{\text{Re}(\text{CO})_3\}_2(\mu\text{-thaq})(\mu\text{-1})\}_2$ (L-7) were synthesized under solvothermal condition. The binding and quenching of them with nitro-aromatic compounds such as picric acid (PA) and 1-chloro-4-nitrobenzene were also investigated. Present study demonstrated that compounds L-2, L-4, L-5, L-6, L-7 showed better sensing ability towards picric acid and 1-chloro-4-nitrobenzene. It was also observed that rhenium(I) metallacycles L-6 and L-7 underwent aggregation in THF-water mixtures and the morphology of the aggregate depends on the water fraction. Thus L-6 and L-7 formed granular or spongy spheres in THF solution, while they formed micron size rods in a THF-water mixture containing 40% and 30% water respectively. Higher water content of 80% afforded amorphous materials. The micron size rods of L-6 and L-7 showed better photoluminescence (PL) over granular or spherical aggregates, while PL is totally quenched in case of amorphous aggregates.

In reference to the previous observations it was revealed that PA formed ground state complexes with the compounds L-2, L-4, L-5, L-6, L-7). To observe binding between hosts [L-2, L-4, L-5, L-6, L-7] and guests [PA] UV-Visible absorption spectroscopy was employed and Beneshi-Hildebrand was applied. The Stern-Volmer plot for PL quenching of L-2 and L-5 by picric acid showed linear fit and L-4, L-6, L-7 showed positive curvature. The positive curvature is attributed to the involvement of both static and dynamic quenching.

1. “Über Fluoreszenz Und Phosphoreszenz, I. Abhandlung” (On Fluorescence And Phosphorescence, First Paper); Wiedemann E.; *Annalen Der Physik*, 34, 446-463.
2. “A Brief History Of Fluorescence And Phosphorescence Before The Emergence Of Quantum Theory”; Valeur B.; Berberan-Santos M. N.; *J. Chem. Educ.*, 2011, 88, 6, 731–738 .
3. “Luminescence Of Pyrimidines, Purines, Nucleosides, And Nucleotides At 77°K. The Effect Of Ionization And Tautomerization”; Longwarth, J. W.; Rahn, R. O.; Schulman, R. G.; *J. Chem. Phys.* 1966, 45, 2930-2939.
4. “Fluorescence Assay In Biology And Medicine”; Udenfriend, S.; *Academic Press, New York* 1969, 269-271.
5. “Optical Detection Of Magnetic Resonance Measurements Of The Effects Of pH On The Triplet States Of Benzimidazole And Purine”; Svejda, P.; Anderson. R. R. Maki. A. H.; *J. Am. Chem-Soc.* 1978, 100, 7131-7138.
6. “On The Luminescence Properties Of Some Purines And Pyrimidines. A Study By Fluorescence Spectrophotometry Of The Sites Of Protonation And Of The Types Of Lowest Excited Singlet States”; Barrensen, H. C.; *Acta Chem. Scand.* 1963, 17, 921-929.
7. “Food Additive Analytical Manual”; Food And Drug Administration; Washington Dc. 1973 ; Food Additive Reg. 121-260.
8. “Luminescent Oligo(Tetraphenyl)Silole Nanoparticles As Chemical Sensors For Aqueous TNT”; Toal, S. J.; Magde, D.; Trogler, W. C.; *Chem. Commun.* 2005, 5465–5467.
9. “Synthesis Of New Benzimidazole Linked Pyrrolo[2,1-c][1,4]benzodiazepine Conjugates With Efficient DNA-Binding Affinity And Potent Cytotoxicity”; Kamal, A.; Kumar, P. P.; Sreekanth, K.; Seshadri, B. N.; Ramulu, P.; *Bioorg. Med. Chem. Lett.* 2008, 18, 2594-2598.
10. (A) “Synthesis Of Some New 2-substituted-phenyl-1H-benzimidazole-5-carbonitriles And Their Potent Activity Against Candida Species”; Göker, H.; Kuş, C.; Boykin, D. W.; Yildiz, S.; Altanlar, N.; *Bioorg. Med. Chem.* 2002, 10, 2589-2596.

- (B) “Synthesis And Antimicrobial Activity Of Some Novel Phenyl And Benzimidazole Substituted Benzyl Ethers”; Güven, Ö.Ö.; Erdoğan, T.; Göker, H.; Yildiz, S.; *Bioorg. Med. Chem. Lett.* 2007, 17, 2233-2236.
- (C) “Chromatographic Elution Profile Of An Analyte Involved In Reversible Chemical Reaction Of The Type $A + B \leftrightarrow AB$ ”; Nobilis, M.; Jira, T.; Líska, M.; Holčapek, M.; Szotáková, B.; Lamka, J.; Skálová, L. J.; *Chromatogr. A.* 2007, 1149, 112-116.
- (D) “Potential Antitumor Agents. 59. Structure-Activity Relationships For 2-phenylbenzimidazole-4-carboxamides, A New Class Of Minimal DNA-Intercalating Agents Which May Not Act Via Topoisomerase II”; Denny, W. A.; Rewcastle, G. W.; Baguley, B. C. J.; *Med. Chem.* 1990, 33, 814.
11. “Self-Assembled Pentacenequinone Derivative For Trace Detection Of Picric Acid”; Bhalla, V.; Gupta, A.; Kumar, M.; Shankar Rao, D. S.; And Prasad, K. S.; *Acs Appl. Mater. Interfaces* 2013, 5, 3, 672–679.
12. “A Novel Preparation Method Of Organic Microcrystals”; Kasai, H.; Nalwa, H. S.; Oikawa, H.; Okada, S.; Matsuda, H.; Minami, N.; Kakuta, A.; Ono, K.; Mukoh, A.; Nakanishi, H.; *Jpn. J. Appl. Phys.* 1992, 31, L1132-L1134.
13. “Fabrication Of Organic Nanocrystals For Electronics And Photonics”; Nalwa, H. S.; Kasai, H.; Okada, S.; Oikawa, H.; Matsuda, H.; Kakuta, A.; Mukoh, A.; Nakanishi, H.; *Adv. Mater.* 1993, 5, 758-760.
14. “Organic Mesoscopic Chemistry”; Kasai, H.; Oikawa, H.; Nakanishi, H.; *Blackwell Science, Oxford* 1999, 145–170.
15. “Crystal Size Dependence Of Emission From Perylene Microcrystals”; Kasai, H.; Kamatani, H.; Yoshikawa, Y.; Okada, S.; Oikawa, H.; Watanabe, H.; Itoh, O.; Nakanishi, H.; *Chem. Lett.* 1997, 26, 1181-1182.
16. “Crystal Size Dependence Of Fluorescence Spectra From Perylene Nanocrystals Evaluated By Scanning Near-Field Optical Microspectroscopy”; Oikawa, H.; Mitsui, T.; Onodera, T.; Kasai, H.; Nakanishi, H.; Sekiguchi, T.; *Jpn. J. Appl. Phys.* 2003, 42, L111-L113.
17. “Supramolecular Structure Of Precipitated Nanosize β -Carotene Particles”; Auweter, H.; Haberkorn, H.; Heckmann, W.; Horn, D.; Ddecke, Lu. E.; Rieger, J.; Weiss, H.; *Angew. Chem. Int. Ed.* 1999, 38, 2188-2191.

18. "In Situ And Ex Situ Observations Of The Growth Dynamics Of Single Perylene Nanocrystals In Water"; Tachikawa, T.; Chung, R.H.; Masuhara, A.; Kasai, H.; Oikawa, H.; Nakanishi, H.; Fujitsuka, M.; Majima, T.; *J. Am. Chem. Soc.* 2006, 128, 15944-15945.
19. "Single Molecule Spectroscopy Of Organic Dye Nanoparticles"; Gesquiere, A. J.; Uwada, T.; Asahi, T.; Masuhara, H.; Barbara, F.P.; *Nano Lett.* 2005, 5, 1321-1325.
20. "Photopatterned Arrays Of Fluorescent Organic Nanoparticles"; An, B. K.; Kawn, K. S.; Park, Y. S.; *Angew. Chem. Int. Ed.* 2007, 46, 1978-1982.
21. "Size Effects On The Optical Properties Of Organic Nanoparticles"; Fu, H. B.; Yao, J. N.; *J. Am. Chem. Soc.* 2001, 123, 1434 –1439.
22. "Enhanced Emission And Its Switching In Fluorescent Organic Nanoparticles"; An, B. K.; Kawn, K. S.; Jung, D. S.; Park, Y. S.; *J. Am. Chem. Soc.* 2002, 124, 14410 – 14 415.
23. "Photoswitchable Organic Nanoparticles And A Polymer Film Employing Multifunctional Molecules With Enhanced Fluorescence Emission And Bistable Photochromism"; Lim, J. S.; An, B. K.; Jung, D. S.; Chung, A. M.; Park, Y. S.; *Angew. Chem.* 2004, 116, 6506 –6510 , *Angew. Chem. Int. Ed.* 2004, 43, 6346 – 6350.
24. "Strongly Fluorescent Organogel System Comprising Fibrillar Self-Assembly Of A Trifluoromethyl-Based Cyanostilbene Derivative"; An, B. K.; Lee, S. D.; Park, Y. S.; Song S. H.; *J. Am. Chem. Soc.* 2004, 126, 10232 –10 233.
25. "Fluorescent Organic Nanoparticles Of Benzofuran-Napthyridine Linked Molecules: Formation And Fluorescence Enhancement In Aqueous Media"; Sun, Y. Y.; Liao H. J.; Fang, M. J.; Chou, T. P.; Shen, H. C.; Hsu, W. C.; Chen, C. L.; *Organic Letters* 2006, 8, 17, 3713-3716.
26. (A) "Crystal Size Dependence Of Emission From Perylene Microcrystals"; Kasai, H.; Kamatani, H.; Yoshikawa, Y.; Okada, S.; Oikawa, H.; Watanabe, A.; Itoh, O.; Nakanishi, H.; *Chem. Lett.* 1997, 26, 1181-1182.
(B) "Size Effects On The Optical Properties Of Organic Nanoparticles"; Fu, H. B.; Yao, J. N.; *J. Am. Chem. Soc.* 2001, 123, 1434-1439.

- (C) “Steps To Demarcate The Effects Of Chromophore Aggregation And Planarization In Poly(phenyleneethynylene)s. 1. Rotationally Interrupted Conjugation In The Excited States Of 1,4-Bis(phenylethynyl)benzene”; Levitus, M.; Schmieder, K.; Ricks, H.; Shimizu, K. D.; Bunz, U. H. F.; Garcia-Garibay, M. A.; *J. Am. Chem. Soc.* 2001, 123, 4259-4265.
- (D) “Aggregation-Induced Emission Of 1-methyl-1,2,3,4,5-pentaphenylsilole” ; Luo, J.; Xie, Z.; Lam, J. W. Y.; Cheng, L.; Chen, H.; Qiu, C.; Kwok, H. S.; Zhan, X.; Liu, Y.; Zhu, D.; Tang, B. Z.; *Chem. Commun.* 2001, 1740-1741.
- (E) “Preparation And Characterization Of Porphyrin Nanoparticles”; Gong, X.; Milic, T.; Xu, C.; Batteas, J. D.; Drain, C. M.; *J. Am. Chem. Soc.* 2002, 124, 14290-14291.
- (F) “Preparation And Photochromic Properties Of Diarylethene Nanoparticles”; Sun, F.; Zhang, F.; Zhao, F.; Zhou, X.; Pu, S.; *Chem. Phys. Lett.* 2003, 380, 206-212.
- (G) “Size-Tunable Emission From 1,3-diphenyl-5-(2-anthryl)-2-pyrazoline Nanoparticles”; Xiao, D.; Xi, L.; Yang, W.; Fu, H.; Shuai, Z.; Fang, Y.; Yao, J.; *J. Am. Chem. Soc.* 2003, 125, 6740-6745.
- (H) “Enhanced Fluorescent Emission Of Organic Nanoparticles Of An Intramolecular Proton Transfer Compound And Spontaneous Formation Of One-Dimensional Nanostructures”; Li, S.; He, L.; Xiong, F.; Li, Yi.; Yang, G.; *J. Phys. Chem. B* 2004, 108, 10887-10892.
- (I) “CD Inversion And Fluorescence Enhancement In Organic Nanoparticles Of (R)-di-2-naphthylprolinol”; Xi, L.; Fu, H.; Yang, W.; Yao, J.; *Chem. Commun.* 2005, 492-494.
27. “Tunable Emission From Doped 1,3,5-triphenyl-2-pyrazoline Organic Nanoparticles”; Peng, D. A.; Xiao, D.; Ma, Y.; Yang, S. W.; Yao, N. J.; *Adv. Mater.* 2005, 17, 2070-2073.
28. “Multiple Emission From Doped 1,3-diphenyl-5-pyrenyl-2-pyrazoline Nanoparticles”; Fu, H. ; Loo, H. B.; Xiao, D.; Xie, R.; Ji, X.; Yao, J.; Zhang, B.; Zang, L.; *Angew. Chem. Int. Ed.* 2002, 41, 6.
29. “Size-Tunable Emission From 1,3-diphenyl-5-(2-anthryl)-2-pyrazoline Nanoparticles”; Xiao, D.; Xi, L.; Yang, W.; Fu, H.; Shuai, Z.; Fang, Y.; Yao, J.; *J. Am. Chem. Soc.* 2003, 125, 6740-6745.

30. "Effects Of Sonication On The Size And Crystallinity Of Stable Zwitterionic Organic Nanoparticles Formed By Reprecipitation In Water"; Kaysi, A.; Mu"ller, O. R.; Ahn, M. A.; Lee, T. S.; Bardeen, S. C.; *J. Langmuir* 2005, 21, 7990–7994.
31. "Organic Core/Diffuse-Shell Nanorods: Fabrication, Characterization And Energy Transfer"; Kang, L.; Chen, Yu.; Xiao, D.; Peng, D. A.; Shen, K. X.; Fu, H.; Yao, J.; *Chem. Commun.* 2007, 2695-2697.
32. "Three-Dimensional Mesoscale Self-Assembly"; Huck, S. T. W.; Tien, J.; Whitesides, M. G.; *J. Am. Chem. Soc.* 1998, 120, 8267.
33. "Porphyrin Nanotubes By Ionic Self-Assembly"; Wang, Z.; Medforth, J. C.; Shelnut, J. A.; *J. Am. Chem. Soc.* 2004, 126, 15954.
34. "Single-Crystal Organic Microtubes With A Rectangular Cross Section"; Zhang, X.; Zhang, X.; Shi, W.; Meng, X.; Lee, S. C.; Lee, T. S.; *Angew. Chem. Int. Ed.* 2007, 46, 1525.
35. "Assembly Of One-Dimensional Organic Luminescent Nanowires Based On Quinacridone Derivatives"; Wang, J.; Zhao, Y.; Zhang, J.; Yang, B.; Wang, Y.; Zhang, D.; You, H.; Ma, D.; *J. Phys. Chem. C.* 2007, 111, 9177.
36. "Nanobelt Self-Assembly From An Organic N-type Semiconductor: Propoxyethyl-PTCDI"; Balakrishnan, K.; Datar, A.; Oitker, R.; Chen, H.; Zuo, J.; Zang, L.; *J. Am. Chem. Soc.* 2005, 127, 10496.
37. "Nanofibril Self-Assembly Of An Arylene Ethynylene Macrocyclic"; Balakrishnan, K.; Datar, A.; Zhang, W.; Yang, X.; Naddo, T.; Huang, J.; Zuo, J.; Yen, M.; Moore, S.J.; Zang, L.; *J. Am. Chem. Soc.* 2006, 128, 6576.
38. "Ultralong Nanobelts Self-Assembled From An Asymmetric Perylene Tetracarboxylic Diimide"; Che, Y.; Datar, A.; Balakrishnan, K.; Zang, L.; *J. Am. Chem. Soc.* 2007, 129, 7234.
39. "Intense Fluorescence From Light-Driven Self-Assembled Aggregates Of Nonionic Azobenzene Derivatives"; Han, M.; Hara, M.; *J. Am. Chem. Soc.* 2005, 127, 10951-10955.
40. "Optical Waveguide Self-Assembled From Organic Dye Molecules In Solution"; Takazawa, K.; Kitahama, Y.; Kimura, Y.; Kido, G.; *Nano Lett.* 2005, 5, 1293.
41. "Waveguiding Properties Of Fiber-Shaped Aggregates Self-Assembled From Thiocyanine Dye Molecules"; Takazawa, K.; *J. Phys. Chem. C* 2007, 111, 8671.

42. “Nanotube Formation From Renewable Resources Via Coiled Nanofibers”; John, G.; Masuda, M.; Okada, Y.; Yase, K.; Shimizu, T.; *Adv. Mater.* 2001, 13, 715.
43. “Ratiometric Fluorescent Mercuric Sensor Based On Thiourea-thiadiazole-pyridine Linked Organic Nanoparticle”; Li, H.; Yan, H.; *J. Phys. Chem. C* 2009, 113, 7526-7530.
44. “Synthesis Of Organic Nanoparticles In Different W/O Microemulsions”; Debuigne, L.; Jeunieu; Wiame, M.; *J. B. Langmuir* 2000, 16, 7605–7611.
45. (A) “Size-Dependent Colors And Luminescences Of Organic Microcrystals”; Kasai, H.; Kamatani, H.; Okada, S.; Oikawa, H.; Matsuda, H.; Nakanishi, H.; *Jpn. J. Appl. Phys.* 1996, 35, L221.
(B) “Photoswitchable Organic Nanoparticles And A Polymer Film Employing Multifunctional Molecules With Enhanced Fluorescence Emission And Bistable Photochromism”; Lim, J. S.; An, B. K.; Jung, D. S.; Chung, A. M.; Park, Y. S.; *Angew. Chem. Int. Ed.* 2004, 43, 6346.
46. “Fabrication And Size-Dependent Optical Properties Of Copper/Lophine Core/Shell Nanocomposites”; Zhao, S. Y.; Hu, F.; Yang, W.; Ma, Y.; Yao, J.; *J. Nanosci. Nanotechol.* 2007, 7, 1021.
47. “A Hierarchical Self-Assembly Of 4, 5-diphenylimidazole On Copper”; Zhao, S. Y.; Hu, F.; Yang, W.; Zhang, H.; Ma, Y.; Yao, J.; *Colloids Surf. A* 2006, 277, 111.
48. “Properties Of A New Pyrazoline Derivative And Its Application In Electroluminescence”; Gao, C. X.; Cao, H.; Zhang, Q. L.; ; Zhang, W. B.; Cao, Y.; Huang, H. C.; *J. Mater. Chem.* 1999, 9, 1077.
49. “Single-Crystal Colloidal Multilayers Of Controlled Thickness”; Jiang, P.; Bertone, F. J.; Hwang, S. K.; Colvin, L. V.; *Chem. Mater.* 1999, 11, 2132.
50. “Influence Of Shell Strength On Shape Transformation Of Micron-Sized, Monodisperse, Hollow Polymer Particles”; Okubo, M.; Minami, H.; Morikawa, K.; *Colloid Polym. Sci.* 2003, 281, 214.
51. “Self-Assembling Sub-Micrometer-Sized Tube Junctions And Dendrites Of Conducting Polymers”; Wei, X. Z.; Zhang, J. L.; Yu, M.; Yang, S.Y.; Wan, X. M.; *Adv. Mater.* 2003, 15, 1382.

52. “High-Yield Synthesis Of Superhydrophilic Polypyrrole Nanowire Networks”; Zhong, W.; Liu, S.; Chen, X.; Wang, Y.; Yang, W.; *Macromolecules* 2006, 39, 3224.
53. “Polyaniline Nanofibers: Facile Synthesis And Chemical Sensors”; Huang, J.; Virji, S.; Weiller, H. B.; Kaner, B. R.; *J. Am. Chem. Soc.* 2003, 125, 314.
54. “Conjugated Polymer Actuators For Biomedical Applications”; Smela, E.; *Adv. Mater.* 2003, 15, 481.
55. “Polypyrrole Nanowire Actuators”; Berdichevsky, Y.; Lo, H. Y.; *Adv. Mater.* 2006, 18, 122.
56. “Electrospun Polyaniline/Polyethylene Oxide Nanofiber Field-Effect Transistor”; Pinto, J. N.; Johnson, T. A.; Macdiarmid, G. A. Jr.; Mueller, Theofylaktos, N.; Robinson, C. D.; Miranda, A. F.; *Appl. Phys. Lett.* 2003, 83, 4244.
57. “Microcavity Effects And Optically Pumped Lasing In Single Conjugated Polymer Nanowires”; Carroll, O. D.; Lieberwirth, I.; Redmond, G.; *Nat. Nanotech-nol.* 2007, 2, 180.
58. “A Single Polymer Nanowire Photodetector”; O’Brien, A. G.; Quinn, J. A.; Tanner, A. D.; Redmond, G.; *Adv. Mater.* 2006, 18, 2379.
59. “Micrometer- And Nanometer-Sized Polymeric Light-Emitting Diodes”; Granstro, M.; Berggren, M.; Ingana S, O.; *Science* 1995, 267, 1479.
60. “Size-Dependent Colors And Luminescences Of Organic Microcrystals”; Kasai, H.; Kamatani, H.; Okada, S.; Oikawa, H.; Matsuda, H.; Nakanishi, H.; *Jpn. J. Appl. Phys.* 1996, 34, L221 –L223.
61. “CD Inversion And Fluorescence Enhancement In Organic Nanoparticles Of (R)-di-2-naphthylprolinol”; Xi, L.; Yang, W.S.; Fu, B. H.; Fang, Y.; Yao, N. J.; Yang, S. W.; *Chem. Commun.* 2005, 492 –494.
62. “Aggregation-Driven Growth Of Size-Tunable Organic Nanoparticles Using Electronically Altered Conjugated Polymers”; Wang, F.; Han, Y. M.; Mya, Y. K.; Wang, B. Y.; Lai, H. Y.; , *J. Am. Chem. Soc.* 2005, 127, 10350 –10 355.
63. “Water-Soluble Hybrid Nanoclusters With Extra Bright And Photostable Emissions: New Tool For Biological Imaging”; Makarava, N.; Parfenov, A.; Baskakov, V. I.; *Biophys. J.* 2005, 89, 572 –580.

64. (A) "Ultrathin Organic Films Grown By Organic Molecular Beam Deposition And Related Techniques"; Forrest, R. S.; *Chem. Rev.* 1997, 97, 1793.
- (B) "Handbook Of Advanced Electronic And Photonic Materials And Devices"; By Nalwa, H. S. *Academic Press* 2001, 6.
65. "Science And Technology At The Nanometer Scale Using Vacuum-Deposited Organic Thin Films"; Forrest, S. R.; *Mrs Bull.* 2001, 26, 2, 108-112.
66. "Excimer Emission Of Anthracene, Perylene, Coronene And Pyrene Microcrystals Dispersed In Water"; Seko, T.; Ogura, K.; Kawakami, Y.; Sugino, H.; Toyotama, H.; Tanaka, J.; *Chem. Phys. Lett.* 1998, 291, 438-444.
67. "Fluorescence Spectral Study Of Wavelength Shifters For Scintillation Plastics"; Sandler, S. R.; Tsou, K. C.; *J. Chem. Phys.* 1963, 39, 1062.
68. "Hole Transport In 1-phenyl-3-((diethylamino)styryl)-5-(p-(diethylamino)phenyl)pyrazoline-Doped Polymers"; Borsenberger, P. M.; Schein, L. B.; *J. Phys. Chem.* 1994, 98, 233.
69. "Use Of Pyrazoline-Based Carrier Transport Layers In Layered Photoconductor Systems For Electrophotography"; Melz, P. J.; Champ, R. B.; Chang, L. S.; Chiou, C.; Keller, G. S.; Liclican, L. C.; Neiman, R. R.; Schattuck, M. D.; Weiche, W. J.; *Photogr. Sci. Eng.* 1977, 21, 73.
70. "Properties Of A New Pyrazoline Derivative And Its Application In Electroluminescence"; Gao, X. C.; Cao, H.; Zhang, L. Q.; Zhang, B. W.; Cao, Y.; Huang, C. H.; *J. Mater. Chem.* 1999, 9, 1077-1080.
71. (A) "Signaling Recognition Events With Fluorescent Sensors And Switches"; De Silva, A. P.; Gunaratne, H. Q. N.; Gunnlaugsson, T.; Huxley, A. J. M.; McCoy, C. P.; Rademacher, J. T.; Rice, T. E.; *Chem. Rev.* 1997, 97, 1515-1566.
- (B) "Design Principles Of Fluorescent Molecular Sensors For Cation Recognition"; Valeur, B.; Leray, I. *Coord. Chem. Rev.* 2000, 205, 3-40.
- (C) "Luminescent Chemosensors For Transition Metal Ions"; Prodi, L.; Bolletta, F.; Montalti, M.; Zaccheroni, N.; *Coord. Chem. Rev.* 2000, 205, 59-83.
72. (A) "Coupling Selectivity With Sensitivity In An Integrated Chemosensor Framework: Design Of A Hg²⁺-Responsive Probe, Operating Above 500 Nm"; Descalzo, A. B.; Martı'Nez-Ma'Ñez, R.; Radeaglia, R.; Rurack, K.; Soto, J.; *J. Am. Chem. Soc.* 2003, 125, 3418-3419.

- (B) “An Optical Fiber Chemical Sensor For Mercury Ions Based On A Porphyrin Dimer”; Zhang, X. B.; Guo, C. C.; Li, Z. Z.; Shen, G. L.; Yu, R. Q.; *Anal. Chem.* 2002, 74, 821–825.
- (C) “Fluorometric Chemosensors. Interaction Of Toxic Heavy Metal Ions Pb^{II} , Cd^{II} , And Hg^{II} With Novel Mixed-Donor Phenanthroline-Containing Macrocycles: Spectrofluorometric, Conductometric, And Crystallographic Studies”; Aragon, M. C.; Arca, M.; Demartin, F.; Devillanova, F. A.; Isaia, F.; Garau, A.; Lippolis, V.; Jalali, F.; Papke, U.; Shamsipur, M.; Tei, L.; Yari, A.; Verani, G.; *Inorg. Chem.* 2002, 41, 6623–6632.
- (D) “A Highly Selective Fluorescent Chemosensor For Lead Ions”; Chen, C. T.; Huang, W. P.; *J. Am. Chem. Soc.* 2002, 124, 6246–6247.
- (E) “Multi-Ion Imaging Using Fluorescent Sensors In A Microtiterplate Array Format”; Mayr, T.; Liebsch, G.; Klimant, I.; Wolfbeis, O. S.; *Analyst* 2002, 127, 201–203.
73. (A) “Bioinorganic Chemistry: Inorganic Elements In The Chemistry Of Life, An Introduction And Guide”; Kaim, W.; Schwederski, B.; *Wiley- Interscience: New York* 1991.
- (B) “The Chemical Cycle And Bioaccumulation Of Mercury”; Morel, F. M. M.; Kraepiel, A. M. L.; Amyot, M.; *Annu. Rev. Ecol. Syst.* 1998, 29, 543–566.
74. “Tools And Tactics For The Optical Detection Of Mercuric Ion”; Nolan, E. M.; Lippard, S. J.; *Chem. Rev.* 2008, 108, 3443–80.
75. “Modulating The Sensory Response Of A Conjugated Polymer By Proteins: An Agglutination Assay For Mercury Ions In Water”; Kim, I.-B.; Bunz, U. H. F.; *J. Am. Chem. Soc.* 2006, 128, 2818–2819.
76. “Tuning The Sensitivity Of A Foldamer-Based Mercury Sensor By Its Folding Energy”; Zhao, Y.; Zhong, Z.; *J. Am. Chem. Soc.* 2006, 128, 9988–9989.
77. “Rational Design Of “Turn-On” Allosteric Dnzyme Catalytic Beacons For Aqueous Mercury Ions With Ultrahigh Sensitivity And Selectivity”; Liu, J. W.; Lu, Y.; *Angew. Chem., Int. Ed.* 2007, 46, 7587–7590.
78. “Highly Sensitive “Turn-On” Fluorescent Sensor For Hg^{2+} In Aqueous Solution Based On Structure-Switching Dna”; Wang, Z. D.; Lee, J. H.; Lu, Y.; *Chem. Commun.* 2008, 6005–6007.

79. "A Blue Fluorescent Antibody–Cofactor Sensor For Mercury"; Matsushita, M.; Meijler, M. M.; Wirsching, P.; Lerner, R. A.; Janda, K. D.; *Org. Lett.* 2005, 7, 4943–4946.
80. "A Highly Selective And Sensitive Fluorescent Chemosensor For Hg²⁺ In Neutral Buffer Aqueous Solution"; Guo, X.; Qian, X.; Jia, L.; *J. Am. Chem. Soc.* 2004, 126, 2272–2273.
81. "Highly Selective Chromogenic And Redox Or Fluorescent Sensors Of Hg²⁺ In Aqueous Environment Based On 1,4-disubstituted Azines"; Caballero, A.; Marti'Nez, R.; Lloveras, V.; Ratera, I.; Vidal-Gancedo, J.; Wurst, K.; Ta'Rraga, A.; Molina, P.; Veciana, J.; *J. Am. Chem. Soc.* 2005, 127, 15666–15667.
82. "Fluorogenic Hg²⁺-Selective Chemodosimeter Derived From 8-Hydroxyquinoline"; Song, K. C.; Kim, J. S.; Park, S. M.; Hung, K.-C.; Ahn, S.; Chang, S.-K.; *Org. Lett.* 2006, 8, 3413–3416
83. "Surfactant Systems: Microemulsions And Vesicles As Vehicles For Drug Delivery"; Lawrence, M. J.; *Eur. J. Drug Metab. Pharmacokinet.*; 1994, 3, 257.
84. "Controlled Drug Delivery With Nanoparticles: Current Possibilities And Future Trends"; Couvreur, P.; Dubernet, C.; Puisieux, F.; *Eur. J. Pharm. Biopharm.* 1995, 41, 2.
85. "A Method For The Preparation Of Submicron Particles Of Sparingly Water-Soluble Drugs By Precipitation In Oil-In-Water Emulsions. Ii: Influence Of The Emulsifier, The Solvent, And The Drug Substance"; Sjo"Stro"m, B.; Bergenstahl, B.; Kronberg, B.; *J. Pharm. Sci.* 1993, 82, 584.
86. "Drug-Loaded Nanoparticles. Preparation Methods And Drug Targeting Issues"; Alle'Mann, E.; Gurny, R.; Doelker, E. *Eur. J. Pharm. Biopharm.* 1993, 39, 173.
87. (A) "About Supramolecular Assemblies Of π -Conjugated Systems"; Hoeben, M. J. F.; Jonkheijm, P.; Meijer, W. E.; Schenning, J. H. P. A. ; *Chem. Rev.* 2005, 105, 1491.
- (B) "Photoconductive Coaxial Nanotubes Of Molecularly Connected Electron Donor And Acceptor Layers"; Yamamoto, Y.; Fukushima, T.; Suna, Y.; Ishii, N.; Saeki, A.; Seki, S.; Tagawa, S.; Taniguchi, M.; Aida, T.; *Science* 2006, 314, 1761.
- (C) "The Chemistry Of Organic Nanomaterials"; Grimsdale, C. A.; Mullen, K.; *Angew. Chem. Int. Ed.* 2005, 44, 5592.

88. "Coloring Of Dragees With Carotinoid Dyes"; Klau, H.; Munzel, K.; *Pharm. Acta Helv.* 1965, 40, 153-164.
89. "Die Anwendung Und Bedeutung Von Synthetischen Carotinoiden In Der Lebens- Und Futtermittel-Sowie In Der Pharmazeutischen Industrie"; Manz, U.; *Chimia* 1967, 21, 329-335.
90. "In: Carotenoids, Ed. O. Isler. Birkhäuser Verlag, Basel And Stuttgart"; Bauernfeind, J. C.; Brubacher, G. B.; Klau, H. M.; Marusich, W. L.; 1971, 743-769.
91. "Carotenoids As Colorants And Vitamin A Precursors"; *Academic Press, New York* 1981.
92. "Optical Nanosensors For Chemical Analysis Inside Single Living Cells. 2. Sensors For pH And Calcium And The Intracellular Application Of Pebble Sensors"; Clark, A. H.; Kopelman, R.; Tjalkens, R.; And Philbert, M. A.; *Anal. Chem.* 1999, 71, 4837.
93. "Noninvasive Monitoring Of Intracellular pH Change Induced By Drug Stimulation Using Silica Nanoparticle Sensors"; Peng, J.; Wang, K. He. X.; Tan, W.; Wang, T.; Liu, Y.; *Anal. Bioanal. Chem.* 2007, 388, 645.
94. "Synthesis And Characterization Of Ratiometric, pH Sensing Nanoparticles With Covalently Attached Fluorescent Dyes: Communications"; Sun, H.; Scharff-Poulsen, M. A.; Gu, H.; Almdal, K.; *Chem. Materials* 2006, 18, 3381.
95. "Synthesis, Characterization, And Application Of Fluorescence Sensing Lipobeads For Intracellular pH Measurements"; Mcnamara, P. K.; Nguyen, T.; Dumitrascu, G.; Rosenzweig, N. Ji. J.; Rosenzweig, Z.; *Anal. Chem.* 2001, 73, 3240.
96. "Synthesis And Application Of Submicrometer Fluorescence Sensing Particles For Lysosomal pH Measurements In Murine Macrophages"; Rosenzweig, N. Ji. J.; Griffin, C.; Rosenzweig, Z.; *Anal. Chem.* 2000, 72, 3497.
97. "Fluorescent Gel Particles In The Nanometer Range For Detection Of Metabolites In Living Cells"; Almdal, K.; Sun, H.; Poulsen, K. A.; Arleth, L.; Jakobsen, I.; Gu, H.; Scharff-Poulsen, M. A.; *Polym. Adv. Technol.* 2006, 17, 790.
98. "Development Of A Quasi-Distributed Optical Fibre pH Sensor Using A Covalently Bound Indicator"; Wallace, A. P.; Elliott, N.; Uttamlal, M.; Holmes-Smith, S. A.; And Campbell, M.; *Meas. Sci. Technol.* 2001, 12, 882.

99. “High-Performance Fiber-Optic pH Microsensors For Practical Physiological Measurements Using A Dual-Emission Sensitive Dye”; Song, A.; Parus, S.; Kopelman, R.; *Anal. Chem.* 1997, 69, 863.
100. A) “Self-Assembled Hexa-peri-hexabenzocoronene Graphitic Nanotube”; Hill, P. J.; Jin, W.; Kosaka, A.; Fukushima, T.; Ichihara, H.; Shimomura, T.; Ito, K.; Hashizume, T.; Ishii, N.; Aida, T.; *Science* 2004, 304, 1481 – 1483;
(B) “Hierarchical Self-Assembly Of Chiral Rod-Like Molecules As A Model For Peptide Beta -Sheet Tapes, Ribbons, Fibrils, And Fibers”; Aggeli, A.; Nyrkova, A. I.; Bell, M.; Harding, R.; Carrick, L.; Mcleish, B. C. T.; Semenov, N. A.; Boden, N.; *Proc. Natl. Acad. Sci.* 2001, 98, 11857 – 11862.
101. (A) “New Triply Hydrogen Bonded Complexes With Highly Variable Stabilities”; Murray, T. J.; Zimmerman, S. C.; *J. Am. Chem. Soc.* 1992, 114, 4010-4011.
(B) “Complexation-Induced Unfolding Of Heterocyclic Ureas. Simple Foldamers Equilibrate With Multiply Hydrogen-Bonded Sheetlike Structures”; Corbin, P. S.; Zimmerman, S. C.; Thiessen, P. A.; Hawryluk, N. A.; Murray, T. J.; *J. Am. Chem. Soc.* 2001, 123, 10475-10488.
(C) “A Highly Stable Quadruply Hydrogen-Bonded Heterocomplex Useful For Supramolecular Polymer Blends”; Park, T.; Zimmerman, S. C.; Nakashima, S.; *J. Am. Chem. Soc.* 2005, 127, 6520-6521.
102. “HPLC Separation Of Dna Adducts Based On Hydrogen Bonding”; Feibush, B.; Saha, M.; Onan, K.; Karger, B.; Giese, R.; *J. Am. Chem. Soc.* 1987, 109, 7531-7533.
103. “Nucleotide Base Recognition: Ditopic Binding Of Guanine To A Macrocyclic Receptor Containing Naphthyridine And Naphthalene Units”; Hamilton, A. D.; Pant, N.; *J. Chem. Soc. Chem. Commun.* 1988, 765-766.
104. (A) “Recognition Of A Single Guanine Bulge By 2-acylamino-1,8-naphthyridine”; Nakatani, K.; Sando, S.; Saito, I.; *J. Am. Chem. Soc.* 2000, 122, 2172-2177.
(B) “Use Of Abasic Site-Containing Dna Strands For Nucleobase Recognition In Water”; Yoshimoto, K.; Nishizawa, S.; Minagawa, M.; Teramae, N.; *J. Am. Chem. Soc.* 2003, 125, 8982-8983.
(C) “Specific Recognition Of Naphthyridine-Based Ligands Toward Guanine-Containing Bulges In RNA Duplexes And RNA–DNA Heteroduplexes”; Tok, J. B. H.; Bi, L.; Saenz, M.; *Bioorg. Med. Chem. Lett.* 2005, 15, 827-831.

- (D) "A New Ligand Binding To G–G Mismatch Having Improved Thermal And Alkaline Stability"; Peng, T.; Murase, T.; Goto, Y.; Kobori, A.; Nakatani, K.; *Bioorg. Med. Chem. Lett.* 2005, 15, 259-262.
105. (A) "2,7-bis(1H-pyrrol-2-yl)ethynyl-1,8-naphthyridine: An Ultrasensitive Fluorescent Probe For Glucopyranoside"; Liao, J. H.; Chen, C. T.; Chou, H. C.; Cheng, C. C.; Chou, P. T.; Fang, J. M.; Slanina, Z.; Chow, T. J.; *Org. Lett.* 2002, 4, 3107-3110.
- (B) "Fluorescent And Circular Dichroic Detection Of Monosaccharides By Molecular Sensors: Bis[(pyrrolyl)ethynyl]naphthyridine And Bis[(indolyl)ethynyl] naphthyridine"; Fang, J. M.; Selvi, S.; Liao, J. H.; Slanina, Z.; Chen, C. T.; Chou, P. T.; *J. Am. Chem. Soc.* 2004, 126, 3559-3566.
- (C) "Two-Stage Sensing Property Via A Conjugated Donor-Acceptor-Donor Constitution: Application To The Visual Detection Of Mercuric Ion"; Huang, J. H.; Wen, W. H.; Sun, Y. Y.; Chou, P. T.; Fang, J. M.; *J. Org. Chem.* 2005, 70, 5827-5832.
106. (A) "Integrated Nanoparticle–Biomolecule Hybrid Systems: Synthesis, Properties, And Applications"; Katz, E.; Willner, I.; *Angew. Chem., Int. Ed.* 2004, 43, 6042–6108.
- (B) "Synthesis, Characterization, And Applications Of Dendrimer-Encapsulated Nanoparticles"; Scott, R. W. J.; Wilson, O. M.; Crooks, R. M.; *J. Phys. Chem. B* 2005, 109, 692–704.
- (C) "Applications Of Nanoparticles In Biology"; De, M.; Ghosh, P. S.; Rotello, V. M.; *Adv. Mater.* 2008, 20, 4225–4241.
- (D) "Biological Applications Of Gold Nanoparticles"; Sperling, R. A.; Gil, P. R.; Zhang, F.; Zanella, M.; Parak, W. J.; *Chem. Soc. Rev.* 2008, 37, 1896–1908.
107. (A) "Simple And Rapid Colorimetric Sensing Of Enzymatic Cleavage And Oxidative Damage Of Single-Stranded DNA With Unmodified Gold Nanoparticles As Indicator"; Shen, Q.; Nie, Z.; Guo, M.; Zhong, C.J.; Lin, B.; Li, W.; Yao, S.; *Chem. Commun.* 2009, 929–931.
- (B) "Optical Detection Of Brain Cell Activity Using Plasmonic Gold Nanoparticles"; Zhang, J.; Atay, T.; Nurmikko, A. V.; *Nano Lett.* 2009, 9, 519-524.

108. (A) "A Glucose Biosensor Based On Deposition Of Glucose Oxidase Onto Crystalline Gold Nanoparticle Modified Carbon Nanotube Electrode"; Rakhi, R. B.; Sethupathi, K.; Ramanprabhu, S.; *J. Phys. Chem. B.* 2009, 113, 3190–3194.
- (B) "Nanocatalyst-Based Assay Using DNA-Conjugated Au Nanoparticles For Electrochemical Dna Detection"; Selvaraju, T.; Das, J.; Jo, K.; Kwon, K.; Huh, C. H.; Kim, T. K.; Yang, H.; *Langmuir* 2008, 24, 9883–9888.
- (C) "Specific And Sensitive Detection Of Nucleic Acids And Rnases Using Gold Nanoparticle–RNA–Fluorescent Dye Conjugates"; Kim, J. H.; Estabrook, R. A.; Braum, G.; Lee, B. R.; Reich, N. O.; *Chem. Commum.* 2007, 4342–4344.
- (D) "Reversible Binding Of Fluorescent Proteins At DNA–Gold Nanoparticles"; Hazarika, P.; Kukolka, F.; Niemeyer, C. M.; *Angew. Chem. Int. Ed.* 2006, 45, 6827–6830.
109. (A) "A Simple Assay For Direct Colorimetric Visualization Of Trinitrotoluene At Picomolar Levels Using Gold Nanoparticles"; Jiang, Y.; Zhao, H.; Zhu, N.; Lin, Y.; Yu, P.; Mao, L.; *Angew. Chem. Int. Ed.* 2008, 47, 8601–8604.
- (B) "Imprinting Of Molecular Recognition Sites Through Electropolymerization Of Functionalized Au Nanoparticles: Development Of An Electrochemical Tnt Sensor Based On π -Donor-Acceptor Interactions"; Riskin, M.; Tel-Vered, R.; Bourenko, T.; Granot, E.; Willner, I.; *J. Am. Chem. Soc.* 2008, 130, 9726–9733.
- (C) "Highly Sensitive And Selective Colorimetric Sensors For Uranyl (UO_2^{2+}): Development And Comparison Of Labeled And Label-Free Dnazyme-Gold Nanoparticle Systems"; Lee, J. H.; Wang, Z.; Liu, J.; Lu, Y.; *J. Am. Chem. Soc.* 2008, 130, 14217–14226.
110. (A) "Synthesis Of Highly Fluorescent Gold Nanoparticles For Sensing Mercury(II)"; Huang, C. C.; Yang, Z.; Lee, K. H.; Chang, H. T.; *Angew. Chem. Int. Ed.* 2007, 46, 6824–6828.
- (B) "Fluorescent Gold Nanoparticles-Based Fluorescence Sensor For Cu^{2+} Ions"; Chen, W.; Tu, X.; Guo, X.; *Chem. Commum.* 2009, 1736–1738.
- (C) "Potassium Ion Recognition By Facile Dithiocarbamate Assembly Of Benzo-15-crown-5–gold Nanoparticles"; Patel, G.; Kumar, A.; Pal, U.; Menon, S.; *Chem. Commum.* 2009, 1849–1851.

- (D) “Lanthanide Luminescent Displacement Assays: The Sensing Of Phosphate Anions Using Eu(III)–Cyclen-Conjugated Gold Nanoparticles In Aqueous Solution”; Massue, J.; Quinn, S. J.; Gunnlaugsson, T.; *J. Am. Chem. Soc.* 2008, 130, 6900–6901.
111. “A Simple And Sensitive Colorimetric Ph Meter Based On Dna Conformational Switch And Gold Nanoparticle Aggregation”; Chen, C.; Song, G.; Ren, J.; Qu, X.; *Chem. Commun.* 2008, 6149–6151.
112. (A) “Photostable Single-Molecule Nanoparticle Optical Biosensors For Real-Time Sensing Of Single Cytokine Molecules And Their Binding Reactions”; Huang, T.; Nallathamby, P. D.; Xu, X. H. N.; *J. Am. Chem. Soc.* 2008, 130, 17095–17105.
- (B) “Surface-Enhanced Raman Spectroscopy For Trace Arsenic Detection In Contaminated Water”; Mulvihill, M.; Tao, A.; Benjauthrit, K.; Arnold, J.; Yang, P.; *Angew. Chem. Int. Ed.* 2008, 47, 6456–6460.
113. (A) “Surface Attached-Poly(acrylic Acid) Network As Nanoreactor To In-Situ Synthesize Palladium Nanoparticles For H₂O₂ Sensing”; Tang, Y.; Cao, Y.; Wang, S.; Shen, G.; Yu, R.; *Sensors And Actuators B* 2009, 137, 736–740.
- (B) “Click” Dendrimers: Synthesis, Redox Sensing Of Pd(OAc)₂, And Remarkable Catalytic Hydrogenation Activity Of Precise Pd Nanoparticles Stabilized By 1,2,3-Triazole-Containing Dendrimers”; Ornelas, C.; Aranzaes, J. R.; Salmon, L.; Astruc, D.; *Chem. Eur. J.* 2008, 14, 50–64.
114. (A) “Electrochemical Coding Technology For Simultaneous Detection Of Multiple DNA Targets”; Wang, J.; Liu, G.; Merkoci, A.; *J. Am. Chem. Soc.* 2003, 125, 3214–3215.
- (B) “CuS Nanotubes For Ultrasensitive Nonenzymatic Glucose Sensors”; Zhang, X.; Wang, G.; Gu, A.; Wei, Y.; Fang, B.; *Chem. Commun.* 2008, 5945–5947.
- (C) “A Modular Nanoparticle-Based System For Reagentless Small Molecule Biosensing”; Sandros, M. G.; Gao, D.; Benson, D. E.; *J. Am. Chem. Soc.* 2005, 127, 12198–12199.
115. (A) “Synthesis, Characterization And Sensing Properties Of Nano-SnO₂ Supported On SBA-15 As Highly Sensitive Semiconductor Gas Sensors”; Yang, J.; Hidajat, K.; Kawi, S.; *J. Mater. Chem.* 2009, 19, 292–298.

- (B) “Nanocrystalline Metal Oxides From The Injection Of Metal Oxide Sols In Coordinating Solutions: Synthesis, Characterization, Thermal Stabilization, Device Processing, And Gas-Sensing Properties”; Epifani, M.; Diaz, R.; Arbiol, J.; Comini, E.; Sergent, N.; Pagnier, T.; Siciliano, P.; Faglia, G.; Morante, J. R.; *Adv. Funct. Mater.* 2006, 16, 1488–1498.
- (C) “Simple And Generalized Synthesis Of Oxide–Metal Heterostructured Nanoparticles And Their Applications In Multimodal Biomedical Probes”; Choi, S. H.; Na, H. B.; Park, Y.; An, K.; Kwon, S. G.; Jang, Y.; Park, M.H.; Moon, J.; Son, J. S.; Song, I. C.; Moon, W. K.; Hyeon, T.; *J. Am. Chem. Soc.* 2008, 130, 15573–15580.
116. (A) “Sensing Proteins With Luminescent Silica Nanoparticles”; Latterini, L.; Amelia, M.; *Langmuir* 2009, 25, 4767–4773.
- (B) “Selective Chromofluorogenic Sensing Of Heparin By Using Functionalised Silica Nanoparticles Containing Binding Sites And A Signalling Reporter”; Climent, E.; Calero, P.; Marcos, M. D.; Manez, R. M.; Sancenon, F.; Soto J.; *Chem. Eur. J.* 2009, 15, 1816–1820.
- (C) “Mesoporous Silica Nanoparticles Functionalized With An Oxygen-Sensing Probe For Cell Photodynamic Therapy: Potential Cancer Theranostics”; Cheng, S. H.; Lee, C. H.; Yang, C. S.; Tseng, F. G.; Mou, C. Y.; Lo, L. W.; *J. Mater. Chem.* 2009, 19, 1252–1257.
- (D) “Surface Modification Of Silica Nanoparticles: A New Strategy For The Realization Of Self-Organized Fluorescence Chemosensors”; Rampazzo, E.; Brasola, E.; Marcuz, S.; Mancin, F.; Tecilla, P.; Tonellato, U.; *J. Mater. Chem.* 2005, 15, 2687–2696.
117. (A) “Ratiometric Single-Nanoparticle Oxygen Sensors For Biological Imaging”; Wu, C.; Bull, B.; Christensen, K.; McNeill, J.; *Angew. Chem. Int. Ed.* 2009, 48, 2741–2745.
- (B) “Cadmium(II) (8Hydroxyquinoline) Chloride Nanowires: Synthesis, Characterization And Glucose-Sensing Application”; Pan, H.; Lin, H.; Shen, Q.; Zhu, J. J.; *Adv. Funct. Mater.* 2008, 18, 3692–3698.

- (C) “A Submicrometer Wire-To-Wheel Metamorphism Of Hybrid Tridentate Cyclometalated Platinum(II) Complexes”; Lu, W.; Chui, S. S. Y.; Ng, K. M.; Che, C. M.; *Angew. Chem. Int. Ed.* 2008, 47, 4568–4572.
118. (A) “Infinite Coordination Polymer Nano And Microparticle Structures”; Spokoyny, A. M.; Kim, D.; Sumrein, A.; Mirkin, C. A.; *Chem. Soc. Rev.* 2009, 38, 1218–1227.
- (B) “Chemically Tailorable Colloidal Particles From Infinite Coordination Polymers”; Oh, M.; Mirkin, C. A.; *Nature* 2005, 438, 651–653
- (C) “Ion Exchange As A Way Of Controlling The Chemical Compositions Of Nano- And Microparticles Made From Infinite Coordination Polymers”; Oh, M.; Mirkin, C. A.; *Angew. Chem. Int. Ed.* 2006, 45, 5492–5494.
- (D) “Dynamic Interconversion Of Amorphous Microparticles And Crystalline Rods In Salen-Based Homochiral Infinite Coordination Polymers”; Jeon, Y. M.; Heo, J.; Mirkin, C. A.; *J. Am. Chem. Soc.* 2007, 129, 7480–7481.
- (E) “Growth-Controlled Formation Of Porous Coordination Polymer Particles”; Cho, W.; Lee, H. J.; Oh, M.; *J. Am. Chem. Soc.* 2008, 130, 16943–16946.
119. (A) “Photophysical Investigations Of Rhenium^ICl(CO)₃(Phenanthroline) Complexes”; Striplin, D. R.; Crosby, G. A.; *Coord. Chem. Rev.* 2001, 211, 163–175.
- (B) “Developing The {M(CO)₃}⁺ Core For Fluorescence Applications: Rhenium Tricarbonyl Core Complexes With Benzimidazole, Quinoline, And Tryptophan Derivatives”; Wei, L.; Babich, J. W.; Ouellette, W.; Zubieta, J.; *Inorg. Chem.* 2006, 45, 3057–3066.
- (C) “Preparative Routes To Luminescent Mixed-Ligand Rhenium(I) Dicarbonyl Complexes”; Smithback, J. L.; Helms, J. B.; Schutte, E.; Woessner, S. M.; Sullivan, B. P.; *Inorg. Chem.* 2006, 45, 2163–2174.
- (D) “A Spectroscopic And Computational Study On The Effects Of Methyl And Phenyl Substituted Phenanthroline Ligands On The Electronic Structure Of Re(I) Tricarbonyl Complexes Containing 2,6-Dimethylphenylisocyanide”; Villegas, J. M.; Stoyanov, S. R.; Huang, W.; Rillema, D. P.; *Dalton Trans.* 2005, 1042–1051.
- (E) “Photophysical, Spectroscopic, And Computational Studies Of A Series Of Re(I) Tricarbonyl Complexes Containing 2,6-Dimethylphenylisocyanide And 5-

- And 6-Derivatized Phenanthroline Ligands”; Villegas, J. M.; Stoyanov, S. R.; Huang W.; Rillema, D. P.; *Inorg. Chem.* 2005, 44, 2297–2309.
- (F) “Complexes Of Substituted Derivatives Of 2-(2-pyridyl)benzimidazole With Re(I), Ru(II) And Pt(II): Structures, Redox And Luminescence Properties”; Shavaleev, N. M.; Bell, Z. R.; Easun, T. L.; Rutkaite, R.; Swanson, L.; Ward, M. D.; *Dalton Trans.* 2004, 3678–3688.
- (G) “Synthesis, Photophysics And Photochemistry Of Novel Luminescent Rhenium(I) Photoswitchable Materials”; Yam, V. W. W.; Lau V. C Y.; Cheung, K. K.; *J. Chem. Soc., Chem. Commun.* 1995, 259–261.
- (H) “Photoswitchable Trinuclear Transition-Metal Complexes. Intramolecular Triplet–Triplet Energy Transfer From *fac*-(diimine)Re(I)(CO)₃ Chromophores To A Stilbene-Like Bridging Ligand”; Sun, S. S.; Robson, E.; Dunwoody, N.; Silva, A. S.; Brinn, I. M.; Lees, A. J.; *Chem. Commun.* 2000, 201–202.
120. (A) “Realizing Green Phosphorescent Light-Emitting Materials From Rhenium(I) Pyrazolato Diimine Complexes”; Ranjan, S.; Lin, S. Y.; Hwang, K. C.; Chi, Y.; Ching, W. L.; Liu, C. S.; *Inorg. Chem.* 2003, 42, 1248–1255.
- (B) “Trifunctional Light-Emitting Molecules Based On Rhenium And Ruthenium Bipyridine Complexes”; Gong, X.; Ng, P. K.; Chan, W. K.; *Adv. Mater.* 1998, 10, 1337.
121. “The Role Of Ruthenium And Rhenium Diimine Complexes In Conjugated Polymers That Exhibit Interesting Opto-Electronic Properties”; Ng, P. K.; Gong, X.; Chan, S. H.; Lam, L. S. M.; Chan, W. K.; *Chem. Eur. J.* 2001, 7, 4358–43.
122. (A) “Synthesis, Characterization, Crystal Structure, And Electrochemical, Photophysical, And Protein-Binding Properties Of Luminescent Rhenium(I) Diimine Indole Complexes”; Lo, K. K. W.; Tsang, K. H. K.; Hui, W. K.; Zhu, N.; *Inorg. Chem.* 2005, 44, 6100–6110.
- (B) “Novel Rhenium(I) Polypyridine Biotin Complexes That Show Luminescence Enhancement And Lifetime Elongation Upon Binding To Avidin”; Lo, K. K. W.; Hui, W. K.; Ng, D. C. M.; *J. Am. Chem. Soc.* 2002, 124, 9344–9345.
123. Yam, V. W. W.; Lo, K. K. W.; Cheung, K. K.; Kong, R. Y. C.; *J. Chem. Soc., Chem Commun.* 1995, 1191–1192.

124. (A) "Synthesis, Characterization, Photophysical Properties, And Biological Labeling Studies Of A Series Of Luminescent Rhenium(I) Polypyridine Maleimide Complexes"; Lo, K. K. W.; Hui, W. K.; Ng, D. C. M.; Cheung, K. K.; *Inorg. Chem.* 2002, 41, 40-46.
- (B) "Luminescent Rhenium(I) Polypyridine Complexes With An Isothiocyanate Moiety-Versatile Labelling Reagents For Biomolecules"; Lo, K. K. W.; Ng, D. C. M.; Hui, W. K.; Cheung, K. K.; *J. Chem. Soc., Dalton Trans.* 2001, 2634–2640.
125. "A Long-Lived Highly Luminescent Re(I) Metal-Ligand Complex As A Biomolecular Probe"; Guo, X. Q.; Castellano, F. N.; Li, L.; Szmecinski, H.; Lakowicz, J. R.; Sipior, J. *Analyt. Biochem.* 1997, 254, 179–186.
126. (A) "Ion Pair Cooperative Binding Of Potassium Salts By New Rhenium(I) Bipyridine Crown Ether Receptors"; Uppadine, L. H.; Redman, J. E.; Dent, S. W.; Drew, M. G. B.; Beer, P. D.; *Inorg. Chem.* 2001, 40, 2860–2869.
- (B) "Electrochemical, Photophysical, And Anion-Binding Properties Of A Luminescent Rhenium(I) Polypyridine Anthraquinone Complex With A Thiourea Receptor"; Lo, K. K. W.; Lau, J. S. Y.; Fong, V. W. Y.; *Organometallics* 2004, 23, 1098–1106.
127. "Proton-Induced Luminescence Of Mono- And Dinuclear Rhenium(I) Tricarbonyl Complexes Containing 4-Pyridinealdazine"; Cattaneo, M.; Fagelde, F.; Katz, N. E.; *Inorg. Chem.* 2006, 45, 6884–6891.
128. "Luminescence-Based Oxygen Sensors: $\text{ReL}(\text{CO})_3\text{Cl}$ And $\text{ReL}(\text{CO})_3\text{CN}$ Complexes On Copolymer Supports"; Kneas, K. A.; Xu, W.; Demas, J. N.; Degraff, B. A.; Zipp, A. P.; *J. Fluorescence* 1998, 8, 295.
129. "Metallocyclic Receptors With ReI/OsII-Based Moieties: Molecular Photophysics And Selective Molecular Sensing"; Xu, D.; Khin, K. T.; Van Der Veer, W. E.; Ziller, J. W.; Hong, B.; *Chem. Eur. J.* 2001, 7, 2425.
130. (A) "Synthesis And Photophysical Properties Of Neutral Luminescent Rhenium-Based Molecular Rectangles"; Rajendran, T.; Manimaran, B.; Liao, R. T.; Lin, R. Y.; Thanasekaran, P.; Lee, G. H.; Peng, S. M.; Liu, Y. H.; Chang, I. J.; Rajagopal, S.; Lu, K. L.; *Inorg. Chem.* 2003, 42, 6388–6394.

- (B) “Aggregate Of Alkoxy-Bridged Re(I)-Rectangles As A Probe For Photoluminescence Quenching”; Thanasekaran, P.; Wu, J. Y.; Manimaran, B.; Rajendran, T.; Chang, I. J.; Rajagopal, S.; Lee, G. H.; Peng, S. M.; Lu, K. L.; *J. Phys. Chem. A* 2007, *111*, 10953–10960.
131. “Accumulation Of Trinitrotoluene (TNT) In Aquatic Organisms: Part 1 - Bioconcentration And Distribution In Channel Catfish (*Ictalurus Punctatus*)”; David, R.; Belden, J. B.; Lotufo, G. R.; Lydy, M. J.; *Chemosphere* 2005, *58*, 1153.
132. “Cytotoxic And Genotoxic Effects Of Energetic Compounds On Bacterial And Mammalian Cells In Vitro”; Lachance, B.; Robidoux, P. Y.; Hawari, J.; Ampleman, G.; Thiboutot, S.; Sunahara, G. I.; *Mutation Research, Genetic Toxicology And Environmental Mutagenesis* 1999, *444*, 1, 25-39.
133. Robidoux, P.; Hawari, J.; Thiboutot, S.; *Environ. Toxicol. Chem.* 1999, *23*, 1026
134. (A) “Fluorescent Porous Polymer Films As TNT Chemosensors: Electronic And Structural Effects”; Yang, J. S.; Swager, T. M.; *J. Am. Chem. Soc.* 1998, *120*, 11864–11873.
- (B) “Polymer Sensors For Nitroaromatic Explosives Detection”; Toal, S. J.; Trogler, W. C.; *J. Mater. Chem.* 2006, *16*, 2871–2883.
135. (A) “Luminescent Oligo(tetraphenyl)silole Nanoparticles As Chemical Sensors For Aqueous TNT”; Toal, S. J.; Magde, D.; Trogler, W. C.; *Chem. Commun.* 2005, 5465–5467.
- (B) “Synthesis, Luminescence Properties, And Explosives Sensing With 1,1-Tetraphenylsilole- And 1,1-Silafluorene-Vinylene Polymers”; Sanchez, J. C.; Dipasquale, A. G.; Rheingold, A. L.; Trogler, W. C.; *Chem. Mater.* 2007, *19*, 6459–6470.
- (C) “Detection Of Nitroaromatic Explosives Based On Photoluminescent Polymers Containing Metalloles”; Sohn, H.; Sailor, M. J.; Magde, D.; Trogler, W. C.; *J. Am. Chem. Soc.* 2003, *125*, 3821–3830.
- (D) “Detection Of TNT And Picric Acid On Surfaces And In Seawater By Using Photoluminescent Polysiloles”; Sohn, H.; Calhoun, R. M.; Sailor, M. J.; Trogler, W. C.; *Angew. Chem. Int. Ed.* 2001, *40*, 2104–2105.
136. (A) “Metalloporphyrins As Sensing Elements For The Rapid Detection Of Trace TNT Vapor”; Tao, S.; Li, G.; Zhu, H.; *J. Mater. Chem.* 2006, *16*, 4521–4528.

- (B) “High-Performance TNT Chemosensory Materials Based On Nanocomposites With Bimodal Porous Structures”; Tao, S.; Yin, J.; Li, G.; *J. Mater. Chem.* 2008, 18, 4872–4878.
137. (A) “Fluorescent Sensors For Nitroaromatic Compounds Based On Monolayer Assembly Of Polycyclic Aromatics”; Zhang, S.; Lu, F.; Gao, L.; Ding, L.; Fang, Y.; *Langmuir* 2007, 23, 1584–1590.
- (B) “Fluorescence Quenching Of Benzo[k]fluoranthene In Poly(vinyl alcohol) Film: A Possible Optical Sensor For Nitro Aromatic Compounds”; Patra, D.; Mishra, A. K.; *Sensors Actuators B* 2001, 80, 278–282.
- (C) “Rapid Nitroaromatic Compounds Sensing Based On Oligopyrene”; Bai, H.; Li, C.; Shi, G.; *Sensors Actuators B* 2008, 130, 777–782.
138. “Handbook Of Physical Properties Of Organic Chemicals”; Howard, P. H.; Meylan, W. M.; 1997.
139. “High-Sensitivity Detection Of TNT”; Pushkarsky, M. B.; Dunayevskiy, I. G.; Prasanna, M.; Tsekoun, A. G.; Go, R.; Kumar, C.; Patel, N.; *Proc. Natl. Acad. Sci.* 2006, 103, 52, 19630-19630.
140. “Fluorescent Porous Polymer Films As TNT Chemosensors: Electronic And Structural Effects”; Yang, J. S.; Swager, T. M.; *J. Am. Chem. Soc.* 1998, 120, 46, 11864-11873.
141. “Porous Shape Persistent Fluorescent Polymer Films: An Approach To TNT Sensory Materials”; Yang, J. S.; Swager, T. M.; *J. Am. Chem. Soc.* 1998, 120, 21, 5321-5322
142. “Conjugated Polymer-Based Chemical Sensors”; Mcquade, D. T.; Pullen, A. E.; Swager, T. M.; *Chem. Rev.* 2000, 100, 7, 2537-2574.
143. “Self-Amplifying Semiconducting Polymers For Chemical Sensors”; Swager, T. M.; Wosnick, J. H.; *Mrs Bull.* 2002, 27, 6, 446-450.
144. “Three-Dimensional Electronic Delocalization In Chiral Conjugated Polymers”; Zahn, S.; Swager, T. M.; *Angew. Chem., Int. Ed.* 2002, 41, 22, 4225-4230.
145. “Sensitivity Gains In Chemosensing By Lasing Action In Organic Polymers”; Rose, A.; Zhu, Z.; Madigan, C. F.; Swager, T. M.; Bulovi, V.; *Nature* 2005, 434, 7035, 876-879.

146. "Chemical Sensors Based On Amplifying Fluorescent Conjugated Polymers"; Thomas, S. W.; Joly, G. D.; Swager, T. M.; *Chem. Rev.* 2007, 107, 4, 1339-1386.
147. "Iptycenes In The Design Of High Performance Polymers"; Swager, T. M.; *Acc. Chem. Res.* 2008, 41, 9, 1181-1189.
148. "Detection Of TNT And Picric Acid On Surfaces And In Seawater By Using Photoluminescent Polysiloles"; Sohn, H.; Calhoun, R. M.; Sailor, M. J.; Trogler, W. C.; *Angew. Chem., Int. Ed.* 2001, 40, 11, 2104-2105.
149. "Detection Of Nitroaromatic Explosives Based On Photoluminescent Polymers Containing Metalloles"; Sohn, H.; Sailor, M. J.; Magde, D.; Trogler, W. C.; *J. Am. Chem. Soc.* 2003, 125, 13, 3821-3830.
150. "Synthesis, Luminescence Properties, And Explosives Sensing With 1,1-Tetraphenylsilole And 1,1-Silafluorene-Vinylene Polymers"; Sanchez, J. C.; Dipasquale, A. G.; Rheingold, A. L.; Trogler, W. C.; *Chem. Mater.* 2007, 19, 26, 6459-6470.
151. "Efficient Blue-Emitting Silafluorene-Fluorene-Conjugated Copolymers: Selective Turn-Off/Turn-On Detection Of Explosives"; Sanchez, J. C.; Trogler, W. C.; *J. Mater. Chem.* 2008, 18, 26, 3143-3156.
152. "Detection Of Explosives By Electronic Noses"; Yinon, J.; *Anal. Chem.* 2003, 75, 5, 99a.
153. "Carbenes May Be Key To Enzymes Power"; Rouhi, A. M.; *Chem. Eng. News* 1997, 75, 12.
154. "Challenge For Physical Chemistry Of Explosives Detection"; Steinfeld, J. I.; Wormhoudt, J. A.; *Rev. Phys. Chem.* 1998, 49, 203-232.
155. (A) "Instrumentation For Trace Detection Of High Explosives"; Moore, S. D.; *Rev. Sci. Instrum.* 2004, 75, 2499.
(B) "High Explosives Vapor Detection By Glow Discharge Ion Trap Mass Spectrometry"; Mcluckey, A. S.; Goeringer, E. D.; Asano, G. K.; Vaidyanathan, G.; Stephenson, L. J.; Rapid, Jr.; *Commun. Mass Spectrom.* 1996, 10, 287.
156. (A) "Self-Assembly Of A Nanoscopic Prism Via A New Organometallic Pt₃ Acceptor And Its Fluorescent Detection Of Nitroaromatics"; Ghosh, S.; And Mukherjee, S. P.; *Organometallics* 2008, 27, 316.

- (B) “Self-Assembly Of Neutral And Cationic Pd^{II} Organometallic Molecular Rectangles: Synthesis, Characterization And Nitroaromatic Sensing”; Bar, K. A.; Shanmugaraju, S.; Chi, W. K.; And Mukherjee, S.P.; *Dalton Trans.* 2011, 40, 2257.
- (C) “Coordination-Driven Self-Assembly Of Metallamacrocycles Via A New Pt^{II}₂ Organometallic Building Block With 90° Geometry And Optical Sensing Of Anions”; Shanmugaraju, S.; Bar, K. A.; Chi, W. K.; And Mukherjee, S. P.; *Organometallics* 2010, 29, 2971.
- (D) “Simple Molecule-Based Fluorescent Sensors For Vapor Detection Of TNT”; Zyryanov, V.G.; Palacios, A. M.; Anzenbacher, P.; *Org. Lett.* 2008, 10, 3681.
- (E) “Photoluminescent Coordination Polymers Of D¹⁰ Metals With 4,4'-Dipyridylsulfide (Dps)”; Muthu, S.; Ni, Z.; Vittal, J. J.; *Inorg. Chim. Acta* 2005, 358, 595
- (F) “Novel Ferrocene Receptors For Barbiturates And Ureas”; Collinson, R. S.; Gelbrich, T.; Hursthouse, B. M.; Tucker, R. H. J.; *Chem. Commun.* 2001, 555.
157. (A) “Synthesis And Photophysical Properties Of Neutral Luminescent Rhenium-Based Molecular Rectangles”; Rajendran, T.; Manimaran, B.; Liao, R. T.; Lin, R. Y.; Thanasekaran, P.; Lee, G. H.; Peng, S. M.; Liu, Y. H.; Chang, I. J.; Rajagopal, S.; Lu, K. L.; *Inorg. Chem.* 2003, 42, 6388–6394.
- (B) “Aggregate Of Alkoxy-Bridged Re(I)-Rectangles As A Probe For Photoluminescence Quenching”; Thanasekaran, P.; Wu, J. Y.; Manimaran, B.; Rajendran, T.; Chang, I. J.; Rajagopal, S.; Lee, G. H.; Peng, S. M.; Lu, K. L.; *J. Phys. Chem. A* 2007, 111, 10953–10960.
158. “Self-Assembly Triangular And Square Rhenium(I) Tricarbonyl Complexes: A Comprehensive Study Of Their Preparation, Electrochemistry, Photophysics, Photochemistry, And Host–Guest Properties”; Sun, S. S.; Lee, A. J.; *J. Am. Chem. Soc.* 2000, 122, 8956–8967.
159. “Supramolecular Polymer For Explosives Sensing: Role Of H-Bonding In enhancement Of Sensitivity In The Solid State”; Gole, B.; Shanmugaraju, S.; Kumar, A.; Mukherjee, S.P.; *Chem. Commun.* 2011, 47, 10046–10048.
160. “Triphenylene Derivatives: Chemosensors For Sensitive Detection Of Nitroaromatic Explosives”; Bhalla, V.; Arora, H.; Singh, H.; Kumar, M.; *Z Dalton Trans.* 2013, 42, 969-974.

161. "Pyrene-Functionalized Ruthenium Nano Particles As Effective Chemosensors For Nitroaromatic Derivatives"; Chen, W.; Zuckerman, N. B.; Konopelski, J. P.; Chen, S.; *Anal Chem.* 2010, 15, 82, 461-465.
162. "Micro And Nanostructure Surface Morphology On Electrospun Polymer Fibers"; Megelski, S.; Stephens, J. S.; Chase, D. B.; Rabolt, J. F.; *Macromolecules* 2002, 35, 22, 8456-8466 .
163. "Attogram Sensing Of Trinitrotoluene With A Self-Assembled Molecular Gelator"; Kartha, K. K.; Babu, S. S.; Srinivasan, S.; Ajayaghosh, A.; *J. Am. Chem. Soc.* 2012, 134, 10, 4834-4841.
164. "Detection Of Explosives With A Fluorescent Nanofibril Film"; Naddo, T.; Che, Y.; Zhang, W.; Balakrishnan, K.; Yang, X.; Yen, M.; Zhao, J.; Moore, J. S.; Zang, L.; *J. Am. Chem. Soc.* 2007, 129, 22, 6978-6979.
165. "Organic Nanofibrils Based On Linear Carbazole Trimer For Explosive Sensing"; Zhang, C.; Che, Y.; Yang, X.; Bunes, B. R.; Zang, L.; *Chem. Commun.* 2010, 46, 30, 5560-5562.
166. "Fluorescent Nanoaggregates Of Pentacenequinone Derivative For Selective Sensing Of Picric Acid In Aqueous Media"; Bhalla, V.; Gupta, A.; Kumar, M.; *Org. Lett.* 2012, 14, 3112.
167. "Structure Solution Of The 6,13-Pentacenequinone Surface-Induced Polymorph By Combining X-Ray Diffraction Reciprocal-Space Mapping And Theoretical Structure Modeling"; Salzmann, I.; Nabok, D.; Oehzelt, M.; Duhm, S.; Moser, A.; Heimel, G.; Puschnig, P.; Ambrosch-Draxl, C.; Rabe, J. P.; Koch, N.; *Crystal Growth & Design* 2011, 11, 2, 600-606.
168. "Phase Separation In Vacuum Codeposited Pentacene/6,13-Pentacenequinone Thin Films"; Salzmann, I.; Opitz, R.; Rogaschewski, S.; Rabe, J. P.; Koch, N.; *Phys. Rev. B.* 2004, 75, 174108.
169. "Bulk Phase Two Dimensional Chiral Growth Of 6, 13-Pentacenequinone On Sio₂"; Marco, P. D.; Fioriti, F.; Bisti, F.; Parisse, P.; Santucci, S.; Ottaviano, L. J.; *Appl. Phys.* 2011, 109, 063508.
170. "Enhanced Fluorescent Intensity Of Graphene Oxide–Methyl Cellulose Hybrid In Acidic Medium: Sensing Of Nitro-Aromatics"; Kundu, A.; Layek, K. R.; Nandi, K. A.; *J. Mater. Chem.*, 2012, 22, 8139-8814.

171. “Inverted Opal Fluorescent Film Chemosensor For The Detection Of Explosive Nitroaromatic Vapors Through Fluorescence Resonance Energy Transfer”; Fang, Q.; Geng, J.; Liu, B.; Gao, D.; Li, F.; Wang, Z.; Guan, G.; Zhang, Z.; *Chemistry*. 2009, 15, 43, 11507-11514.
172. “Electrochemical Detection Of Ultratrace Nitroaromatic Explosives Using Ordered Mesoporous Carbon”; Zang, J.; Guo, C.X.; Hu, F.; Yu, L.; Li, Cm.; *Anal Chim Acta*. 2011, 683, 2, 187-191.
173. “Detection Of Nitrobenzene, DNT, And TNT Vapors By Quenching Of Porous Silicon Photoluminescence”; Content, S.; Trogler, W. C.; Sailor, M.; *Chemistry*. 2000, 6, 12, 2205-2213.
174. (A) “N-Heterocyclic Carbenes: Reagents, Not Just Ligands”; Nair, V.; Bindu, S.; Sreekumar, V.; *Angew. Chem. Int. Ed.* 2004, 43, 5130.
(B) “Nucleophilic Carbenes In Asymmetric Organocatalysis”; Enders, D.; Balensiefer, T.; *Acc. Chem. Res.* 2004, 37, 534.
175. “A Modular Approach To Main-Chain Organometallic Polymers”; Boydston, A.J.; Williams, K.A.; Bielawski, C.W.; *J. Am. Chem. Soc.* 2005, 127, 12496.
176. “The Chemistry Of The Benzimidazoles”; Wright, B.J.; 1951.
177. (A) “Trois Nouvelles Voies De Synthèse Des Dérivés 1,3-Azoliques Sous Micro-Ondes”; Bourgrin, K.; Loupy, A.; Soufiaoui, M.; *Tetrahedron* 1998, 54, 8055–8064.
(B) “A Simple And Efficient Method For The Synthesis Of Novel Trifluoromethyl benzimidazoles Under Microwave Irradiation Conditions”; Reddy, G. V.; Rao, V. V. V. N. S. R.; Narsaiah, B.; Rao, P. S.; *Synth. Commun.* 2002, 32, 2467.
(C) “Benzimidazoles: Oxydation Hétérocyclisante Par Le Nitrobenzène Ou Le Diméthylsulfoxyde Sur Silice Et Sous Irradiation Micro-Ondes Ou Ultra-Violet”; Ben-Alloum, A.; Bakkas, S.; Soufiaoui, M.; *Tetrahedron Lett.* 1998, 39, 4481.
178. “A Simple And Efficient Procedure For The Synthesis Of Benzimidazoles Using Air As The Oxidant”; Lin, S.; Yang, L.; *Tetrahedron Letters* 2005, 46, 4315–4319.
179. “Microwave-Assisted One Step High-Throughput Synthesis Of Benzimidazoles”; Lin, Y. S.; Isome, Y.; Stewart, E.; Liu, F. J.; Yohannes, D.; Yu, L.; *Tetrahedron Letters* 2006, 47, 2883–288.

180. “NaHSO₄-SiO₂ Promoted Synthesis Of Benzimidazole Derivatives”; Kumar, R.V.; Satyanarayana, V. V. V.; Srinivaasa R. B.; *Scholars Research Library, Archives Of Applied Science Research* 2012, 4, 3, 1517-1521.
181. “An Efficient Synthesis Of Benzimidazole By Cyclization–Oxidation Processes Using Fe/MgO As A Heterogeneous Recyclable Catalyst”; Borhade, V. A.; Tope, R. K.; Dattaprasad R. P.; , *Journal Of Chemical And Pharmaceutical Research*, 2012, 4, 5, 2501-2506.
182. “p-TsOH Catalyzed Synthesis Of 2-Arylsubstituted Benzimidazoles”; Xiangming, H.; Huiqiang, M.; And Yulu, W.; *General Papers Arkivoc* 2007, 13, 150-154
183. “Synthesis And Biological Activity Of 2-(trifluoromethyl)-1H-benzimidazole Derivatives Against Some Protozoa And Trichinella Spiralis”; Yépez-Mulia, L.; Rafael Castillo, R.; *European Journal Of Medicinal Chemistry* 2010, 45, 3135-3141.
184. “Synthesis Of 6-Nitrobenimidazol-1-acetyl Amino Acids And Peptides As Potent Anthelmintic Agents”; Himaja, R. M.; , Ramana, V. M.; *Indian Journal Of Hetero Cyclic Chemistry* 2002, 2, 121-124.
185. “Synthesis And HIV Inhibition Of Novel Benzimidazole Derivatives, John M. Gardiner”; *Bioorganic And Medicinal Chemistry Letters* 1995, 5, 1251-1254.
186. “Derivative Of Benzimidazole Pharmacophore: Synthesis, Anticonvulsant, Antidiabetic And DNA Cleavage Studies”; Hosmani, M. K.; Keri, S. R.; *European Journal Of Medicinal Chemistry* 2010, 45, 1753-1759.
187. “In-vivo Analgesic And Anti-Inflammatory Activities Of Newly Synthesized Benzimidazole Derivatives”; Hosamani, M. K.;, *European Journal Of Medicinal Chemistry* 2010, 45, 2048–205.
188. “Design And Synthesis Of Novel Benzimidazole Derivatives As Inhibitors Of Hepatitis B Virus”; Luo, Yu.; Yao, P. J.; *Bioorganic & Medicinal Chemistry Letters* 2010, 18, 5048-5055.
189. “Synthesis Of Triazoles Thiadiazole And Oxadiazole Bearing 2-thiomethyl benzimidazole And Their Biological Evaluation”; Murugan, V.; Ramaprasad, K.; 2001, *Indian Journal Of Hetero Cyclic Chemistry* 2001, 11, 169-170.

190. “Synthesis And DNA Interaction Of Benzimidazole Dication Which Have Activity Against Opportunistic Infections”; Lombardy, L. R.; Tanious, F.A.; *Journal Of Medicinal Chemistry* 1996, 39, 1452-1462.
191. “2-piperidin-4-yl-benzimidazoles With Broad Spectrum Antibacterial Activities”; Yun, H.; Baogen, W.; Yang, J.; Robinson, D.; Risen, L.; Ranken, R.; Blyn, L.; Eric, Ss.; Swayze, E.; *Bioorg Med Chem Lett.* 2003, 13, 3253-3256.
192. “Hydrazones Of 2-aryl-4-carboxylic Acid Hydrazides: Synthesis And Preliminary Evaluation As Antimicrobial Agents”; Metwally, K. A.; Abdel-Aziz, L. M.; Lashine, S. M.; Husseiny, M. I.; Badawy, R. H.; *Bioorg Med Chem.* 2006;14, 24, 8675-82.
193. “Benzimidazole Derivatives: Spectrum Of Pharmacological Activity And Toxicological Properties”; Spasov, A.; Yozhitsa, L.; Bugaeva, I.; Anisimova Va.; *Pharmaceutical Chemistry Journal.*, 33, 5, 232-243.
194. “Synthesis, Antibacterial, Antifungal Activity And Interaction Of CT-DNA With A New Benzimidazole Derived Cu (II) Complex”; Arjmand, F.; Mohani, B.; Ahmad, S.; *Eur J Med Chem.* 2005, 40, 11, 1103-1110.
195. “Efficient Telomerization Of 1,3-Butadiene With Alcohols In The Presence Of In Situ Generated Palladium(0)Carbene Complexes”; Jackstell, R.; Frisch, A.; Beller, M.; Rottger, D; Malaun, M.; Bildstein, B.; *J Molec. Cat. A: Chemica.*, 2002, 185, 1-2, 105–112.
196. “Solvent-Controlled Selective Synthesis Of A Trans-Configured Benzimidazoline-2-ylidene Palladium (II) Complex And Investigations Of Its Heck-Type Catalytic Activity”; Huynh, H. V.; Ho, J. H. H.; Neo, T. C.; Koh, L. L.; *J Organometal. Chem.* 2005, 690, 16, 3854–3860.
197. “Influence Of Shell Strength On Shape Transformation Of Micron-Sized, Monodisperse, Hollow Polymer Particles”; Okubo, M.; Minami, H.; Morikawa, K.; *Colloid Polym. Sci.* 2003, 281, 214.
198. “Self-Assembling Sub-Micrometer-Sized Tube Junctions And Dendrites Of Conducting Polymers”; Wei, X. Z.; Zhang, J. L.; Yu, M.; Yang, S. Y.; Wan, X. M.; *Adv. Mater.* 2003, 15, 1382.

199. "High-Yield Synthesis Of Superhydrophilic Polypyrrole Nanowire Networks"; Zhong, W.; Liu, S.; Chen, X.; Wang, Y.; Yang, W.; *Macromolecules* 2006, 39, 3224.
200. "Polyaniline Nanofibers: Facile Synthesis And Chemical Sensors"; Huang, J.; Virji, S.; Weiller, H. B.; Kaner, B. R.; *J. Am. Chem. Soc.* 2003, 125, 314.
201. "Conjugated Polymer Actuators For Biomedical Applications"; Smela, E.; *Adv. Mater.* 2003, 15, 481.
202. The Merck Index, 13th Edition, Ed. M. J. O'Neil; Smith, M.; Heckelman, E. P.; Merck & Co. Inc., Nj. P-1785, Monograph Number: 10074, 2001.
203. Nakamura, S.; Tsuno, N.; Yamashita, M.; Kawasaki, I.; Ohta, S.; Ohishi, Y.; *J. C. S. Perkin* 1995.
204. (A) "Design, Synthesis, And Antiviral Activity Of A-Nucleosides: D- And L- Isomers Of Lyxofuranosyl- And (5 deoxylyxofuranosyl) benzimidazoles"; Migawa, M. T.; Gardet, J. L.; Walker-Ii, J. A.; Koszalka, G. W.; Chamberlain, S. D.; Drach, J. C.; Townsend, L. B.; *J. Med. Chem.* 1998, 41, 1242.
- (B) "Design, Synthesis, And Antiviral Activity Of Certain 2,5,6-trihalo-1-(.beta.-d-ribofuranosyl)benzimidazoles"; Townsend, L. B. ; Devivar, R. V.; Turk, S. R.; Nassiri, M. R.; Drach, J. C.; *J. Med. Chem.* 1995, 38, 4098.
205. "Synthesis, Reactions, And Spectroscopic Properties Of Benzimidazoles"; Preston, P. N.; *Chem. Rev.* 1974, 74, 279.
206. (A) "2h-Benzimidazoles (Isobenzimidazoles). Part 10. Synthesis Of Polysubstituted O-Phenylenediamines And Their Conversion Into Heterocycles, Particularly 2-Substituted Benzimidazoles With Known Or Potential Anthelmintic Activity"; Hazelton, J. C.; Iddon, B.; Suschitzky, H.; Woolley, L. H.; *Tetrahedron* 1995, 51, 10771.
- (B) Labaw, C. S.; Webb, R. L.; *Chem. Abstr.* 1981, 95, 168837.
- (C) "The Biochemical Basis Of Anthelmintic Action And Resistance"; Kohler, P.; *Int. J. Parasitol.* 2001, 31, 336.
207. (A) Meisel, P.; Heidrich, H. J.; Jaensch, H. J.; Kretzschmar, E.; Henker, S.; Laban, G.; *Chem. Abstr.* 1987, 107, 217629.
- (B) Kyle, D.; Goehring, R. R. ; Shao, B.; *Chem. Abstr.* 2001, 135, 33477.

208. "Some 3-Thioxo/Alkylthio-1,2,4-Triazoles With A Substituted Thiourea Moiety As Possible Antimycobacterials"; Kuchkguzel, I.; Kucukguzel, G.; Rollas, S.; Kiraz, M.; *Bioorg. & Med. Chem. Lett.* 2001, 11, 1703.
209. (A) "Synthesis, Tubulin Binding, Antineoplastic Evaluation, And Structure-Activity Relationship Of Oncodazole Analogs"; Kruse, L. L.; Ladd, D. L. ; Harrsch, P. B. McCabe, F. L.; Mong, S. M. ; Faucette, L.; Johnson, R.; *J. Med. Chem.* 1989, 32, 409.
- (B) "Structure-Activity Studies Of Antitumor Agents Based On Pyrrolo[1,2-a]benzimidazoles: New Reductive Alkylating Dna Cleaving Agents"; Islam, I.; Skibo, E. B. ; Dorr, R. T.; Alberts, D. S.; *J. Med. Chem.* 1991, 34, 2954 .
210. "Benzimidazole Synthesis And Biological Evaluation: A Review" Rathod, C. P.; Rajurkar, R. M.; Thonte, S. S.; *Indo American Journal Of Pharmaceutical Research* 2013 .
211. (A) "Conjugated Polymer-Based Chemical Sensors"; Mcquade, T. D.; Pullen, E. A.; Swager, M. T.; *Chem. Rev.* 2000, 100, 2537.
- (B) "Polymer Sensors For Nitroaromatic Explosives Detection"; Toal, J. S.; Trogler, C. W.; *J.Mater.Chem.* 2006, 16, 2871.
- (C) "Optical Explosives Detection: From Color Changes To Fluorescence Turn-On"; Germain, E. M.; Knapp, J. M.; *Chem. Soc. Rev.* 2009, 38, 2543.
212. (A) Moore, D. S.; *Rev. Sci. Instrum.* 2004, 75, 2499.
- (B) Mcluckey, A. S.; Goeringer, E. D.; Asano, G. K.; Vaidyanathan, G.; Stephenson, L. J.; Rapid, J. R.; *Commun. Mass Spectrom.* 1996, 10, 287.
213. (A) "Self-Assembly Of A Nanoscopic Prism Via A New Organometallic Pt₃ Acceptor And Its Fluorescent Detection Of Nitroaromatics"; Ghos, S.; H And Mukherjee, S. P.; *Organometallics* 2008, 27, 316.
- (B) Bar, K. A.; Shanmugaraju, S.; Chi, W.K.; Mukherjee, S. P.; *Dalton Trans.* 2011, 40, 2257.
- (C) "Coordination-Driven Self-Assembly Of Metallamacrocycles Via A New Pt^{II}₂ Organometallic Building Block With 90° Geometry And Optical Sensing Of Anions"; Shanmugaraju, S.; Bar, K. A.; Chi, W. K.; Mukherjee, S. P.; *Organometallics.* 2010, 29, 2971.

- (D) “Simple Molecule-Based Fluorescent Sensors For Vapor Detection Of TNT”; Zyryanov, V. G.; Palacios, A. M.; And Anzenbacher, P.; *Org. Lett.* 2008, 10, 3681.
- (E) “Photoluminescent Coordination Polymers Of D10 Metals With 4,4'-dipyridylsulfide (dps)”; Muthu, S.; Ni, Z.; Vittal, J. J.; *Inorg. Chim. Acta.* 2005, 358, 595.
- (F) “Novel Ferrocene Receptors For Barbiturates And Ureas”; Collinson, R. S.; Gelbrich, T.; Hursthouse, B. M.; Tucker, R. H. J.; *Chem. Commun.* 2001, 555.
214. “Microwave-Assisted One Step High-Throughput Synthesis Of Benzimidazoles”; Lin, Y. S.; Isome, Y.; Stewart, E.; Liu, F. J.; Yohannes, D.; Yu, L.; *Tetrahedron Letters* 2006, 47, 2883–2886.
215. “Crystal Structure Of 2,5-bis(1-butyl-benzimidazol-2-yl)thiophene”; Wen-Long P.; Yan-Mei X.U.; Yifeng S.; Chen S.; Dan-Yan L.; Hua-Can S.; *Analytical Sciences* 2007, 23, 95.
216. “Rhenium-Based Molecular Rectangles As Frameworks For Ligand-Centered Mixed Valency And Optical Electron Transfer”; Dinolfo, P. H.; Williams, M. E.; Stern, C. L.; Hupp, J. T.; *J. Am. Chem. Soc.* 2004, 126, 12989–13001.
217. (A) “Quantitative Studies Of Ground And Excited State Charge Transfer Complexes Of Fullerenes With N,N-Dimethylaniline And N,N-Diethylaniline”; Sun, Y. P.; Bunker, C. E.; Ma, B.; *J. Am. Chem. Soc.* 1994, 116, 9692–9699.
- (B) “Nonlinear Fluorescence Quenching And The Origin Of Positive Curvature In Stern-Volmer Plots”; Keizer, J.; *J. Am. Chem. Soc.* 1983, 105, 1494–1498.
218. Thanasekaran, P.; Wu, J. Y.; Manimaran, B.; Rajendran, T.; Chang, I. J.; Rajagopal, S.; Lee, G. H.; Peng, S. M.; Lu, K. L.; *J. Phys. Chem. A.* 2007, 111, 10953–10960.
219. (A) “Color-Tunable, Aggregation-Induced Emission Of A Butterfly-Shaped Molecule Comprising A Pyran Skeleton And Two Cholesteryl Wings”; Tong, H.; Hong, Y.; Dong, Y.; Ren, Y.; Haeussler, M.; Lam, J. W. Y.; Wong, K. S.; Tang, B. Z.; *J. Phys. Chem. B.* 2007, 111, 2000–2007.
- (B) “Tunable Aggregation-Induced Emission Of Diphenyldi-benzofulvenes”; Tong, H.; Dong, Y.; Haeussler, M.; Lam, J. W. Y.; Sung, H. H. Y.; Williams, I. D.; Sun, J.; Tang, B. Z.; *Chem. Commun.* 2006, 1133–1135.

220. (A) "Aggregation-Induced Emission Of 1-Methyl-1,2,3,4,5 pentaphenylsilole"; Luo, J. D.; Xie, Z. L.; Lam, J. W. Y.; Cheng, L.; Chen, H. Y.; Qiu, C. F.; Kwok, H. S.; Zhan, X. W.; Liu, Y. Q.; Zhu, D. B.; Tang, B. Z.; *Chem. Commun.* 2001, 1740–1741.
- (B) "Fluorescent "Light-Up" Bioprobes Based On Tetraphenylethylene Derivatives With Aggregation-Induced Emission Characteristics"; Tong, H.; Hong, Y.; Dong, Y. Haeussler, M.; Lam, J. W. Y.; Li, Z.; Guo, Z.; Guo, Z.; Tang, B. Z.; *Chem. Commun.* 2006, 3705–3707.
- (C) Chen, J.; Law, C. C. W.; Lam, J. W. Y.; Dong, Y.; Lo, S. M. F.; Williams, I. D.; Zhu, D. B.; Tang, B. Z.; *Chem. Mater.* 2003, 15, 1535–1546.
- (D) "Supramolecular Structure Of Precipitated Nanosize β -Carotene Particles"; Auweter, H.; Haberkorn, H.; Heckmann, W.; Horn, D.; Lüddecke, E.; Rieger, J.; Weiss, H.; *Angew. Chem. Int. Ed.* 1999, 38, 2188–2191.
221. (A) "Effects Of Grafted Alkyl Groups On Aggregation Behavior Of Amphiphilic Poly(aspartic Acid)"; Kang, H. S.; Yang, S. R.; Kim, J. D.; Han, S. H.; Chang, I. S.; *Langmuir* 2001, 17, 7501–7506.
- (B) "Reversible Thermoresponsive Aggregation/Deaggregation Of Water-Dispersed Polymeric Nanospheres Exhibiting Structural Transformation"; Kaneko, T.; Hamada, K.; Kuboshima, Y.; Akashi, M.; *Langmuir* 2005, 21, 9698–9703.
222. (A) "Hydrogen Bonding Networks And Anion Coordination In (η^6 -Arene)Cr(CO)₃ Complexes: Metal Carbonyls As Hydrogen Bond Acceptors"; Camiolo, S.; Coles, S. J.; Gale, P. A.; Hursthouse, M. B.; Mayer, T. A.; Paver, M. A.; *Chem. Commun.* 2000, 275–276.
- (B) "Supramolecular, Bifurcated N-H \cdots OC-M Bonding Explains Unusually Low ν_{CO} Frequencies In Metal Carbonyl Compounds: A Case Study"; Braunstein, P.; Taquet, J. P.; Siri, O.; Welter, R.; *Angew. Chem. Int. Ed.* 2004, 43, 5922–5925.
223. "Aggregation-Driven Growth Of Size-Tunable Organic Nanoparticles Using Electronically Altered Conjugated Polymers"; Wang, F.; Han, M. Y.; Mya, K. Y.; Wang, Y.; Lai, Y. H.; *J. Am. Chem. Soc.* 2005, 127, 10350–10355.

Appendix

Experimental Data

Table-1 : Observation of binding of L-2 with PA by UV-Visible spectroscopy

Vol. of PA (10^{-3} M) added (μ l) With 0.25×10^{-4} (M) L-2	Final conc. of [PA] $\times 10^{-4}$ [M]
0	0
50	0.24
75	0.36
100	0.47
125	0.58
150	0.69
200	0.9
275	1.1

Table-2 : Observation of binding of L-4 with PA by UV-Visible spectroscopy.

Vol. of PA (10^{-3} M) added (μ l) With 0.25×10^{-4} (M) L-4	Final conc. of [PA] $\times 10^{-4}$ [M]
0	0
50	0.24
75	0.36
100	0.47
125	0.58
150	0.69
175	0.8
200	0.9
225	1
275	1.1
325	1.39

Table-3 : Observation of binding of L-5 with PA by UV-Visible spectroscopy

Vol. of PA (10^{-3} M) added (μ l) With 0.25×10^{-4} (M) L-5	Final conc. of [PA] $\times 10^{-4}$ [M]
0	0
25	0.12
50	0.24
60	0.29
70	0.33
80	0.38
90	0.43
100	0.47
120	0.57

Table-4 : Observation of binding of L-6 with PA by UV-Visible spectroscopy.

Vol. of PA (10^{-4} M) added (μ l) With 1×10^{-5} (M) L-6	Final conc. of [PA] $\times 10^{-5}$ [M]
0	0
50	0.24
75	0.36
150	0.69
175	0.8
225	1
375	1.5
450	1.8

Table-5 : Observation of binding of L-7 with PA by UV-Visible spectroscopy.

Vol. of PA (10^{-4} M) added (μ l) With 0.5×10^{-5} (M) L-7	Final conc. of [PA] $\times 10^{-5}$ [M]
0	0
75	0.36
125	0.58
150	0.69
200	0.9
250	1.1
300	1.3
350	1.48

Table-6 : Absorption maxima of compound L-2, L-4, L-5, L-6, L-7.

Compound	λ_{\max} (nm)
L-2	300, 350
L-4	350
L-5	350
L-6	250, 280, 400, 610, 660
L-7	250, 350, 410, 590, 630

Table-7 : Observation of binding of L-2 with 1-chloro-4-nitrobenzene by UV-Visible spectroscopy.

Vol. of 1-chloro-4-nitrobenzene (10^{-3} M) (μ l) added With 0.25×10^{-4} (M) L-2	Final conc. of [1-chloro- 4-nitrobenzene] $\times 10^{-4}$ [M]
0	0
50	0.24
75	0.36
100	0.47
125	0.58
150	0.69
200	0.9
225	1
275	1.1

Table-8 : Data for Benesi-Hildebrand plot [Compound : L-2]

Final [PA] $\times 10^{-4}$ M	$1/[PA] \times 10^4$ M	Absorbance(A)	$1/\Delta A = 1/A - A_0$
0.69	1.449	1.112	2.958
0.8	1.256	1.174	2.5
0.9	1.111	1.217	2.257
1	1	1.256	2.074
1.1	0.909	1.327	1.808
1.3	0.769	1.393	1.615

Table-9 : Data for Benesi-Hildebrand plot [Compound : L-4]

Final [PA] x 10 ⁻⁴ M	1/[PA] x 10 ⁴ M	Absorbance(A)	1/ΔA=1/A-A ₀
0.36	2.777	0.839	6.756
0.47	2.127	0.891	5
0.58	1.724	0.940	4.016
0.69	1.449	0.980	3.460
0.8	1.256	1.051	2.777
0.9	1.111	1.112	2.375
1	1	1.157	2.145
1.1	0.909	1.237	1.831
1.3	0.769	1.326	1.574

Table-10 : Data for Benesi-Hildebrand plot [Compound : L-5]

Final [PA] x 10 ⁻⁴ M	1/[PA] x 10 ⁴ M	Absorbance(A)	1/ΔA=1/A-A ₀
0.29	3.448	0.818	5
0.33	3.03	0.864	4.065
0.38	2.631	0.911	3.412
0.43	2.325	0.977	2.785

Table-11 : Data for Benesi-Hildebrand plot [Compound : L-6]

Final [PA] x 10 ⁻⁵ M	1/[PA] x 10 ⁵ M	Absorbance(A)	1/ΔA=1/A-A ₀
0.24	4.166	1.126	16.393
0.36	2.777	1.153	10.989
0.47	2.127	1.177	8.695
0.58	1.724	1.197	7.407
0.69	1.449	1.209	6.802

Table-12 : Data for Benesi-Hildebrand plot [Compound : L-7]

Final [PA] x 10 ⁻⁵ M	1/[PA] x 10 ⁵ M	Absorbance(A)	1/ΔA=1/A-A ₀
0.12	8.333	0.616	47.61
0.24	4.166	0.628	30.30
0.36	2.777	0.640	22.22
0.47	2.127	0.651	17.857
0.69	1.449	0.666	14.084
0.8	1.256	0.674	12.658

Table-13: Observation of quenching of L-2 with PA by fluorescence spectroscopy.

Vol. of PA (10 ⁻³ M) added (μl) With 0.25 x 10 ⁻⁴ (M) L-2	Final conc. of [PA] × 10 ⁻⁴ [M]
0	0
50	0.24
75	0.36
100	0.47
125	0.58
150	0.69
225	1

Table-14: Observation of quenching of L-4 with PA by fluorescence spectroscopy.

Vol. of PA (10 ⁻³ M) added (μl) With 0.25 x 10 ⁻⁴ (M) L-4	Final conc. of [PA] × 10 ⁻⁴ [M]
0	0
50	0.24
75	0.36
100	0.47
125	0.58
150	0.69
275	1.1

Table-15: Observation of quenching of L-5 with PA by fluorescence spectroscopy.

Vol. of PA (10^{-3} M) added (μ l) With 0.25×10^{-4} (M) L-5	Final conc. of [PA] $\times 10^{-4}$ [M]
0	0
25	0.12
50	0.24
60	0.29
70	0.33
80	0.38
90	0.43
110	0.52
130	0.62

Table-16: Observation of quenching of L-6 with PA by fluorescence spectroscopy.

Vol. of PA (10^{-4} M) added (μ l) With 1×10^{-5} (M) L-6	Final conc. of [PA] $\times 10^{-5}$ [M]
0	0
50	0.24
125	0.58
175	0.8
225	1
275	1.2
300	1.3
325	1.39
375	1.5

Table-17: Observation of quenching of L-7 with PA by fluorescence spectroscopy.

Vol. of PA (10^{-4} M) added (μ l) With 0.5×10^{-5} (M) L-7	Final conc. of [PA] $\times 10^{-5}$ [M]
0	0
50	0.24
100	0.47
150	0.69
275	1.1
350	1.48
450	1.8

Table-18 : Data of Stern-Volmer plot for PL quenching of L-2 by PA.

[PA] x 10 ⁻⁴ M	I ₀ /I-1
0.24	0.0556
0.36	0.788
0.47	1.003
0.58	1.329
0.69	1.645
0.8	2.044
0.9	2.348
1	2.844

Table-19 : Data of Stern-Volmer plot for PL quenching of L-4 by PA.

[PA] x 10 ⁻⁴ M	I ₀ /I-1
0.24	0.612
0.36	0.782
0.47	1.074
0.58	1.545
0.69	1.991
0.9	3.376
1.1	6.064

Table-20 : Data of Stern-Volmer plot for PL quenching of L-5 by PA.

[PA] x 10 ⁻⁴ M	I ₀ /I-1
0.12	0.3
0.24	0.678
0.29	0.887
0.33	1.068
0.38	1.232
0.43	1.420
0.47	1.581
0.52	1.702

Table-21 : Data of Stern-Volmer plot for PL quenching of L-6 by PA.

[PA] x 10 ⁻⁵ M	I ₀ /I-1
0.9	0.1165
1	0.1193
1.1	0.1253
1.3	0.1356
1.39	0.1479
1.48	0.1712
1.5	0.2026

Table-22 : Data of Stern-Volmer plot for PL quenching of L-7 by PA.

[PA] x 10 ⁻⁵ M	I ₀ /I-1
0.24	0.035
0.47	0.061
0.9	0.099
1.3	0.142
1.6	0.209
1.8	0.220

Table-23 : Data of Modified stern-Volmer plot for the PL quenching of L-4 by PA.

[PA] x 10 ⁻⁴ M	(I ₀ /I-1)/[PA] x10 ⁵ M
0.36	2.0578
0.47	2.2851
0.58	2.6637
0.69	2.8855
0.9	3.7511

Table-24 : Data of Modified stern-Volmer plot for the PL quenching of L-7 by PA.

[PA] x 10 ⁻⁵ M	(I ₀ /I-1)/[PA] x10 ⁵ M
0.9	0.11
1.1	0.1172
1.48	0.1263
1.6	0.1306

Table-25 : Dynamic and Static Stern-Volmer constants for L-2, L-4, L-5, L-6, L-7.

Compound	K_{sv}, M^{-1}	K_s, M^{-1}
L-2	3.37312	0.0327
L-4	18.397 ^a	0.1751
L-5	3.62719	0.8900
L-6		0.3563
L-7	0.01824 ^a	1.5470

Here, a = K_{sv} for modified Stern-Volmer plot.